Akademia Górniczo – Hutnicza
im. Stanisława Staszica w Krakowie
Wydział Inżynierii Metali i Informatyki Przemysłowej

PRACA DOKTORSKA

PhD DISSERTATION

Author: mgr inż. Łukasz Madej

Title: Development of the multi-scale analysis model to simulate strain localization occurring during material processing

Supervisor: Professor Maciej Pietrzyk

Kraków 2006

ACKNOWLEDGMENTS

I would like to sincerely thank the people who contributed to the completion of this thesis. Firstly, thanks must go to my supervisor, Maciej Pietrzyk, for his help, for the inspiration he gave me, for scientific discussions and most importantly for his time. Special thanks must go to Peter Hodgson who believed in my work and always gave me his support and enormous enthusiasm.

I would like to say thank you to all my professors, friends and colleagues from the AGH department for a very good atmosphere at work. I would also like to say thank you to the people from Sheffield University for their knowledge imparted to me at the beginning of my work. Particular thanks must go to all my friends from Deakin University who helped me a lot while I was staying far away from home. Thanks to them I have spent great times in Australia.

And last but certainly not least, I am most grateful to all my family for their support and understanding during my work. I would like to give special thanks to my Mother and Father, Dominika, James, Klaudia and my beautiful niece Ola for their wholehearted support during my work and my life.

Thank you for everything.

„Truth is much too complicated to allow anything but approximation”

Janos Von Neumann

Content

List of Symbols

a(t)	nodal displacement vector
a	constant
b	Burgers vector
C	constant
$G(T)$	shear modulus
$E^t(T)$	stiffness at time t and temperature T
f	scaling factor
FFI	final failure index
h_{sm}	smoothing length
$H_s(x)$	Heaviside function
K	material consistency
l	mean free path of dislocation
k	yield stress in pure shear
m	strain rate sensitivity coefficient
$M_S^h(x)$	unit jump function
M	constant
n	vector normal to the surface
n	exponent
N(x)	standard shape function matrix
N_{CA}	number of CA cells associated with one integration point
N_{ke}	linear shape function of the k_e node
n_{el}	number of finite elements in the FE mesh
$N(i)$	surrounding of the i^{th} cell
Q	activation energy
R	gas constant
S	discontinuity path
t	time
T	temperature
u	displacement field
$\hat{u}$	regular part of the displacement field
[[u]](x t)	displacement jump function
V_j	volume associated with the j^{th} particle
W_{ij}	kernel function
$\hat{W}_{ij}$	corrected kernel function
$\alpha(x)$	correction factor in the SPH method
α_r	disorientation angle
α_d	constant
α_{MSB_fr}	fraction of micro shear bands in the SB cell
$\boldsymbol{\beta}(x)$	correction factors in the SPH method
β	damage variable calculated from the Rousselier [Rou89] model
δ_S	Dirac delta function
$d\dot{\varepsilon}_i$	equivalent strain rate increment
$d\dot{\varepsilon}_{ij}$	strain rate increment tensor

ε	strain
$\dot{\varepsilon}_{ij}$	strain rate tensor
$\dot{\varepsilon}_i$	equivalent strain rate
$\dot{\varepsilon}_1\ \dot{\varepsilon}_2\ \ \dot{\varepsilon}_3$	principal value of the strain rate tensor
ε_{ij}	strain tensor
ε_i	equivalent strain
ε_{cr}^*	critical value of strain
ε_{CA}	strain calculated in the CA spaces
$\|\mathbf{e}\|$	error norm
Φ	sensitivity parameter
θ^{rot}	rotation angle
θ_F	critical value of the disorientation angle
κ	constant related to the support domain
ξ	correction coefficient in the CAFE model
Γ	boundary of the domain of the solution
η	heat transfer coefficient
μ	friction coefficient
v_{gb}	grain growth velocity
Ω	domain of the solution
ρ	dislocation density
σ_{ij}	stress tensor
$\hat{\sigma}_{ij}$	deviatoric part of the stress tensor
σ_1, σ_3	principal stresses
σ_p	flow stress value in the Levy Mises flow rule
σ_i	equivalent stress
σ_f	flow stress calculated by the inverse analysis
σ_e^*	stress equal to theoretical shear strength
σ_{cr}^*	critical value of stress
σ_I	maximum value of the principal stress
σ_F	fracture stress
σ_p^{CA}	flow stress calculated in the CA spaces
τ_{hard}	critical value for initiation of the hard slip system
Y_i	state of the i^{th} cell
ς	coefficient in the flow rule correction [Waj04]

1. Introduction

Numerical modeling of material behavior under conditions of processing, manufacturing and exploitation is widely used in many research and industrial facilities. The Finite Element (FE) method is commonly applied to create a complex description of a particular deformation, thermomechanical or heat treatment process. Applications of the FE method are wide, from modeling of simple plastometric tests (e.g., compression, tension, torsion) to modeling the complicated behavior of entire structures (e.g., cars, buildings, implants). FE models are able to replicate the real processes and phenomena that take place in materials, as well as in the surroundings. These days the FE method is used not only in material application but also in almost every aspect of science and is still evolving. Advanced finite element techniques capable of handling new requirements and new numerical algorithms (e.g., hp adaptation method) to solve increasingly complex problems are being developed by many researchers [Dau00, Pas06, Str01, Zhu03, Zie06]. This also includes the creation of new advanced finite elements and meshes capable of more accurate prediction of material behavior, such as enhanced finite elements [Oli95], which take into account discontinuities in materials.

However, there are several constraints that limit FE applications and capabilities. Simultaneous prediction of material behavior in different scales during processing (e.g., development of micro shear and shear bands) is one of these constraints. Large computational costs and lack of flexibility are also disadvantages of this method. More efficient numerical techniques achieve greater commercial impacts. That explains the search in recent years for an alternative new multi scale computational technique to solve problems in various length scales during material processing [All06, Cha06, Dau00, Gan94, Mak00, Mro06, Mro07, Pec98a, Ron06, Shi05, Str01].

One solution is multi scale analysis CAFE model (Cellular Automata Finite Element) [Gan94]. Such a combination of two numerical methods (FE and CA) represents a truly multi scale approach to describe material behavior under complex loading conditions. Analysis based on the CAFE method is more complex and accurate than that used in the conventional FE method. In the CAFE approach, material behavior is completely separated from the structural response because calculations are coupled between the cellular automata technique and the finite element method. The CAFE approach makes it possible to model various processes that occur in materials during deformation at different scales and at the same time. The possibility to use a stochastic description of materials rather than deterministic is another advantage of this model. This makes CAFE models a very effective computational tool, which may be useful in different areas of engineering, such as modeling of strain localization.

Recent scientific experiments have shown that prediction of strain localization related to initiation and development of micro shear bands and shear bands is crucial for accurate modeling of the plastic deformation in a variety of metallic materials [Kor04]. These phenomena have been experimentally and theoretically studied over recent years by several researchers. It has been stated that the development of strain localization due to shear banding in material is often a precursor to material failure. On the other hand, it is proven that control of the shear banding phenomena may lead to reduction in applied loads. This is the basis of the proposed Structure Based Design of Metal Forming Operations (SBDMFO) [Kor95], which eventually led to the development of new types of forming industrial operations (i.e. KOBO type forming) [Boc03]. It is proven that certain process conditions (e.g., change in temperature or strain path) may lead to an increase in the forming capabilities of many materials that are difficult to form by conventional metal forming operations. However, an efficient numerical model to support experimental observations is required to further analyze these problems and to obtain a significant reduction in production costs.

There is still lack of an efficient numerical model that accounts for the influence of the formation of shear bands and micro shear bands during industrial processes, because of the multi scale and discontinuous nature of those phenomena [Kor95, Ciz02a]. That is a reason why the advantages of the multi scale CAFE method are used in this work to solve the problem of modeling strain localization. Particular emphasis is put on an intelligent definition of the transition rules based on the knowledge of experts and scientists, experimental observation and available data. It is believed that increased knowledge input into the transition rules allow for a more accurate and realistic CA model to be created. Thus the CAFE approach is one of the artificial intelligence techniques. The developed multi scale CAFE model for the prediction of strain localization occurring during thermo-mechanical processing improves the quality in modeling of various processes occurring in materials.

A detailed review of the strain localization problem from the experimental and numerical point of view as well as a review of the application of the multi scale CAFE method is presented in this thesis. On the basis of this knowledge, a proposed solution to create an efficient numerical model for strain localization that overcomes the limitations of current FE approaches is described, discussed and validated with results obtained from the flat rolling process and channel die compression. The present work concludes with a discussion of the possibilities of further application and development of the proposed model.

2. Strain Localization Phenomena

The multi scale CAFE model dedicated to simulate specific phenomena is always based on properly defined transition rules, which replicate real processes occurring in materials. The more accurate these rules are, the more realistic is the description of material behavior. That is the reason why creation of valuable transition rules is of importance during the model design stage. In this work, definition of the transition rules for strain localization phenomena is based on the knowledge of experts and scientists and experimental observations, which are described in detail below.

Plastic deformation of metallic materials is performed by two main mechanisms: slip and twinning, which affect the microstructure and deformation texture. These mechanisms have been the subject of research performed for decades by scientists from all over the world [Ana80, Bal03, Boc03, Ciz02a, Dev89, Kor98, Mak00, Nak07, Nav04, Oli95, Oli01, Pec92]. Several complex theoretical and mathematical models describing slip and twinning in various metallic materials (steel [Hum95], aluminum [Cru04], magnesium [Nav04] and titanium [Sea05]) have been used in theoretical analyses supporting the experimental knowledge. However, some of the mechanisms are still not fully understood.

Particular attention has been given to slip activity in polycrystalline materials, which is based on band-like features [Hum95], such as deformation bands, microbands and shear bands. Deformation bands are usually characterized as parts of a crystal that have rotated differently during deformation and have produced different orientation bands within given grains. When neighboring volumes of a grain have deformed on several slip systems and have rotated to a different orientation, so called transition bands develop. They are usually formed from long narrow cell clusters or subgrains. When the previously developed cell structure is no longer stable, microbands develop due to changes in the strain path within a single grain. This is an instability, which carries only the deformation at medium strains when homogeneous slip is excluded. Two theories describing initiation of microbands have been developed [Hum95]. The first suggests a connection with a low work hardening rate and eventually with dynamic recovery. The second claims that microbands develop due to flow instability, which involves mixed dislocations on parallel planes.

Shear bands are the last deformation features that operate at large strains carrying most of the deformation. This phenomenon is also the least known and explained. However, a proper understanding of the processes leading to initiation and propagation of these bands is crucial for understanding material behavior during deformation in industrial conditions.

The current work is a natural outcome from industrial demand and is particularly focused on the development of a proper transition rules dedicated to describe shear banding phenomena and their incorporation into the created multi scale CAFE model.

2.1. Shear Band Theory

As mentioned above, one of the possible mechanisms leading to material plastic deformation is the cooperative work of two parallel processes [Ana80, Ciz02a, Dev89, Hum95, Kor98]: development of micro shear and shear bands. Recent work has shown that initiation and development of micro shear bands and shear bands are crucial for the development of plastic deformation in a variety of metallic materials [Kor98, Kor04]. The problem of strain localization in materials during deformation has been investigated by scientists for over thirty years. Much effort has been made both experimentally and theoretically to study shear band propagation during various kinds of deformation: compression [Ana94, Col93, Dev89, Nou86], rolling [Dil79, Dug78, Emb84, Kor83, Kor86a, Lee91, Liu87, Nou80] and extrusion [Kaz05, Lib92]. As a result of these studies several forming processes, which benefit from the change of deformation path and shear band propagation, have already been designed and used in industry [Boc03, Kor85, Kor92, Kor95, Ric95]. However, there is still lack in scientific literature a single complex theory that describes these two phenomena. During past years several contributory theories commonly used by researchers have been developed independently.

Korbel and co-workers have attempted to create a consistent theory on shear banding phenomena [Ber92, Emb84, Kor85, Kor86a, Kor86b, Kor88, Kor90, Kor92, Kor95, Kor97, Kor98**,** Kor04, Ric95]. The author [Kor98] has claimed that coarse slip already develops when deformation is small and that coarse slip employs similar slip systems to those in a single crystal of the same metal. The development of coarse slip systems affects the hardening of polycrystals sooner than in a single crystal, but it does not lead to strain localization in the macroscale. Based on this process a micro shear band usually develops in one grain. When crossing to adjacent grains, the transition occurs without any change in orientation inside the material. Shear is distributed along the grains in very thin micro shear layers, which are able to cluster with increasing strain. As a result, a macroscopic feature termed *shear band* develops (Figure 2.1).

a) 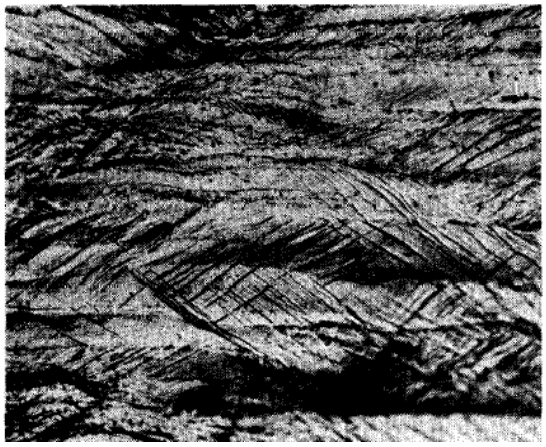 b) 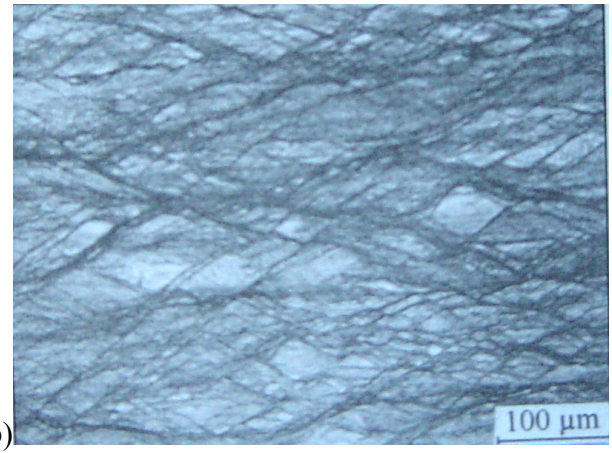

Figure 2.1. Micro shear bands and shear bands observed in a) [Kor86b] b) [Bli02].

Shear bands in materials have the same orientation as micro shear bands. In this work [Kor98] the thickness of a micro shear band was estimated to be in the order of 0.1 to 0.2 μm. Similar observations are reported in [Ciz02a, Ciz04, Mor85].

A characteristic feature of a micro shear band is that a shear employs other than an easy slip system in the material. One explanation is that when micro shear band slip plane coincides with the easy slip system, a channel-like penetration of the substructure, typical for the coarse slip system, is observed. Another explanation is the involvement of several slip systems within this very thin band. But according to [Kor98] there is no evidence supporting this multi slip system theory. From the observations performed in [Ber92, Emb84, Kor85, Kor88, Kor98], it is clear that the deformation in a micro shear band is simple shear. Slip on a non-easy slip system is possible, but it involves much higher critical stresses than that necessary for the initiation of an easy slip system, which is a key parameter in shear banding theory supported by other researchers [Mor85].

In [Kor98], the author claims that initiation of micro shear bands is connected with very high and very local stress concentrations. The source of these local stresses and, furthermore, the initiation of micro shear bands may be the coarse slip in an easy slip system. This statement is the major assumption of the theory proposed in [Kor98]. Another very important conclusion from [Kor98] is that a change in the deformation scheme and increase of temperature can cause instant initiation of micro shear bands in metallic materials. It seems that under these conditions that shear banding phenomena become the major mode of plastic deformation. In the work [Kor98] the author also claims that the shear band phenomenon is responsible for many instabilities occurring in the material during the deformation of metallic materials, such as Luders deformation or the Portevin-LeChatelier deformation.

A slightly different theory describing the origin of the micro shear banding phenomenon has been presented in [Ciz02a, Ciz02b, Ciz04], which supports the observations in [Mor85]. The development of micro shear bands in the material proposed in this approach [Ciz02b] has been chosen as the basis of the transition rules in the developed multi scale

model presented in this work. Therefore, a more detailed explanation of the major assumptions made by Cizek are presented below.

In [Ciz02b] the author claims that micro shear bands develop through the formation of slip domains, discrete cells aligned along the band propagation direction. Shear bands can nucleate on the isolated cells or small groups of cells. During the deformation process, misorientation angles between these cells and the surrounding matrix increase, which is clearly shown in Figure 2.2.

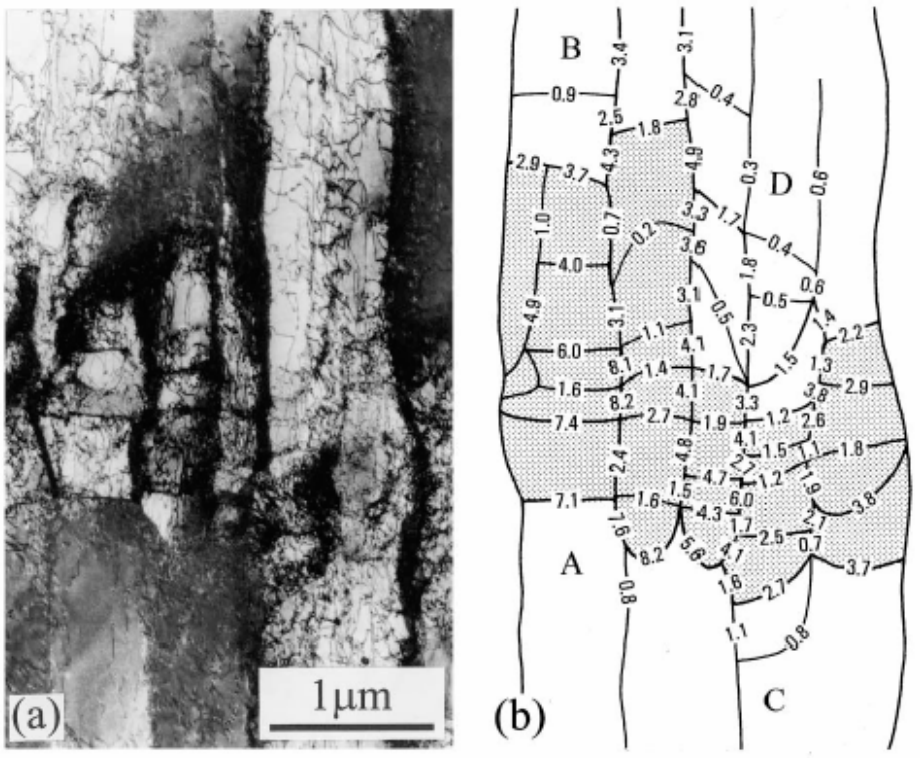

Figure 2.2. a) TEM observation of nucleating micro shear bands, b) corresponding misorientation map with the domain misorientation values [Ciz02b].

It is shown in [Ciz02b] that even at low strain values, misorientation angles of the cell boundaries have already reached values far higher than 8^{o}. Eventually they form narrow bands that than become thicker due to the formation of new cells. This process is connected with micro stress fields generated during the rotation of the previously formed cells. A schematic illustration of this process is presented in Figure 2.3. The shade of gray in each particular cell indicates different values of the boundary misorientation angles.

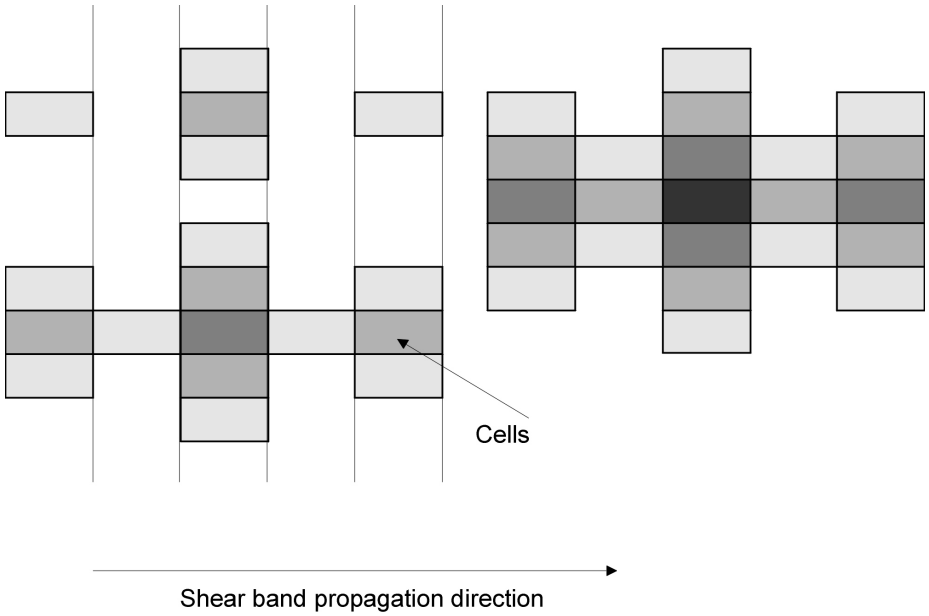

Figure 2.3. Scheme of the initiation and development of shear bands [Ciz02b]. Shade of gray represents the value of the misorientation angle.

Finally, at larger strains micro shear bands, composed of cells with significant misorientation with respect to the surrounding matrix, occur in the sample. It was observed in [Ciz02b] that micro shear bands propagate across the grains in a similar direction. However, these directions are not always parallel. Misorientation angles of two almost parallel microshear bands are shown in Figure 2.4. It is clear that these two micro shear bands nucleated at different strains, but during further deformation the two micro shear bands merge due to thickening, and a macroscopic shear band nucleates. The same mechanism of shear band formation is reported in [Kor98].

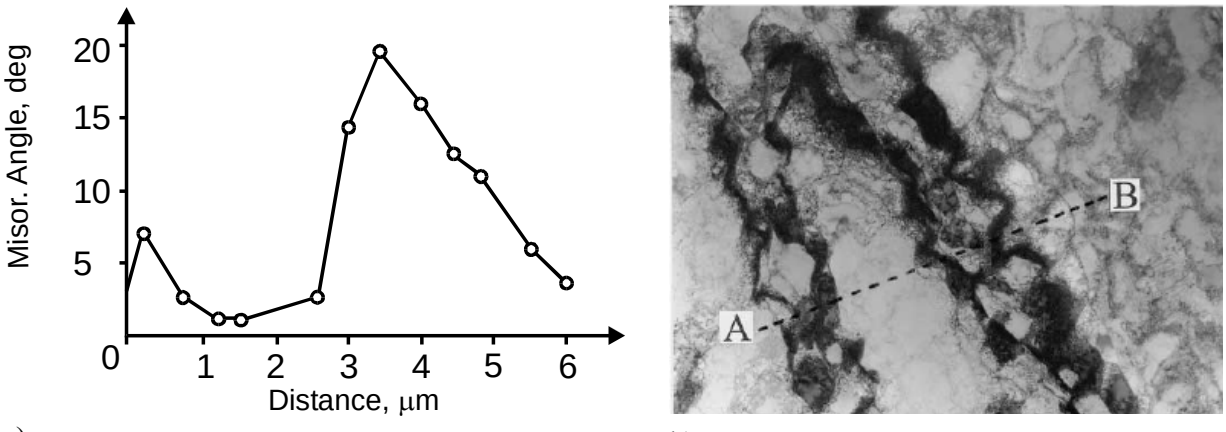

a) b)

Figure 2.4. Misorientation of the developing micro shear bands as a function of distance (a) between points A and B (b) [Ciz02b].

It was observed in [Mor85] that inside cell clusters some of their crystallographic orientations were distorted, and some of the cells were fragmented into small blocks. Based on those small blocks with large misorientation angles, micro shear bands nucleate. In general, the presence of lamellar structures such as mechanical twins [Mor85] or microbands [Nak87], which are built from the dislocation walls, are needed for shear band formation. These observations support the theory described in [Ciz02b].

Other theories, slightly different than the approaches proposed in [Ciz02a, Ciz02b] and [Kor98], have also been developed. Works by [Dev89, Har88, Sem82], which mainly focus on the detailed explanation of macroscopic shear band formation, also need to be considered. It has been shown in [Har88] that development of shear bands is a result of crystalline slip or geometrical softening. Such a softening provides the path for shear localization and shear band formation. Two important parameters were identified to control the initiation of shear bands in plain strain channel die compression. The first is achievement of the critical value of the strain hardening rate, and the second is attainment of favorable slip geometry. In other work [Sem82] axisymmetrical compression tests were performed to explore the shear banding phenomenon. A typical evolution of the developed shear band is presented in that work. The author claims a strong influence of material properties, geometry and friction on micro shear occurrence during deformation. However, the shear bands always initiated as regions of very intense deformation in the form of an X structure along the sample. During further deformation the intersecting parts of the two shear bands form a flat region with intense deformation. Whenever strain increases, this flat region bends towards one of the die, which is shown in Figure 2.5. Similar development of macroscopic shear bands has been observed by many other researchers [Dev89, Dug78, Hou78, Kor98, Lee91, Liu87, Nou80, Nou86].

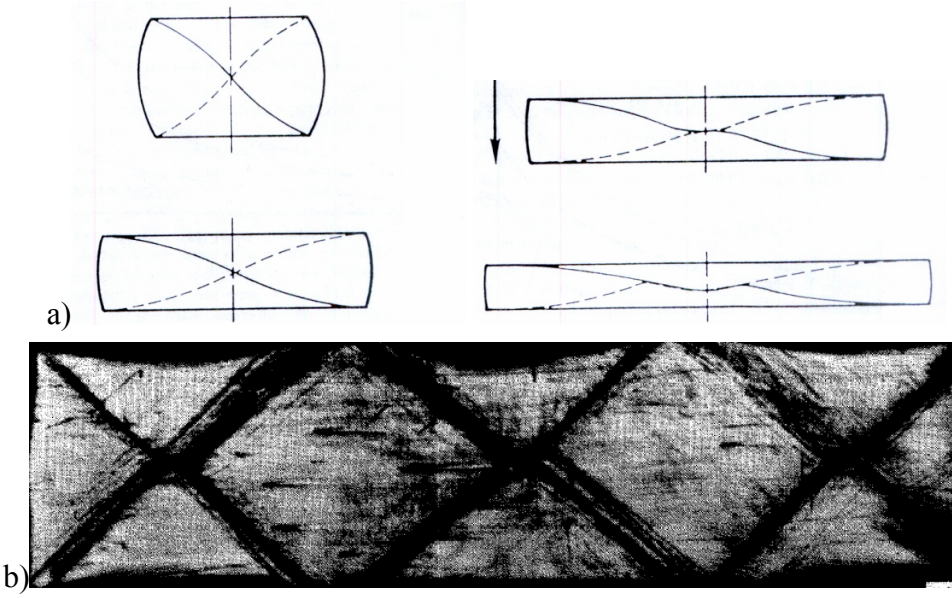

a)

b)

Figure 2.5. a) Development of strain localization in form of an X structure [Sem78], b) strain localization in 70-30 brass [Nou86] revealed under optical micrograph.

As demonstrated thus far, the micro shear and shear band initiation processes have been a subject of significant research. The length scale of these analyses vary significantly from the investigation of micro shear band initiation at the microscale level to development and formation of shear bands at the mezoscale level. Interactions between these two phenomena have also been intensely studied for different materials, plastometric tests and sample shapes.

The physical aspects of the processes leading to micro shear and shear bands development presented in this Chapter show the degree of complexity of the strain localization problem. Numerical models attempting to replicate this real material behavior are usually based on conventional differential equations, which face difficulties describing discontinuous and stochastic processes that lead to strain localization. More often than not, the developed models incompletely describe the processes responsible for strain localization development. A detailed discussion about the possibilities and limitations of the proposed numerical approaches thus far is presented in the next section of this work. On the other hand the physical aspects of strain localization are crucial in the creation of alternative approaches such as the multi scale CAFE model. In this approach, defining differential equations to describe material behavior is not required. Instead, in the CAFE model all processes are included in the CA method through a set of precisely defined transition rules created on the basis of the literature and experimental knowledge presented in this Chapter. The most important aspects of the shear banding theories are used in the present work to create transition rules in the CAFE model for strain localization phenomena and are summarized in Chapter 5.

Previously described experimental knowledge has been a starting point for many researchers to create a detailed mathematical and numerical description of shear banding phenomena [Ana80, Dev89, Oli01, Oli95]. Several different theories, mainly including macroscopic shear band formation, have been developed. A short review of the ideas presented in scientific literature is shown in the next section of this work.

2.2. Shear Band Modeling

Parallel to the work on theoretical models of the development of micro shear bands and shear bands, research focused on the creation of numerical models have been performed in various laboratories. Development of such models is very important from both scientific and economical points of view, because they provide the possibility to solve many problems that may occur during industrial tests by changing the material properties, shapes of the samples or test conditions. Based on these numerical simulations a final product with the required properties can be obtained without numerous expensive industrial trials. However, reliable results cannot be obtained without a numerical model that includes the real phenomena occurring in materials during thermo-mechanical processing. For years more and

more advanced Finite Element (FE) [Ana94, Pec92, Pec98, Pec98b], Finite Difference (FD) [Mak00a, Mak00b, Mak01] and Mesh Free [Li00] models have been developed. Usually they are able to describe one particular process, which is the key phenomenon during material deformation. While these models are commonly used, they are still being further developed to create more accurate and more flexible theories.

A shear band phenomenon, as presented in the first part of this Chapter, is one of the most important phenomena to occur in metal during different stages of deformation. Creation of a numerical model to describe the initiation and development of micro shear and shear bands has been attempted for several years [Ana80, Ana94, Fen99]. Models with different complexity and accuracy have been developed, but there are problems with the general description of these phenomena. Introducing modified elements into the FE mesh [Oli95] or introducing a modified flow rule, which is particularly sensitive to shear banding phenomena [Pec98, Waj04], are possible solutions to this problem. Several alternative approaches based on discrete methods such as Cellular Automata (CA) have been introduced as well during creation of the more complex and accurate models [Bal03, Mak00a]. A short description of several numerical models taking into account shear banding phenomena is given below.

The approach to solve a problem with strong discontinuities such as shear bands, is proposed in publications [Oli95] and is further used in other works [Arm95]. A method based on special finite elements with special points emerging from strong discontinuity analysis is presented in [Oli95]. By using these special points it is possible to combine a continuum approach with the discrete approach, which is based on discrete constitutive equations. The author of [Oli95] considered the existence of a body Ω subjected to strong discontinuity conditions along the discontinuity path *S* (Figure 2.6).

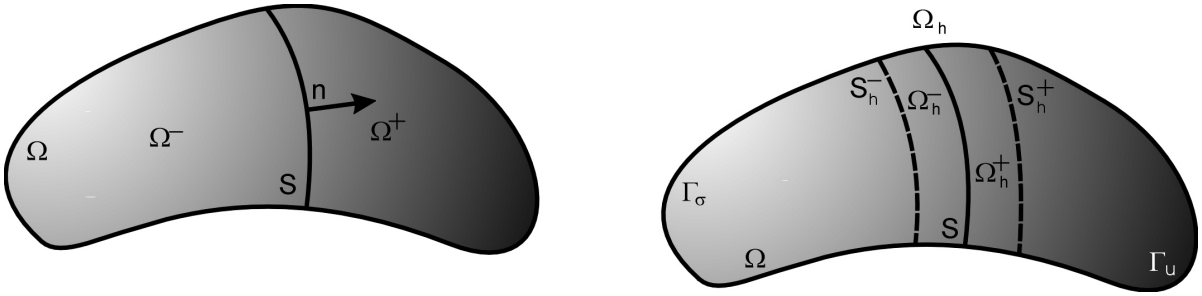

a) b)

Figure 2.6. Discontinuity path (a) and domains (b) created in [Oli95].

S is a discontinuity path, which is fixed at the reference configuration and characterized by the normal vector **n**. The *S* path is introduced in a way that divides the Ω domain into Ω^+ and Ω^- parts and a Heaviside function $H_s(x)$ is defined on Ω:

$$H_S(\mathrm{x}) = \begin{cases} 1 & \forall \mathrm{x} \in \Omega^- \\ 0 & \forall \mathrm{x} \in \Omega^+ \end{cases} \tag{2.1}$$

An illustration of a body with discontinuity path *S* is presented in Figure 2.6 where Γ_u and Γ_σ are the Ω boundaries subjected to the usual essential and natural boundary conditions, respectively, and obey three conditions:

$$\Gamma_u \cup \Gamma_\sigma = \partial\Omega, \quad \Gamma_u \cap \Gamma_\sigma = 0, \quad \Gamma_u \cap \Omega^h = 0 \tag{2.2}$$

S_h^+ and S_h^- are the two boundaries of the Ω_h^+ and Ω_h^- subdomains, which surround the *S* path. It is also assumed that a function $\varphi^h(\mathrm{x})$ is defined as:

$$\varphi^h(\mathrm{x}) = \begin{cases} 0 & \forall \mathrm{x} \in \Omega^- \setminus \Omega_h^- \\ 1 & \forall \mathrm{x} \in \Omega^+ \setminus \Omega_h^+ \end{cases} \tag{2.3}$$

In the work [Oli95] a unit jump function, which takes the zero value everywhere in Ω excluding Ω_h, was introduced:

$$M_S^h(\mathrm{x}) = H_S(\mathrm{x}) - \varphi^h(\mathrm{x}) \tag{2.4}$$

Such a function exhibits a jump across the discontinuity path *S*. An expression for the displacement field *u*(*x*, *t*) under a strong discontinuity condition on *S* is:

$$u(\mathrm{x},t) = \hat{u}(\mathrm{x},t) + M_S^h(\mathrm{x})[[u]](\mathrm{x},t) \tag{2.5}$$

where: $\hat{u}$ - the conventional part of the displacement field, [[*u*]](x, *t*) - displacement jump function.

A strain field is calculated based on the symmetric part of the gradient of the displacement field:

$$\varepsilon = (\nabla \mathrm{u})^S = \bar{\varepsilon} + \delta_S([[\mathrm{u}]] \times \mathrm{n})^S \tag{2.6}$$

where: $\bar{\varepsilon}$ – conventional part of the strain field, *S* – superscript denoting the symmetric part of the vector and δ_S - the Dirac delta function along *S* path.

Decomposition of the displacement field is illustrated in Figure 2.7.

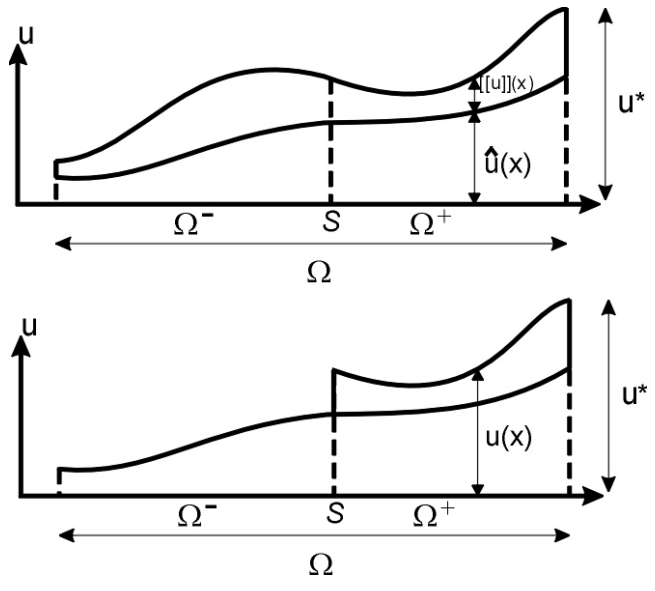

Figure 2.7. Illustration of the displacement field decomposition [Oli95].

Based on this knowledge [Oli95], a finite element approximation of the strong discontinuity problem is illustrated in Figure 2.8, where: l_e – length of a straight line in the element, n_e – the normal vector to S_e.

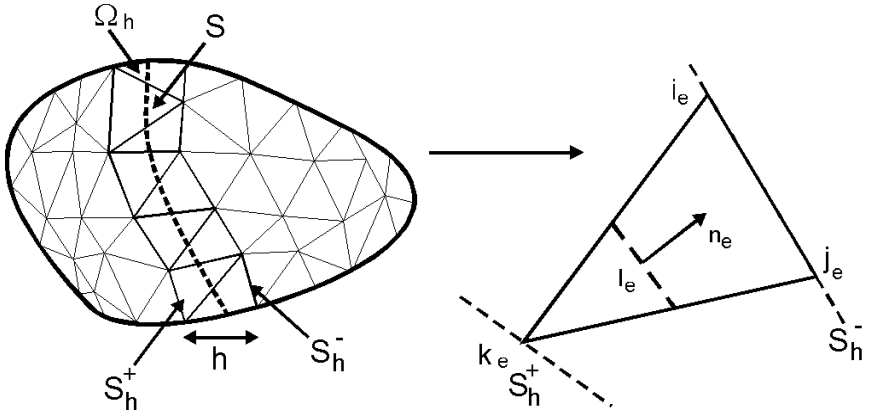

Figure 2.8. Illustration of the finite element approximation [Oli95].

By extending equation (2.5) to the whole boundary S, an approximation of the displacement field in the FE method is expressed as:

$$u^h(x,t) = \hat{u}^h(\mathrm{x},t) + \sum_{e=1}^{n_{el}} M_{Se}^h(\mathrm{x})[[u]]^h(t) \tag{2.7}$$

$$M_{Se}^h(\mathrm{x}) = H_{Se}(\mathrm{x}) - N_{ke}(\mathrm{x}) \tag{2.8}$$

where: $H_{Se}(\mathrm{x})$ – Heaviside function, N_{ke} – standard linear shape function of the k_e node, n_{el} – number of all finite elements in the mesh.
Equation (2.8) is illustrated [Oli95] in Figure 2.9:

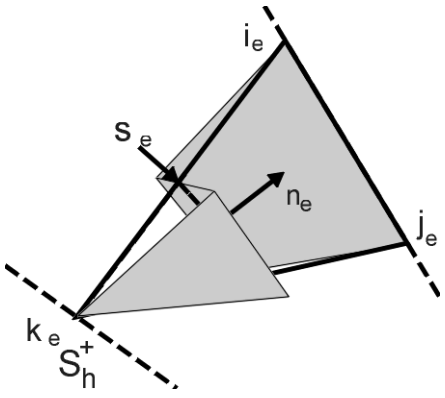

Figure 2.9. Illustration of the unit jump function finite element approximation [Oli95].

The strain field is then finally calculated as:

$$\varepsilon^h(\mathrm{x},t) = \left(\nabla \hat{\mathrm{u}}^h\right)^S + \sum_{e=1}^{n_{el}} \left(\nabla M_{Se}^h \times [[u]]^h(t)\right)^S \Rightarrow regular + enhanced \tag{2.9}$$

Based on this approach, interesting simulation results, including uniaxial tension or shear tests, are shown in [Arm95, Oli95]. However, an artificial method was used to trigger a discontinuity such as shear band formation. In [Oli95] the peak stress value of the upper element in the band was artificially reduced. The same procedure was used in [Arm95]. Therefore the initiation of strain localization is not a natural outcome of the processes taking place during deformation, which is the main disadvantage of methods involving enhanced finite elements. A different approach has been proposed by others [Pec98, Waj04]. The idea is not based on modified finite elements, as in [Oli95], but on creation of the modified flow rule, which is capable of including strain localization phenomena.

In the work [Pec98], the author defined a modified flow rule based on the assumption that the strain localization phenomenon is a multi scale problem. It appears as cooperative work of the micro shear bands and shear bands, which is in agreement with the theory described in [Ciz02b, Kor98]. The modified flow rule proposed in [Pec98] is expressed as follows:

$$d\dot{\varepsilon}_{ij} = \frac{3d\dot{\varepsilon}_i}{2(1-f_{MS})\sigma_p}\sigma_{ij} \tag{2.10}$$

where: $d\dot{\varepsilon}_i$ - equivalent strain rate increment, $\sigma_{ij}, d\dot{\varepsilon}_{ij}$ - stress and strain rate increment tensors, σ_p - equivalent stress value in the Huber-Mises-Hencky criterion, which is equal to the flow stress insensitive to the state of stress.

The main disadvantage of this approach is lack of flexibility when different plastometric tests are taken into account. The f_{MS} function has to be identified for a specific deformation test and cannot be generalized. The theoretical basis of this model is widely explained in the work [Pec98]. The commonly used expression for the f_{MS} function is defined as:

$$f_{\mathrm{MS}}(\varepsilon) = \frac{f_{\mathrm{MS0}}}{1+\exp(a-b\dot{\varepsilon}_i)} \tag{2.11}$$

where: a, b and f_{MSO} are coefficients determined from plastometric tests, $\dot{\varepsilon}_i$ – equivalent strain rate.

A slightly different approach to the strain localization problem was developed in [Waj04] and introduced into the FE code as a correction to the conventional flow rule. Analysis was performed for different plastometric tests, such as ring compression, uniaxial compression and plane strain channel die compression. Based on the inverse analysis [Sze02, Sze06] performed for those results, a correction coefficient ς was defined. The principal value of the strain rate tensor $\dot{\varepsilon}_2$ is the key parameter controlling the correction coefficient:

$$\varsigma = 1.25 - \frac{1}{2\pi}\arctan\left(10\frac{\dot{\varepsilon}_2}{\dot{\varepsilon}_i}\right) \tag{2.12}$$

where: $\dot{\varepsilon}_2$ - principal value of the strain rate tensor, $\dot{\varepsilon}_i$ - equivalent strain rate.

The coefficient presented in the form of equation (2.12) is used to modify the flow stress value calculated using the inverse analysis in the Levy-Mises flow rule:

$$\sigma_p = \frac{\sigma_f}{\varsigma} \tag{2.13}$$

where: σ_p - flow stress value in the Levy-Mises flow rule, σ_f - flow stress calculated based on the inverse analysis for a particular plastometric test.

The model [Pec98], as well as a similar approach of [Waj04], were used for simulation of the plain strain compression tests and have proven their capability for modeling strain localization phenomena during deformation. For evaluation purposes, the following norm has been used.

$$\|\mathbf{e}\| = \int_0^t \int_V \left(\hat{\sigma}_{ij}^r - \hat{\sigma}_{ij}^h\right)^T \left(\dot{\varepsilon}_{ij}^r - \dot{\varepsilon}_{ij}^h\right) dV dt \tag{2.14}$$

where: $\hat{\sigma}_{ij}^r, \hat{\sigma}_{ij}^h$ - vectors with the deviatoric part of the stress tensor components for the two solutions, $\dot{\varepsilon}_{ij}^r, \dot{\varepsilon}_{ij}^h$ - vectors with the strain rate tensor components for the two solutions, *r* – model with the f_{MS} function, *h* - model with the conventional flow rule.

Error $\|\mathbf{e}\|$ represents differences in plastic deformation energy dissipated in the material, calculated based on two solutions: with and without the modified flow rule. Results obtained based on equation (2.12) with the norm (2.14) are presented in Figure 2.10.

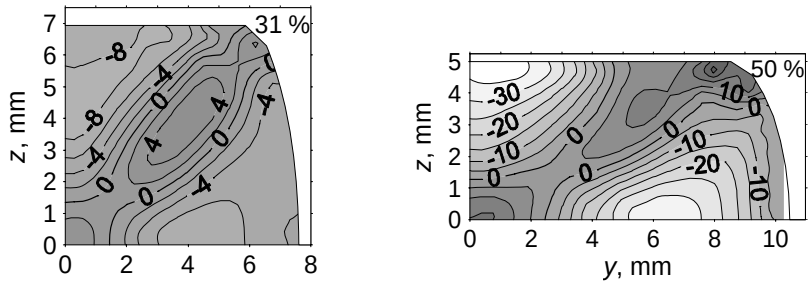

Figure 2.10. Distribution of the norm (2.14) at ¼ of the transverse section of the sample in the channel test.

Distribution of the norm (2.14) in the sample area reveals a relatively narrow band with positive values of $\|\mathbf{e}\|$ at the cross section, where a strain localization is observed during deformation. Positive values of the norm $\|\mathbf{e}\|$ indicate that more energy is dissipated in the material during deformation than in the model without the proposed correction. At the same time the integral of the norm 2.14 takes negative values, which proves that overall work is lower when correction is applied. All the above mentioned facts confirm that corrections proposed in [Pec98, Waj04] properly predict strain localization during simple deformation processes.

In order to put more light on the discussed approach, the Author of this work performed analysis of the strain localization phenomena during ring compression tests [Mad05b]. These tests were selected because the state of strains in ring compression vary depending on the friction coefficient. A short discussion of that work is presented in the next section. A series of FE simulations was conducted to analyze the ς coefficient (equation 2.12) behavior during ring compression tests performed to obtain $\varepsilon = 0.5$. Detailed information about dimensions and friction conditions are presented in Figure 2.11 and Tables 2.1 and 2.2.

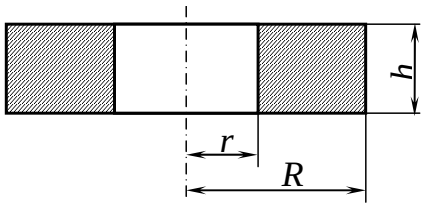

Figure 2.11. Ring compression sample with basic dimensions.

Table 2.1. Ring dimensions and friction coefficients used in the first set of simulations.

R, mm	10								
r, mm	3			5			7		
h, mm	4			6.7			10		
μ	0.03	0.08	0.15	0.03	0.08	0.15	0.03	0.08	0.15

Table 2.2. Ring dimensions and values of the friction coefficients used in the second set of simulations.

R/r	2								
h, mm	4			6.7			10		
μ	0.03	0.08	0.15	0.03	0.08	0.15	0.03	0.08	0.15

Results of analysis seem to support literature observations that the strain field in the sample depends on the friction and sample dimensions. When the friction coefficient and sample height are higher, material changes its deformation mode to plane strain compression, as shown in Figures 2.12 and 2.13.

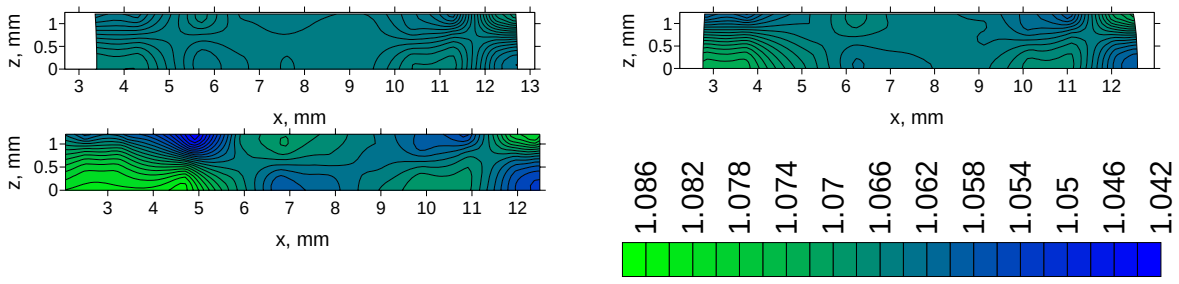

Figure 2.12. Sample (ϕ20×ϕ6×4 mm) cross section after deformation showing distribution of the ς coefficient defined by equation (2.12). Friction coefficients are $\mu = 0.03$, 0.08 and 0.15, respectively.

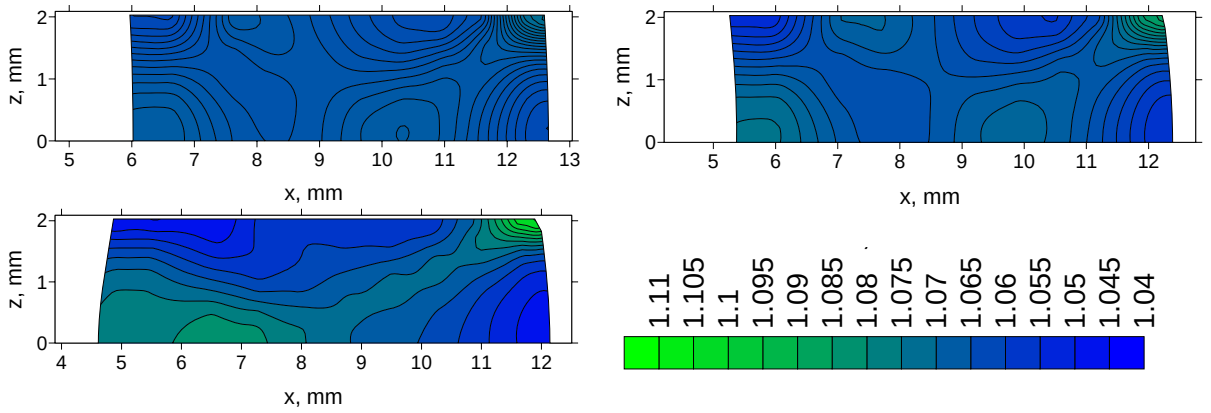

Figure 2.13. Sample (ϕ20xϕ10x6.7 mm) cross section after deformation showing distribution of the ς coefficient defined by equation (2.12). Friction coefficients are μ = 0.03, 0.08 and 0.15, respectively.

Furthermore, sensitivity analysis was performed based on the results obtained from simulation. Graphs showing behavior of the average ς coefficient value as a function of friction and radius r are presented in Figure 2.14.

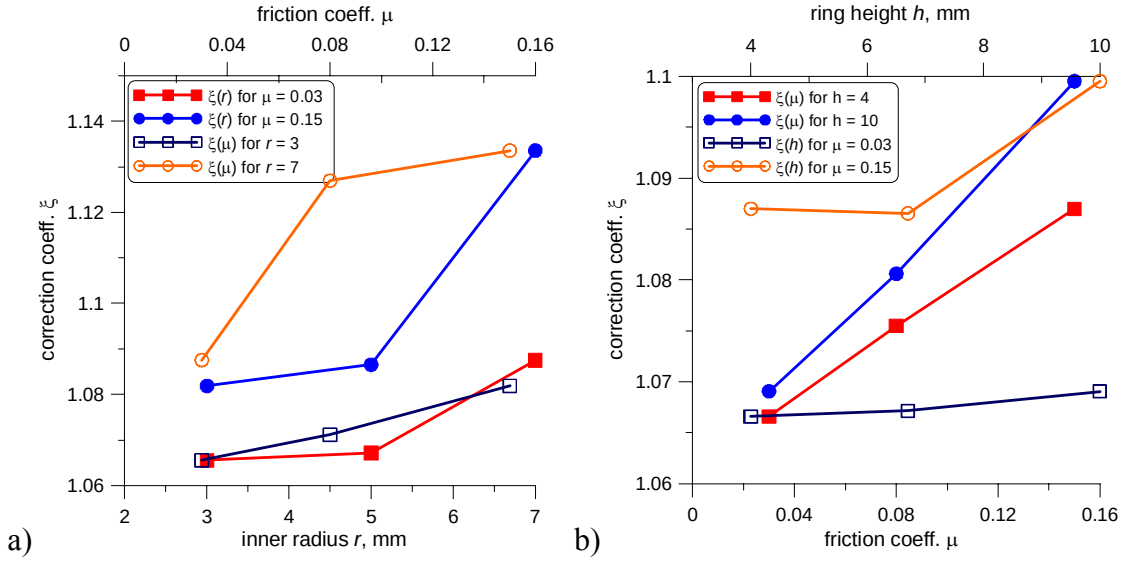

Figure 2.14. a) ς vs. μ and ς vs. r for the case when R = 10 mm and h/r = *const.* = 3/2. b) ς vs. μ and ς vs. h for the case when R = 10 mm and r = 5 mm.

It is clearly seen that values of the ς coefficient are higher when values of μ and r are higher, which indicates a change of the deformation mode to plane strain compression. A similar relationship can be observed for the case of increasing sample height h (Figure 2.14b).

Sensitivity analysis was performed according to the following equations:

$$\Phi_{\varsigma,\mu} = \frac{\mu}{\varsigma}\frac{d\varsigma}{d\mu}, \Phi_{\varsigma,r} = \frac{r}{\varsigma}\frac{d\varsigma}{dr} \tag{2.15}$$

The sensitivity parameter Φ is a weighted limit difference approximation of the derivative of the coefficient with respect to the selected variable μ or r.

Results of the analysis are presented in Figure 2.15. In general, an increase of the parameter sensitivity for increasing values of μ and r is observed; however, some exceptions are observed as well.

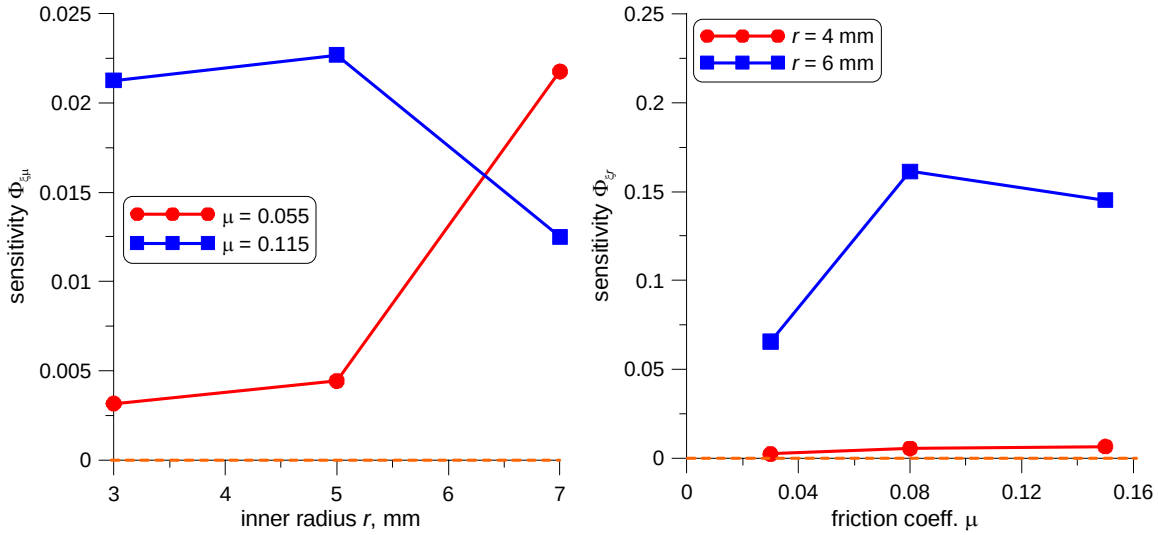

Figure 2.15. Sensitivity analysis of the ς parameter with respect to r and μ, respectively.

Similar analysis was performed for the set of samples presented in Table 2.2. Again change of the deformation mode to plane strain is observed when sample height and friction coefficient increase. Results of the performed simulations are presented in Figures 2.16 and 2.17.

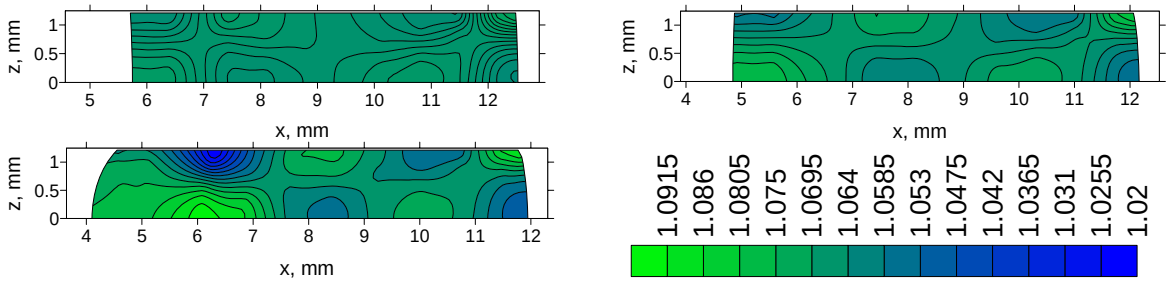

Figure 2.16. Sample (h = 4 mm) cross section after deformation showing distribution of the ς coefficient defined by equation (2.12). Friction coefficients are μ = 0.03, 0.08 and 0.15, respectively.

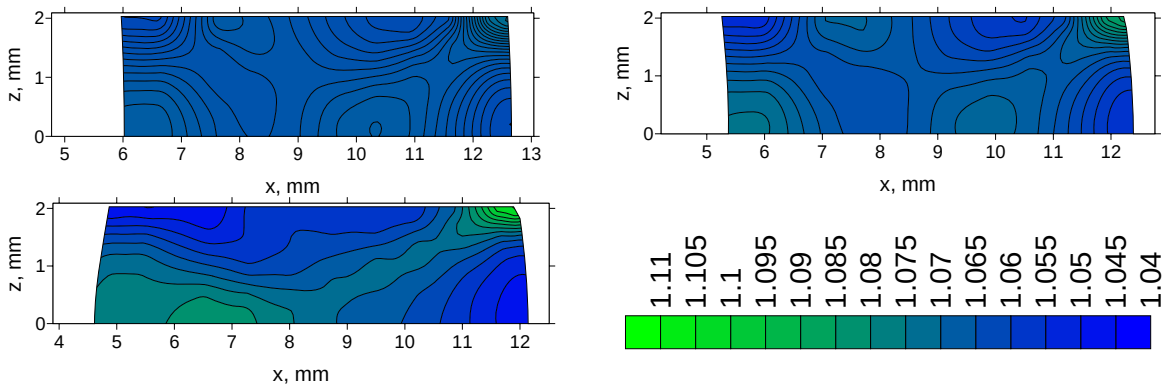

Figure 2.17. Sample (h = 6.7 mm) cross section after deformation showing distribution of the ς coefficient defined by equation (2.12). Friction coefficients are μ = 0.03, 0.08 and 0.15, respectively.

Sensitivity analysis was performed according to equations:

$$\Phi_{\varsigma,\mu} = \frac{\mu}{\varsigma}\frac{d\varsigma}{d\mu}, \Phi_{\varsigma,h} = \frac{h}{\varsigma}\frac{d\varsigma}{dh} \tag{2.16}$$

This analyzes reveals high sensitivity of the ς parameter with respect to changes in μ and h values, as shown in Figure 2.18.

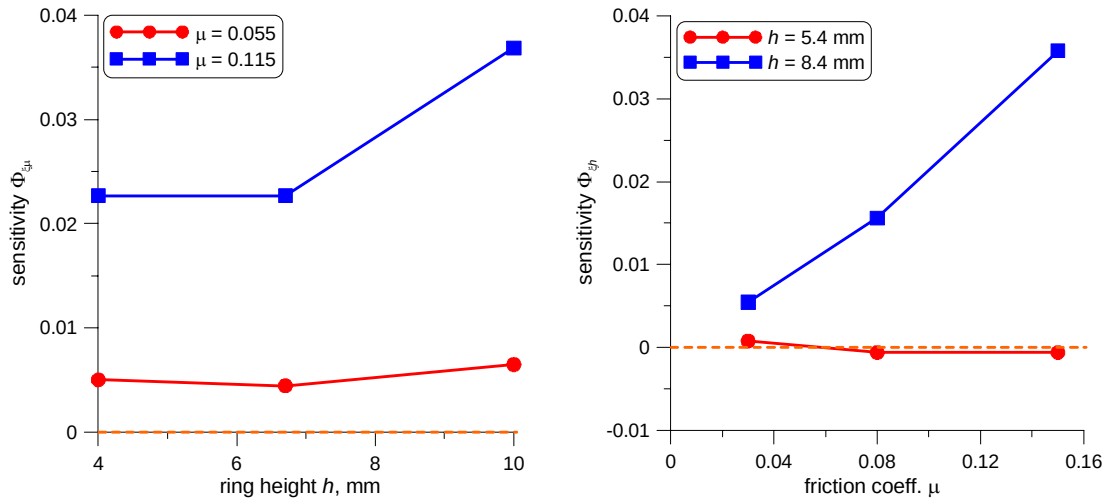

Figure 2.18. Sensitivity analysis of the ς parameter with respect to h and μ coefficients, respectively.

It has been shown that strain state in the sample influences the development of micro and macro shear bands. The Author confirmed that strain localization is higher when the deformation mode approaches a plane strain compression. This indicates that the model for strain localization developed in the work [Waj04] should be analyzed for processes under the plane strain deformation mode (i.e. channel die test). The presented analysis on strain localization in ring compression shows the significance of the work dedicated to shear

banding phenomena performed by scientists. It reveals how strain localization development can be modeled and controlled by changing the deformation conditions. Such analysis may be used to obtain a positive effect (i.e. load reduction during deformation) instead of a highly localized zone, which may lead to fracture initiation.

This preliminary work on ring compression inspired the Author of this work to further research strain localization phenomena and to analyze possibilities of creating a complex numerical model dedicated to this problem.

The presented work on ring compression, as well as results obtained in [Waj04, Pec98] describing experimental forces and calculated ones, reveal good predictive capabilities of the proposed models. This indicates that such an approach is efficient for particular plastometric tests. However, the presented models cannot be easily generalized to simulate complex industrial deformation operations. Lack of flexibility is one of the main disadvantages of the developed approaches. The other important problem is the discontinuous and stochastic character of processes leading to strain localization. It is very difficult to include such behavior in conventional models [Arm95, Oli95, Pec98, Waj04]. As previously stated, a model accounting for discontinuities in material is crucial for industry to design the most efficient deformation processes. All the above mentioned aspects are fundamental disadvantages of both approaches presented in [Pec98, Waj04], which also inspired the Author of the present work to explore other alternative possibilities of modeling shear band influence on materials deformation.

During last several years, research has been conducted, which focused on developing an alternative approach to the strain localization phenomena occurring during deformation. Interesting work was performed in [Li00] to avoid the problems with mesh influence during FE calculations accounting for strain localization. The author of [Li00] created a model based on one of the mesh free methods: the reproducing kernel particle method RKPM [Fri04]. Such methods are free of any nonphysical mesh behavior. Results obtained in the 2D and 3D cases support the general belief that mesh free methods will become more and more popular for solving many metallurgical problems. Another interesting series of works [Bal03, Mak00a, Mak00b, Mak01] includes processes occurring at the mezoscale and their influence on the macroscale. This was one of the first multi scale approaches based on the combination of continuous and discrete methods. Because of this, the theory described in [Bal03] is worth mentioning due to the subject of this literature review. A model capable of including the strain localization and fracture initiation was developed by Makarov and co-workers [Bal03]. Makarov in his earlier publications had already taken into account local values of the flow parameters at the mezo scale. They vary significantly from the average macroscopic data. Following this concept, slipping systems of the individual crystals and their activation under loading, nucleation of the shear bands, and initiation and propagation of structural elements rotation were included in the model. Due to the averaging process all the above mentioned phenomena are not taken into account in the macroscale simulation. Makarov combined the

advantages given by the continuous approach with the cellular automata CA [Neu66] method, which is capable of including shear band generation and development. Proper transition rules for the CA spaces used to control changes between the CA cells states (*plastic* and *elastic*) where than defined as shown in Figure 2.19.

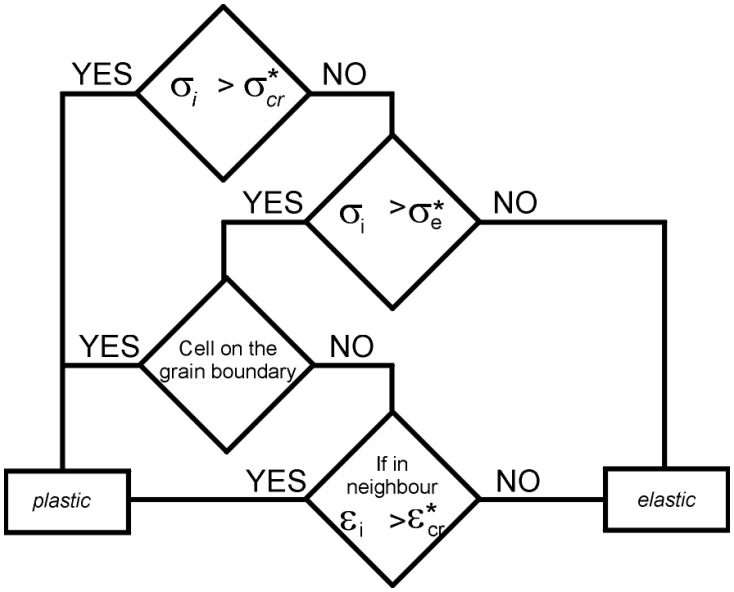

Figure 2.19. Illustration of the developed transition rules applied in the multi scale model for strain localization [Mak00a].

In works [Mak00a, Mak00b, Mak01] grain boundaries, inclusions and phase boundaries are sites for plastic shear initiation. A particular CA cell can change state to plastic when equivalent stress σ_i reaches critical value σ^*_{cr}, which varies for different microstructural features (e.g., grain boundary, internal region of a particular grain) or when a stress value is higher than the critical value of shear strength σ^*_e. A CA cell can also change state to plastic if equivalent strain ε_i in any neighboring cells reaches critical value ε^*_{cr}. In the case when these two transition rules are not fulfilled, a particular CA cell remains in an elastic state. The CA method has been added to the Finite Difference (FD) method in the process of creating a multi scale model of strain localization phenomena. Results of the analysis presented in Figure 2.20 and in [Mak00a, Mak00b, Mak01] confirm the predictive capabilities given by such an alternative approach to the strain localization phenomena. Lack of results obtained for the real deformation process is the main disadvantage of the developed model.

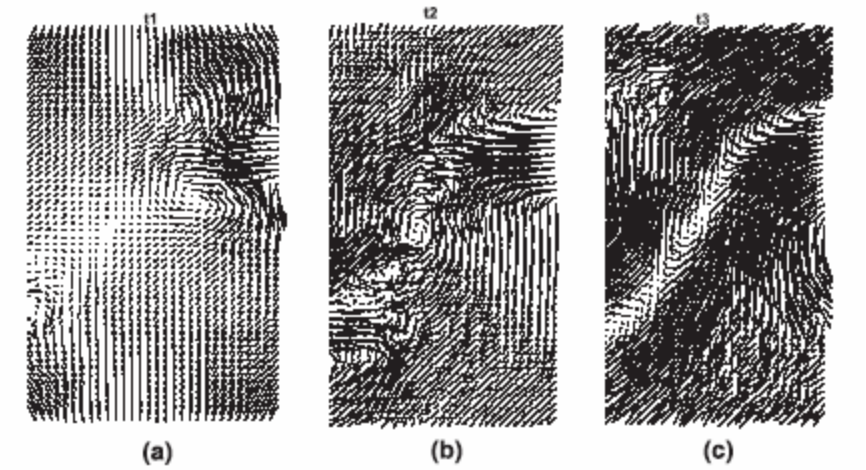

Figure 2.20. Velocity fields of the elastic-plastic deformed specimen under tension loading for different times [Mak00a].

According to these literature findings it is clear that strain localization is interesting from the experimental and theoretical points of view. Despite many attempts to solve the problem of strain localization in materials and create a numerical model describing this phenomenon, there still lacks a complex multi scale numerical model. As previously discussed, a numerical method based on the discrete approach gives a possibility to describe discontinuous and stochastic processes such as the development of micro shear and shear bands in materials. Several different attempts to create multi scale models based on these discrete methods can be found in literature.

This is the reason why the Author of this work decided to create a numerical model based on the Cellular Automata method, which is capable of handling calculations at the microscale, mezoscale and macroscale and of replicating the real multi scale nature of strain localization mechanisms. The multi scale CAFE method provides possibilities not only to describe material behavior in different scales, but also to predict the stochastic and discontinuous nature of these processes. A short review of these alternative multi scale simulation methods based on the Cellular Automata method is described in the next Chapter.

3. Cellular Automata (CA)

The cellular automata technique was originally developed in the early 1960s by Janos Von Neumann [Neu66] to simulate the behavior of discrete and complex systems. Initially the limited capabilities of computers were the main obstacle in the development of this method. However, this technique is becoming more popular due to the continuously increasing computational power of computers [Con76, Wol94]. Nowadays the CA method is used in different scientific areas, from biology and chemistry to solid phase physics and electronics [Kul00, Mal03]. During the last few years the CA method has also been applied to model material behavior during thermomechanical processing. This includes modeling of static and dynamic recrystallization behavior, precipitate coarsening, grain boundary migration and solidification [Bau96, Bur04, Dav95, Dav97, Dav99, Din01, Din 02, Din04, Gan99, Gan94, Gaw04, Gaw05a, Gaw05b, Goe05, Goe98, Goe98b, Gui04, Hes91, Kro01, Kro03, Kro01b, Kro02, Kro05, Mad04, Mar99, Muk04, Qia04, Raa98, Raa02, Raa04, Raa05, Rol01, Svy05, Yu05]. A more detailed review of the CA method application is described in another Author's work [Gaw05c].

The main idea of the cellular automata technique is to divide a specific part of the material into one-, two-, or three-dimensional lattices of finite cells. Each cell in this space is called a cellular automaton, while the lattice of the cells is known as cellular automata space. Each cell in this CA space is surrounded by neighbors, which affect one another. Neighborhoods can be specified in one-, two-, and three-dimensional spaces (Figure 3.1).

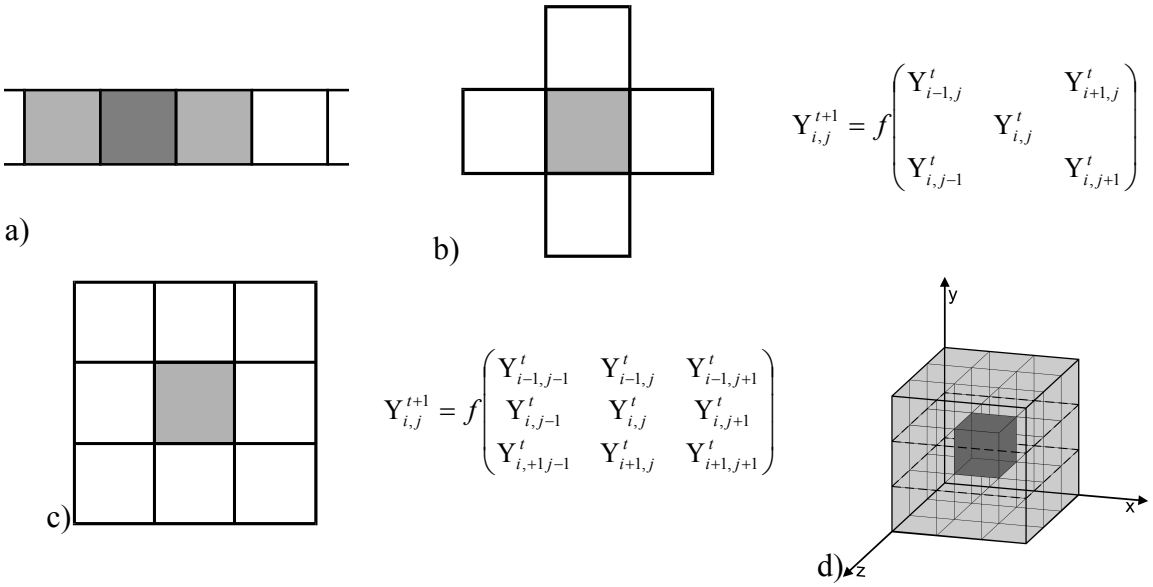

Figure 3.1. Examples of CA neighborhoods in (a) 1D, (b) 2D Von Neumann, (c) 2D Moore, and (d) 3D space.

The most popular examples are the von Neumann and the Moore neighborhoods (Figure 3.1), where in the 2D case each cell is surrounded by either four or eight neighboring cells, respectively. However, several examples of alternative CA neighborhoods such as extended Moore, hexagonal or irregular neighborhood [Gaw05b, Jan04, Ter03, Wol94] can be found in literature.

The cells interactions within the CA space are based on the knowledge defined while studying a particular phenomenon. In every time step, the state of each cell in the lattice is determined by the previous states of its neighbors and the cell itself by a set of precisely defined transition rules f:

$$Y_i^{t+1} = f\left(Y_j^t\right) \text{ where } j \in N(i) \tag{3.1}$$

where: $N(i)$ – surrounding of the i^{th} cell, Y_i – state of the i^{th} cell.

Since the transition rules control the cells behavior during calculations (i.e., during the deformation process), the proper definition of these rules in the process of designing a CA model critically affects the accuracy of this approach.

When the advantages provided by this method are combined with the advantages of macroscale analysis – Finite Element method, a complete multi scale analysis model such as the CAFE (Cellular Automata Finite Element) model is established.

3.1. Cellular Automata Finite Element (CAFE)

The combination of the microscale technique – Cellular Automata with the commonly used macroscale method – Finite Element represents a truly multi scale approach for describing material behavior under loading conditions. The analysis based on the CAFE method is more complex and accurate in comparison with conventional methods. A short review of developed multi scale models based on the CAFE approach is presented below.

The first work based on the application of the CAFE model to material science is presented in [Gan94]. A CAFE method is applied to model the development of dendritic structures appearing during solidification processes. In this approach a differential equation describing the temperature field is solved using the FE model. However a CA method was applied to model microstructure development and heat generation during solidification. In this work [Gan94] the sample area is overlaid by the two separate meshes: FE and CA one. The square CA space is defined to be much thicker than the FE triangle mesh. Proper transition rules between spaces are defined as well.

Further works on this subject dealing with a 3D multi scale approach are presented in [Gan99]. Introduction of the multi scale approach in the microscale is the innovation presented in that work. CA cells were divided into “blocks” and “user windows”. Such windows are created by grouping several adjacent blocks. A schematic illustration of this approach is presented in Figure 3.2.

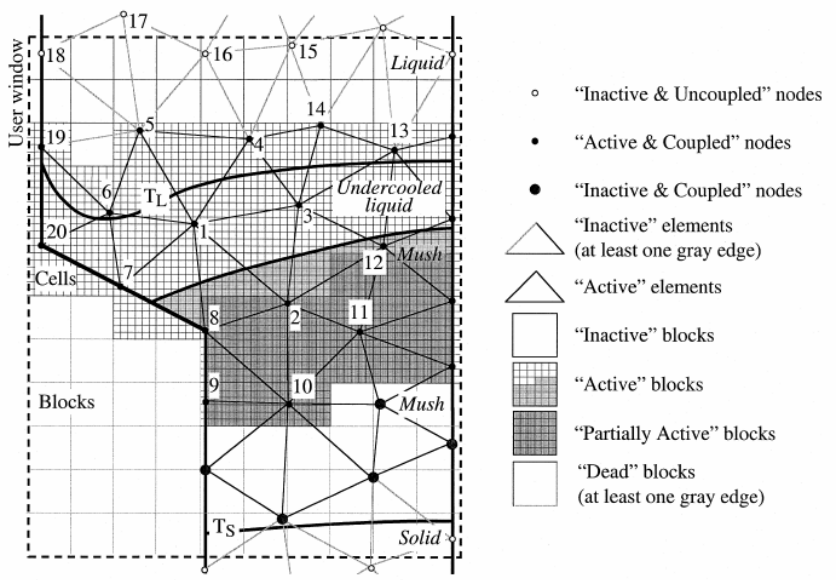

Figure 3.2. Illustration of the multi scale CAFE approach proposed in [Gan99].

The capability of predicting the changes in texture during solidification is one of the advantages of the proposed model. In [Gan01] a comparison with the experimental results was performed using the Electron Back Scattered Diffraction (EBSD) technique. The material microstructure obtained from CAFE simulation, as well as pole figures, agree well with the experimental results.

All the assumptions made in [Gan99] were verified in [Gui04] by comparing the results of the CAFE method with results obtained using the Front Tracking (FT) method. Overestimation of the heat released during solidification is mentioned as the weak point of the proposed CAFE method, and several solutions to avoid this problem have been proposed. A similar model was proposed in [Bur04] but related only to microscale behavior.

In the papers by [Bey00, Bey02, Das02a, Das02b] a multi scale CAFE method was applied to model fracture phenomena occurring during various forming processes. The developed model has capabilities to predict microstructure development, as well as crack propagation in the surface layer during rolling operations. Microstructural features such as grain boundaries, other phase particles and grain interior are included during simulation in the CA spaces. The developed algorithm incorporates three major steps: development of the primary microstructure, flow of the macroscopic parameters obtained from the FE simulation to the CA mezoscale and, finally, back propagation of the parameters calculated in the CA spaces to the FE model. In the developed approach information from integration points in the FE mesh is send to the underlying CA spaces.

An approach proposed by [Dav97] was used to create a primary microstructure for further calculations. A random generation of the CA cells, which can become nuclei for newly formed grains, is performed in the CA space area. In the following steps, the nuclei growth process is simulated according to the equation:

$$v_{gb} = C\ t^{-n} \tag{3.2}$$

where: v_{gb} – grain growth velocity, C – constant, n – exponent equal to 0.6.

The nuclei growth is blocked in the case of impingement of the two developing grains. Such an approach is commonly used in scientific literature; however, grain size in the final microstructure depends on the initial number of nuclei in the CA space, which is a disadvantage of this approach.

The developed microstructure model in the CA mezoscale was then combined with the FE code. CA spaces are not rigorously attached to a particular gauss point, and they can deform during rolling, which is an immense advantage of the developed model. A triangulation method described in [Das02a] is used to obtain information about CA cells associated with an integration point. This is a crucial part of the developed model because efficient information exchange between mezo- and macroscales leads to the establishment of a truly multi scale CAFE model.

In the next step of simulation, information about stress and temperature field, achieved from each gauss point in the FE mesh, is used as input data for the CA calculation of the microstructure development and crack propagation. The strain for the microscale is calculated on the basis of FE strain according to equation:

$$\varepsilon_{CA}^{i} = f^{i}\varepsilon_{FE}^{j} \tag{3.3}$$

where: f – scaling factor related to a particular feature in a material: (f = 1 for the grain interior, 1.2 for the grain boundary, 3 for the inclusions), i – CA space number, j – integration point number (e.g., j = 1, 2, 3, 4 when four integration points are considered).

In the developed model, dislocation density during deformation is calculated with respect to the creation and annihilation phenomena of dislocations with opposite signs:

$$d\rho_{CA}^{i} = d\rho_{CA}^{+} - d\rho_{CA}^{-} = \left(\frac{M}{bl} - A\rho_{CA}^{i}\exp\frac{Q}{RT}\right)d\varepsilon_{CA}^{i} \tag{3.4}$$

where: ρ – dislocation density, M – constant, Q – activation energy, R – gas constant, T – temperature, b – Burgers vector, l – mean free path of dislocation.

During the CA calculations, detailed information about dislocation density in the CA cells with respect to fracture development and dynamic recrystallization is obtained. The author in [Das02a] assumed that when a critical value of dislocation density is reached, a particular cell can become nucleus for dynamic recrystallization, and its dislocation density is set to the reference level. A similar mechanism is commonly used during modeling of dynamic recrystallization [Gaw05b, Mad04].

Despite modeling of microstructure development, crack propagation in surface layers has been included in the CAFE model as well. Critical value of strain is a main parameter in this part of the model. If strain in a CA cell is higher than the defined critical value, such a

cell changes its state and is considered as a cell with a crack. The Final Failure Index (FFI), which describes the ratio of CA cells with cracks to the overall number of CA cells in the CA space, increases during crack propagation. The modified Moore neighborhood was implemented to obtain more realistic behavior for the modeling of crack propagation; however, such an artificial interaction in the CA model should be avoided.

The establishment of a complete back propagation between CA and FE is the last stage in the developed model. Information calculated in the CA spaces is agglomerated to acquire one macroscopic value, which is later send to a particular Gauss point in the FE mesh. Calculation of the stress value may be an example of such an agglomeration:

$$\sigma_{FE}^{j} = \sigma_0 + \alpha G(T) b \sqrt{\rho_{FE}^{j}} \tag{3.5}$$

$$\rho_{FE}^{j} = \frac{\sum_{i=1}^{N_A} \rho_{CA}^{i}}{N_{CA}} \tag{3.6}$$

where: α – constant, $G(T)$ – shear modulus, N_{CA} – number of CA cells associated with one integration Gauss point.

Stiffness in the macroscale is modified while modeling crack propagation in the surface layer, as well:

$$E^{t+1}(T) = E^{t}(T)\left(1 - FFI^{t}\right) \tag{3.7}$$

where: t – time.

Such a modification in the element stiffness solves the problem with removing destroyed FE elements from the mesh. Parallel to the calculation of element stiffness, calculation of friction and heat transfer coefficients based on the crack propagation information, obtained at the microscale, is performed at the macroscale according to the following equations:

$$\mu_{CAFE} = \mu_{lower} + FFI\left(\mu_{upper} - \mu_{lower}\right) \tag{3.8}$$

$$\eta_{CAFE} = \eta_{lower} + FFI\left(\eta_{upper} - \eta_{lower}\right) \tag{3.9}$$

where: indices *upper* and *lower* describe lower and upper limit of the coefficient, μ - friction coefficient, η - heat transfer coefficient.

Agglomeration of the microscale parameters into one macroscale value is an approach frequently used by researchers dealing with multi scale models based on the CAFE method to describe thermomechanical processes.

The developed model [Das02a] is an example of complex multi scale model capable of predicting phenomena related to microstructure development, as well as crack propagation in the surface layer (Figure 3.3). Such a detailed analysis makes possible a detailed explanation of the processes that occur during rolling.

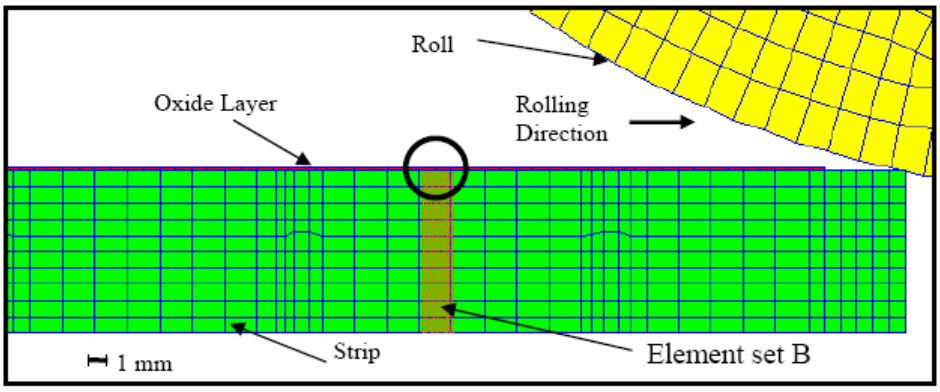

Figure 3.3. Illustration of the rolling process set up for the multi scale CAFE approach [Das02b].

The previously described model [Das02b] became an inspiration for the CAFE model created by Shterenlikht [Sch03]. This approach describes propagation of the brittle and ductile fracture in material during the Charpy test (Figure 3.4). A short description of this approach is presented below.

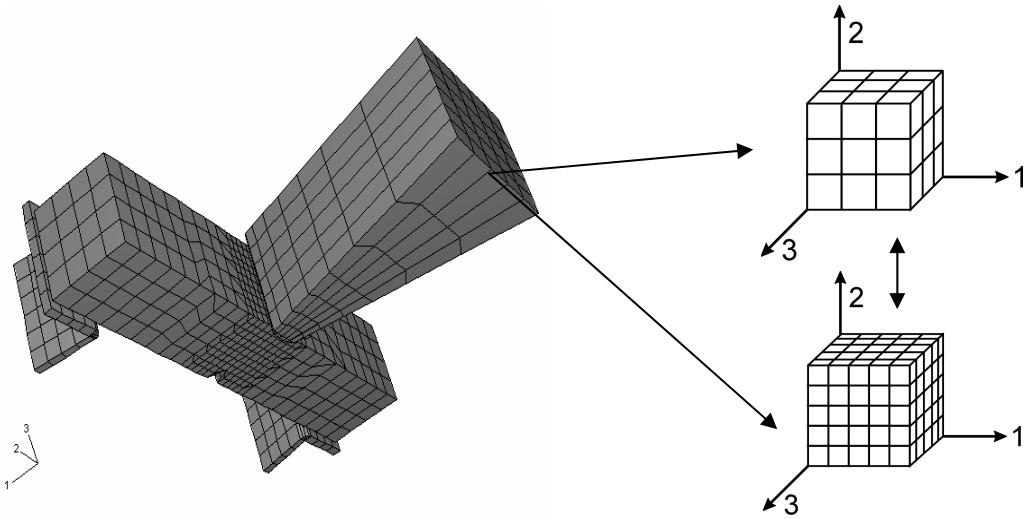

Figure 3.4. Finite element model of the Charpy test created for CAFE simulation with the ductile CA space and brittle CA space [Sch03].

Brittle and ductile fractures are two phenomena, which take place at two different scales in material during deformation. The length scale of the brittle fracture is 0.005-0.05 mm, and the scale for the ductile fracture is 0.1-0.5 mm. The small scales of these phenomena cause difficulties in modeling. In conventional FE modeling, the brittle and ductile fractures are modeled using the size of the finite elements connected to the size of a computational cell [How00, She98], which is between the length scales of the two fracture mechanisms. To achieve greater accuracy, a large number of FE elements is used, which leads

to high computational costs. However, the CAFE approach does not have such limitations. In the created model, two separate 3D cellular automata spaces are introduced (Figure 3.4). The first one, called ductile space, describes phenomena connected with ductile fracture. The second one, called brittle space, describes phenomena connected with brittle fracture during the Charpy test. Because sizes of brittle and ductile fractures differ, a different number and different dimensions of the CA cells are used in those CA spaces.

In [Sch03] each cell in ductile and brittle spaces is described by several state variables. The most important one is the variable that refers to the state of a particular cell. It is assumed that in ductile CA space each cell can be in two different states: *alive* or *dead*. For this case, a proper transition rule, which describes real material behavior during deformation, is defined to control ductile fracture initiation and propagation. Changes between the states *alive* and *dead* are due to equation:

$$\mathrm{Y}_{m(D)}(t_{i+1}) = \begin{cases} alive \Leftrightarrow \beta_m(t_{i+1}) < \beta_{cr} \\ dead \end{cases} \tag{3.10}$$

where: $\mathrm{Y}_{m(D)}(t_{i+1})$ – state of the m^{th} cell from the ductile space at the t+1 time step, β – damage variable calculated from the Rousselier [Rou89, Sch03] model describing the ductile fracture [Sch03], t – time step.

The same analysis was performed for brittle CA space, although the situation concerning this CA space is more complex. Each cell in the automata is described by four different states: *alive*, *aliveC*, *deadD*, *deadB*. *AliveC* is a special cell containing crack carbide. It is assumed that a cell in the state *AliveC* is a precursor of the initiation of brittle crack in the material. State *deadB* refers to the selected cell, which died according to the brittle mode, and *deadD* represents a cell that died according to the ductile transition rules (3.10). These states are related to mapping operations, which take place during the calculations and are used for information exchange between brittle and ductile CA spaces. The transitions among the states in brittle CA space are controlled by a set of transition rules defined as:

$$\mathrm{Y}_{m(B)}(t_{i+1}) = \begin{cases} deadB \Leftrightarrow A \\ \mathrm{Y}_{m(B)}(t_i) \end{cases} \text{ where:}$$

$$A = \sigma_m(t_i) > \sigma_F \wedge \left\{ \begin{cases} \mathrm{Y}_{m(B)}(t_i) = aliveC \vee \\ \left(\begin{bmatrix} \mathrm{Y}^m_{l(B)}(t_i) = deadB \vee \\ \mathrm{Y}^m_{l(B)}(t_i) = deadD \end{bmatrix} \wedge \left| \alpha_r^m - \alpha_r^l \right| < \theta_F \right) \end{cases} \right\} \tag{3.11}$$

where**:** $\mathrm{Y}_{m(B)}(t_{i+1})$ – state of the m^{th} cell from the *brittle* space at the t_{i+1} time step, σ_I – maximum value of the principal stress, σ_F – fracture stress, α_r – disorientation angle, θ_F – critical value of the disorientation angle.

In [Sch03] cellular automata spaces are connected to single Gauss point in each 3D element via the ABAQUS user defined VUMAT procedure. From the FE solver, information

about macroscopic parameters such as stress and strain is sent to cellular automata and is distributed along the CA spaces. The transition rules (3.10) and (3.11) operate during each time step. As a result of calculations in the CA spaces, information about brittle and ductile fracture propagation is returned to the FE solver according to the FE-CA mapping functions. The transition rule between the FE solver and CA solver is defined as follows: whenever a specific part of the dead cell in one of the CA spaces exceeds a declared critical value, then a particular FE element is removed from the FE mesh during further calculations in the next time step. A full description of this CAFE model can be found in [Sch03]. A typical result obtained from this model is shown in Figure 3.5.

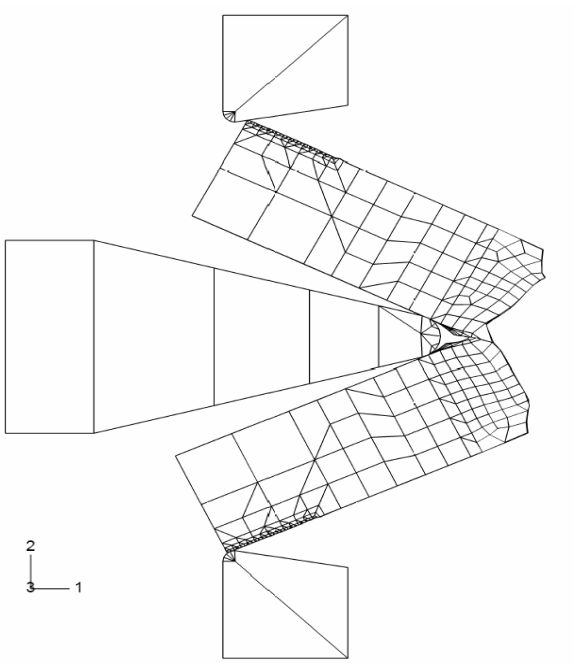

Figure 3.5. Final result of CAFE simulation obtained after deformation [Sch03].

The major advantage of this approach is a significant reduction in the computing time when compared to conventional FE models. This reduction is attributed to the lower number of FE elements.

The ability to modeling discontinuous and stochastic phenomena, which occur during material deformation, is another advantage of the CAFE model over conventional FE models. This is the reason why the multi scale approaches based on the combination of microscale models based on the cellular automata technique with macroscale methods (i.e. finite element or finite difference) are used to deal with processes appearing during material deformation.

Another example of such an application is modeling of strain localization phenomena, which often lead to material failure under loading conditions. Because of the subject of this PhD thesis, which is the creation of a model describing processes that lead to localization, these phenomena are particularly important for the Author. Due to the discontinuous and multi scale nature of processes leading to strain localization, conventional model fail to

describe them properly. An interesting approach to model strain localization phenomena was presented earlier in Chapter 2 [Mak00].

Phase transformation modeling is another area in which methods based on the combination of the Finite Element method with Cellular Automata are applied. In [Lan05] a detailed description of the developed model is presented; however, the reported idea of the cellular automata – finite element model is different than presented previously in [Bey00, Bey02, Das02a, Das02b, Gan99, Gan01, Mak00a, Mak00b, Mak01]. The cellular automata model was created independently of the finite element model, which is a simplification of the CAFE approach because the back propagation step between the micro- and macroscales in each time step is crucial. The information flow between scales is one of the main advantages of the CAFE method when compared to conventional approaches.

In the work [Lan05] the FE method was used to simulate hot compression test of the C-Mn steel. An area of the sample was limited to a few grains to reduce calculation time because several finite elements are applied to describe each particular grain. The amount of energy accumulated during deformation, as well as grain crystallographic orientation, is obtained from the FE model and used as input data for the CA calculations of the austenite-ferrite phase transformation process after deformation. A schematic of the proposed model is presented in Figure 3.6.

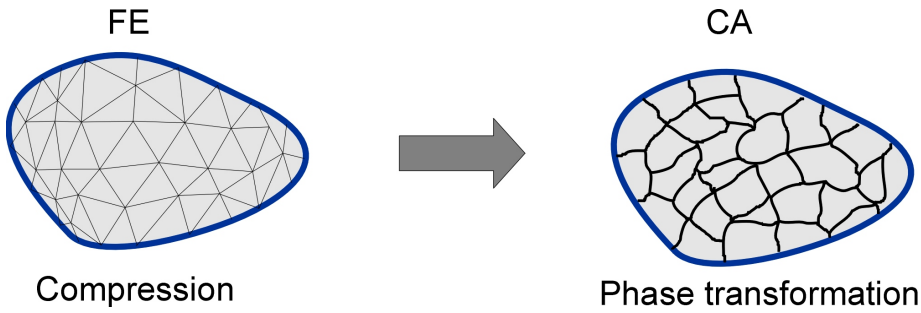

Figure 3.6. Information flow in the multi scale model applied to the ferrite-austenitic phase transformation simulation [Lan05].

Hexagonal neighborhood is used to describe microstructure in the CA space. Internal variables for each CA cell are defined as follows: ferrite nuclei crystallographic orientation; value of the accumulated energy; ferrite, austenite or α-γ phase; carbon concentration and ferrite volume fraction in the particular cell.

The author of [Lan05] assumed that ferrite grain nuclei appear on the austenite grain boundary. Carbon from ferrite grains migrates to the α-γ phase, and energy accumulated in the ferrite CA cell is reset to zero. Carbon diffusion between the ferrite and austenite phases is established according to analytical model [Lan05]. Additionally, when ferrite volume fraction in the particular α-γ phase cell reaches the value of one, the cell changes its state to a ferrite CA cell and all the neighboring cells become α-γ phase CA cells. Carbon migrates from the

ferrite cell to the neighboring cells in this case. All these described transition rules have been created to replicate real material behavior under phase transformation conditions.

Information from the FE model is sent to the CA space only once during the calculation and is used to establish material initial conditions for the CA simulations, so there is no back propagation effect between scales.

The described CAFE models reveal elevated capabilities of the multi scale CAFE approach for modeling of various metallurgical processes.

The literature review performed by the Author shows that the strain localization problem is a truly multi scale phenomenon. Micro shear and shear band development are two processes, which take place at different scales, but at the same time they depend on one other. Additionally, the stochastic and discontinuous nature of these processes was clearly stated in Chapter 2. All these facts result in difficulties in the creation of a numerical model supporting research on strain localization. Based on the knowledge from Chapter 3, it seems that the multi scale CAFE method should be an efficient method to create an alternative approach to describe strain localization phenomena. Models based on the CAFE method are multi scale approaches, which include phenomena taking place at different scales in the material, such as the initiation and development of micro shear and shear bands during various forming processes. This multi scale nature is a limiting factor of the FE approach, in which the size of the FE elements is between the scales of these two processes, which in the end leads to inaccurate results. The CAFE approach is free of this limitation regarding these two scales because two cellular automata spaces representing the material behavior at the micro- and mezoscale are introduced and are attached to the finite element code, which handles the calculation of material behavior at the macroscopic scale. The CAFE approach also has the capability to model discontinuous and stochastic processes leading to strain localization development. This was the main limitation of the conventional strain localization models described in Chapter 2. Based on the literature knowledge described in Chapters 2 and 3, the Author of this work decided to create a multi scale CAFE model capable of replicating real processes, which lead to strain localization. A detailed discussion about the developed model is presented in the following chapters.

4. Aim of the Work

As was shown in Chapter 2, for over thirty years scientists have investigated the problem of modeling strain localization in materials during deformation. Several numerical approaches have been applied to create a model capable of strain localization modeling, but none of them has been completely successful. When strain localization is not precisely controlled during deformation, instead of lowering the loads it can be a precursor of fracture and material failure. Therefore development of a numerical model which supports theoretical analysis is important from both the scientific and industrial point of view.

All the preliminary research performed by the Author [Mad04, Mad05a, Mad05c, Mad05d, Mad06a, Mad06b], as well as research presented in Chapter 3 as a literature review, have shown that: *the multi scale CAFE method should be an efficient method for modeling of strain localization development in the material subjected to plastic deformation in real industrial processes.* It is expected that proper definition of transition rules in the CAFE model, which are based on experimental, literature and researchers knowledge as presented in the literature review, will allow the model to avoid the limitations observed in the conventional methods discussed in Chapter 2.

To support this statement, several major goals of the research were defined as follows:

- Development of the proper algorithm dedicated to the multi scale CA model, composed of two different CA spaces.
- Collection of the most important literature and experimental facts about physical aspects of micro shear and shear band formation and their interactions. This is a crucial step in the creation of the CAFE model. The CAFE method can be classified as one of the artificial intelligence methods. However, methods such as Artificial Neural Networks (ANN) are based on arbitrary - not controlled by the knowledge of researchers - selection of the transfer function with proper weights. Weights are selected without interference from the researcher. Selection is only due to the criterion of the best convergence between ANN output and global material response. Instead of this arbitrary method in the CAFE method proper selection of knowledge from gathered information will allow creation of transition rules in the CA spaces that are strongly related to the physics of the particular investigated processes. Transition rules are designed in a sensible way, and they play a key role in the CAFE simulation because they create the capability of proper reproduction of phenomena leading to strain localization.
- The main aim of this work is the development of the multi scale CAFE model, which predicts micro shear band and shear band development in two different scales at the same time during the deformation process. These two processes are responsible for the

development and propagation of strain localization during deformation. Both the stochastic and discontinuous nature of those phenomena can be taken into account in the multi scale CAFE model.

- Creation of the flexible CAFE approach. Contrary to the model described in Chapter 2, the developed model should be more universal and efficient. It should be applicable not only to simple plastometric tests (e.g., ring compression, channel die test), but it should also be easily applicable to real industrial processes such as rolling or extrusion.
- Experimental analysis of strain localization phenomenon is another crucial stage of this work. Based on the obtained experimental results, proper validation of the CAFE model can be performed.
- Creation of a final version of the strain localization CAFE model with corrected transition rules and application of the developed CAFE model to simulate various industrial processes.

Work performed to realize these goals is described in the following chapters:

Chapter 5 contains a detailed description of the developed cellular automata model dedicated to the prediction of micro shear and shear band development. The defined internal variables and transition rules created based on the knowledge gathered in Chapter 2 for these two spaces are described. Information flow between scales in this model is explained. Difficulties with attaching CA spaces to the FE mesh and proposed solutions to the remeshing problem are discussed in this Chapter as well. Initial results of the CAFE simulations are presented because they show in a natural way how the model was improved to satisfy all the goals of this work.

Results obtained with the completed CAFE model are presented in Chapter 6. Various applications to real industrial processes and comparison with selected experimental results from literature are demonstrated. Additionally, in each case the CAFE results are compared to the results obtained from the conventional FE approach to show limitations of the latter model.

A series of experiments involving flat rolling were performed to support the correctness of the results obtained from the CAFE model. A description of the material and experimental procedure is given in Chapter 7. Selected results showing the development of micro shear and shear bands leading to strain localization at the macroscale are demonstrated.

Finally, Chapter 8 is dedicated to the conclusions regarding the developed model, and advantages and disadvantages of the model are discussed. Following this discussion, this work concludes with a plan for further model improvements and possibilities for future application.

5. Multi Scale Model for Strain Localization

5.1. Description of the Developed Multi Scale CAFE Model

The CAFE model developed by the Author is a real multi scale approach, including phenomena which take place at two scales within material: micro shear bands initiate in the microscale, while shear bands appear in the mezoscale. For conventional FE approaches modeling of the phenomena, which appear simultaneously in different scales, is difficult. Usually the size of the FE elements is selected to be between scales of these two phenomena, which negatively influences the accuracy. In the CAFE approach this is not an issue because two CA spaces can be introduced for these two phenomena: one describing development of micro shear bands and the other describing development of shear bands.

5.1.1. CA Model

Following the concept presented in [Sch03], the cell sizes in each CA space were linked to the specific microstructure feature relevant to micro shear and shear band phenomena, respectively. A schematic illustration of the multi scale nature of the CAFE model is presented in Figure 5.1.

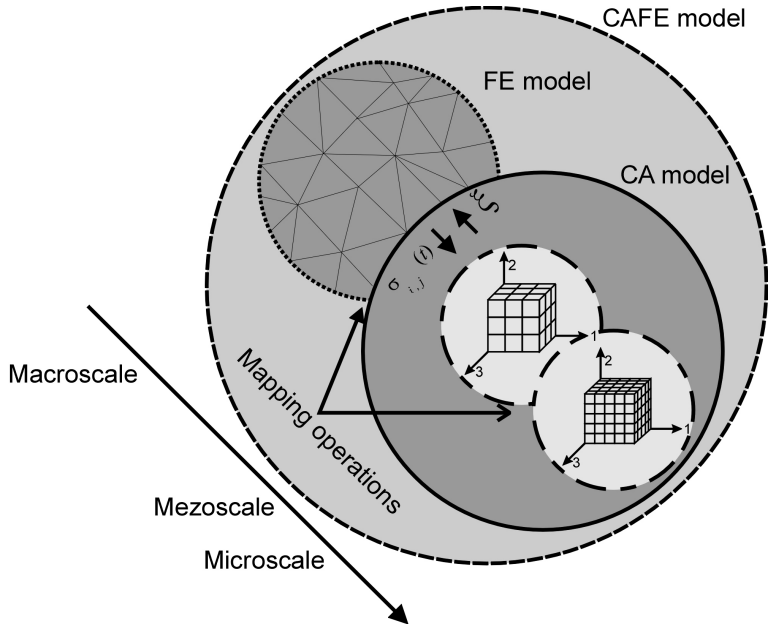

Figure 5.1. Illustration of the information flow between macro-, mezo-, and microscales of the CAFE model, where: $\sigma_{i,j}$ – stress tensor, ξ – correction coefficient.

During the calculations a three dimensional Moore neighborhood was selected for both CA spaces. The Author decided to create a 3D CA model. To obtain space continuity, commonly used 3D periodic boundary conditions were introduced. For simplicity, only the 2D representation of the boundary conditions is presented in Figure 5.2.

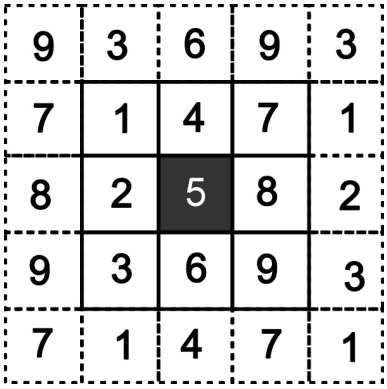

Figure 5.2. Periodic boundary condition in the 2D case.

Before the CA spaces could be attached to each particular integration point, they have to be defined. Internal variables describing particular cells were created, and transition rules controlling changes between cell states were defined. The same procedure was performed for both MSB and SB spaces. The Author of this work placed high emphasis on defining CA spaces capable of simulating micro shear band and shear band processes. In the CAFE model both CA spaces, micro shear band space (MSB space) and shear band space (SB space), are characterized by several state variables, which describe each particular cell, as well as by a set of transition rules defined specifically for those spaces.

After analysis of the physical aspects of the micro shear band development and propagation, which was discussed in detail in Chapter 2, the following internal variables were introduced to the MSB space:

- *state* – representing the state of each particular cell,
- *old state* – representing the state of each particular cell in the previous time step,
- *rotation angle* – describing the cell rotation,
- *old rotation angle* – describing the cell rotation in the previous time step,
- *tau_h*, *tau_e* – critical values of stress necessary to initiate a hard and an easy slip system in the material.

These internal variables were designed to replicate the most important aspects of micro shear banding theories. Each particular MSB cell can be in two possible states: *activeMSB* and *nonactiveMSB*. The *activeMSB* state indicates that micro shear band was initiated and developed in a particular cell, while the *nonactiveMSB* state refers to the surrounding matrix. The remaining variables are more related to micro shear band phenomena rather than to CA theory. At the beginning of the deformation process, critical values of variables describing

stresses are generated for each MSB cell using the gauss distribution function (Figure 5.3). This process is responsible for initiation of the hard and easy slip systems in the MSB space. This operation was designed to relate the initiation of micro shear bands with the hard slip systems described in [Kor98]. This approach is used instead of explicit inclusion of the grain orientations.

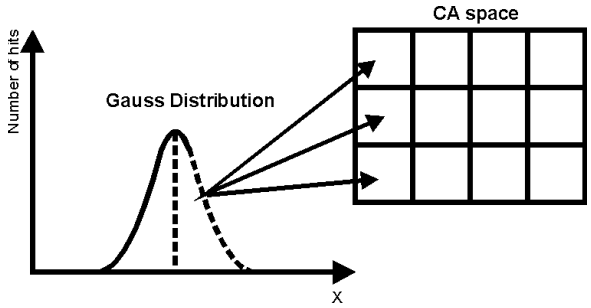

Figure 5.3. Illustration of the critical stresses *tau_h* and *tau_e* generation.

From the artificial intelligence point of view, transition rules are crucial because they control changes between two states in the MSB space. They were defined by the Author based on experimental knowledge gathered in Chapter 2. The transition rules, which provide a change from the *nonactiveMSB* to *activeMSB* state, are described by:

$$\mathrm{Y}_{m(MSB)}(t_{i+1}) = \begin{cases} activeMSB \Leftrightarrow A \\ \mathrm{Y}_{m(MSB)}(t_i) \end{cases} \quad \text{where: } \begin{array}{l} A = \left(\sigma_i > \tau_{hard}\right) \vee \\ \left(\mathrm{Y}^{m}_{l(MSB)} = activeMSB \wedge \right. \\ \left. \theta^{rot}_{m} - \theta^{rot}_{l} > \theta^{rot} \right) \end{array} \tag{5.1}$$

where: $\mathrm{Y}_{m(MSB)}(t_{i+1})$ – state of the m^{th} cell from the MSB space at the t_{i+1} time step, σ_i - equivalent stress value obtained from the FE program, τ_{hard} - critical value for initiation of the hard slip system, $\mathrm{Y}^{m}_{l(MSB)}$ - state of the l^{th} neighbor of the m^{th} cell from the MSB space, θ^{rot} - rotation angle.

Each particular cell can change its state to *activeMSB* when an equivalent stress value obtained from the FE code exceeds a critical value necessary to initiate a hard slip system in the material. This part of the transition rule is a description of a statement from Chapter 2, which is that characteristic feature of a micro shear band is that a shear employs a system different than an easy slip system in the material [Kor98]. The second part of the designed transition rule describes change in a cell state when a neighbor of this particular cell in the previous time step was *activeMSB* and the rotation angle between those two cells goes above a critical value. This rule was created based on the idea proposed in [Ciz02a] and presented in Figures 2.2 and 2.3. Generally, all the proposed internal variables, as well as transition rules, were defined to match as closely as possible the micro shear banding mechanisms described in Chapter 2. This process illustrates the idea of intelligent creation of transition rules, which replicate real material processes.

Similar analysis was performed for the SB space. After detailed analysis of the gathered knowledge regarding shear band phenomenon and its multi scale nature, each cell in the SB space can be described by the designed internal variables:

- *state* – representing the state of each particular cell,
- *old state* – representing the state of each particular cell in the previous time step,
- *MSB_fraction* α_{MSB_fr} – describing the fraction of micro shear bands in the SB cell.
- *old MSB_fraction* α_{MSB_fr} – describing the fraction of micro shear bands in the SB cell in the previous time step.

Values of the α_{MSB_fr} parameter are in the range $\langle 0,1 \rangle$, where 0 means that there are no micro shear bands in a particular SB cell and 1 means that the whole cell is filled with micro shear bands. Based on this, the Author introduced three possible states of the SB cells: *activeSB, nonactiveSB* and *activeMSB.* The *activeSB* state refers to a cell in which a shear band appears. The *nonactiveSB* state is used to describe the surrounding matrix. The *activeMSB* state refers to an SB cell in which micro shear bands — but not shear bands — are observed. The Author created the *activeMSB* state and α_{MSB_fr} parameter as natural outcomes from the claims described in Chapter 2 that shear bands develop on the basis of previously formed micro shear bands [Kor98]. This indicates that the development of shear bands in the SB space is dependent on the development of micro shear bands in the first CA space - MSB space. This multi scale character is well visible in Figure 2.1. To replicate this hierarchical character of shear band formation, proper mapping functions had to be designed and created to perform information exchange between the two CA spaces (Figure 5.4).

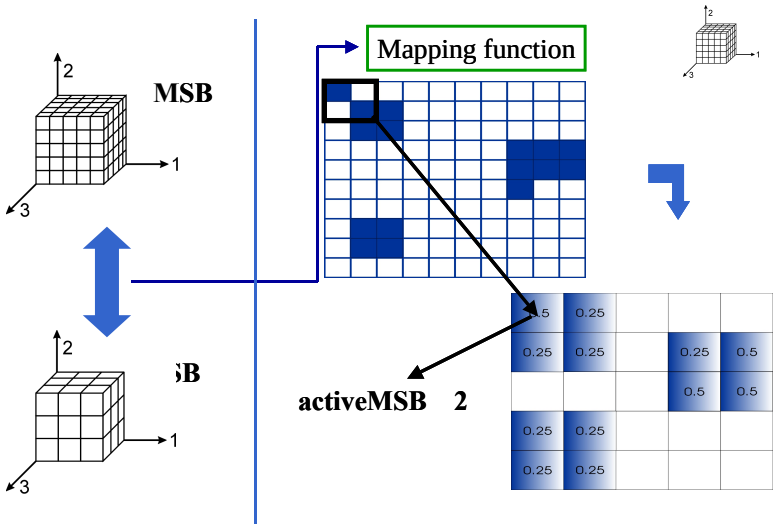

Figure 5.4. Illustration of the designed mapping functions defined between MSB and SB CA spaces to replicate the hierarchical character of strain localization phenomena described in Chapter 2.

The designed mapping functions are key parameters in the multi scale approach. They control information flow from the mezo- to microscale, as well as from the micro- to mezoscale. Such feedback between microstructural behavior features is one of the main advantages of the proposed CAFE approach because it allows the model to replicate the real nature of the strain localization problem described in Chapter 2. In the model, the Author assumed that when a number of cells in the *activeMSB* state in the MSB space related to one SB cell exceeds a certain critical value, such an SB cell can change its state to *activeMSB*. This cell is considered as a cell in the SB space in the area where micro shear bands develop. This is a natural consequence from the experimental observations from Chapter 2 [Kor86, Kor98]. Such an information exchange is not only from MSB to SB space, but also from SB to MSB space.

Algorithms capable of taking into account the relationship between the modeled phenomena in two CA spaces were designed, and a set of transition rules were created for the SB space. Again the Author created transition rules to match theories and observations of shear band formation:

$$\mathrm{Y}_{m(SB)}(t_{i+1}) = \begin{cases} activeSB \Leftrightarrow A \\ \mathrm{Y}_{m(SB)}(t_i) \end{cases} \quad \text{where:} \quad \begin{aligned} A = & \begin{pmatrix} \mathrm{Y}_{m(SB)}(t_i) = activeMSB \wedge \\ \alpha_m(t_i) > \alpha_{cr} \end{pmatrix} \\ \vee & \begin{pmatrix} \mathrm{Y}^{m}_{l(SB)}(t_i) = activeMSB \wedge \\ \alpha^{m}_{MSB\_fr}(t_i) > \alpha^{cr}_{MSB\_fr} \end{pmatrix} \\ \vee & \left(\mathrm{Y}^{m}_{l(SB)}(t_i) = activeSB\right) \end{aligned} \tag{5.2}$$

where: $\mathrm{Y}_{m(SB)}(t_{i+1})$ – state of the m^{th} cell from the SB space at the t_{i+1} time step, $\mathrm{Y}^{m}_{l(SB)}$ - state of the l^{th} neighbor of the m^{th} cell from the SB space.

An SB cell can change its state to *activeSB* whenever this particular cell in the previous time step was *activeMSB* and an *MSB_fraction* exceeds the critical value or else whenever a neighbor of this cell in the previous time step was *activeMSB* and also when the *MSB_fraction* exceeds critical value. The third transition rule is related to shear band propagation throughout the material. A cell can change state to *activeSB* when a neighbor of this cell in the previous time step was in the *activeSB* state.

To make the idea of the CAFE model clear it must be emphasized that the presented rules for MSB and SB spaces are directly related to the knowledge regarding the micro shear and shear band phenomena presented in Chapter 2 [Boc03, Ciz02a, Kor98]. In contrast to the rules for transition between elastic and plastic deformation described in [Mak00a], in this work transition rules describe processes occurring in the plastic region of deformation. In [Ciz02a] the author claims that micro shear bands develop through the formation of slip domains, which are discrete cells aligned along the band propagation direction. The misorientation angles between these cells and the surrounding matrix increase during the deformation process. They form narrow bands that afterward become thicker due to the

formation of new cells. This process is connected with micro stress field generation during the rotation of the previously formed cells. Finally, micro shear bands, which are composed of cells with significant misorientation with respect to the surrounding matrix, appear at larger strains. This statement from Chapter 2 (Figures 2.2, 2.3 and 2.4) is directly included in the second part of the MSB transition rule (5.1) and is related to the *rotation angle* internal variable (Figure 2.4). Furthermore in Chapter 2 it is stated that the development of micro shear bands is due to employing a coarse slip system in the grain [Kor98]. This was a motivation for the first part of transition rule (5.1) controlled by the *tau_h* value, which is necessary to initiate the hard slip system in the material. The theory by [Kor98] describes micro shear band and shear band phenomena as two processes taking place in two different scales in materials at the same time. Micro shear bands are usually related to one particular grain or several adjacent grains, while shear bands cross grains with no respect to their orientation (Figures 2.1 and 2.5). This behavior is replicated by the transition rule for the SB space. Development of shear bands is connected with micro shear bands clustering in the material. To replicate these interactions, proper mapping functions described in Figure 5.4 were defined, and the *activeMSB* state in the SB space was created.

Based on the information described above, it is clear that the idea of CA is to take into account experimental facts and include them in transition rules created for specific spaces (i.e. MSB and SB spaces). This makes a detailed literature review, experimental observation and researchers expertise extremely important during the creation of the CAFE method.

After creation of the internal variables and transition rules, the CA spaces are defined and are ready to be attached to the macroscale simulation method. Information about the occurrence of micro shear and shear bands is exchanged not only between the CA spaces during each time step according to the defined mapping operations. The key parameter of the CAFE model is the relationship between the FE part and the CA spaces. In each time increment, information about the stress tensor is sent from the finite element solver to the MSB space, where development of micro shear bands is calculated according to (5.1). After the information exchange between the CA spaces, the transition rules for the SB space (5.2) are introduced, and propagation of the shear band is modeled. Based on information supplied by the CA spaces, an equivalent stress σ_p^{CA} is calculated and is used to obtain the correction coefficient ξ:

$$\xi = \frac{\sigma_p^{CA}}{\sigma_p} \tag{5.3}$$

This coefficient is returned to the FE program and is used to modify the flow stress for each particular integration point in the next step of FE calculations:

$$\sigma_p \Leftarrow \xi \sigma_p\left(\varepsilon, \dot{\varepsilon}, T\right) \tag{5.4}$$

where: σ_p - flow stress, which does not account for the influence of micro shear bands and shear bands, ξ - correction coefficient, ε - strain, $\dot{\varepsilon}$ - strain rate, *T*- temperature.

The presented CA model was then implemented by the Author using the C++ programming language and can be attached with the FE code to establish the multi scale strain localization CAFE model. The CAFE model was used during the simulations described in the following part of the work.

5.1.2. FE Model

Forge2 code with the viscoplastic flow rule [Che98] was used in the FE model. It is based on the Norton-Hoff law in the form:

$$\sigma_{ij} = 2K\left(\sqrt{3}\dot{\varepsilon}_i\right)^{m-1}\dot{\varepsilon}_{ij} \tag{5.5}$$

where: σ_{ij} – deviatoric stress tensor, $\dot{\varepsilon}_{ij}$ – strain rate tensor, $\dot{\varepsilon}_i$ – effective strain rate, *K* – the material consistency, *m* – strain rate sensitivity coefficient. *K* is the material parameter used in Forge2, which represents the flow stress and is calculated from the following equation:

$$K = \frac{\sigma_p}{\sqrt{3}\left(\sqrt{3}\dot{\varepsilon}_i\right)^m} \tag{5.6}$$

These equations lead to the Levy-Mises flow rule, which describes the relationship between deviatoric stress and the strain rate tensor:

$$\sigma_{ij} = \frac{2}{3}\frac{\sigma_p}{\dot{\varepsilon}_i}\dot{\varepsilon}_{ij} \tag{5.7}$$

In the developed CAFE model the flow stress in equation (5.7) is modified by the correction coefficient ξ calculated from equation 5.3 on the basis of simulations performed in the CA spaces, according to equations (5.1) and (5.2), as well as according to flow information presented in Figures 5.1 and 5.4.

5.2. Initial Simulations Based on the Developed CAFE Approach

Initial calculations using the CAFE model for strain localization were performed for simple compression in the channel die test. The channel die test is a variation of the plane strain compression test, in which material flow is constrained by an additional tool (Figure 5.5). Since the plane strain condition fosters initiation of shear bands, this test is commonly used to investigate strain localization [Ana80, Har88, Nou80, Nou86]. The yielding in plane strain deformation is due to shear and is not affected by the presence of hydrostatic stress:

$$\sigma_1 - \sigma_3 = 2k \tag{5.8}$$

where: σ_1, σ_3 – principal stresses of the Cauchy stress tensor, *k* – yield stress in pure shear.

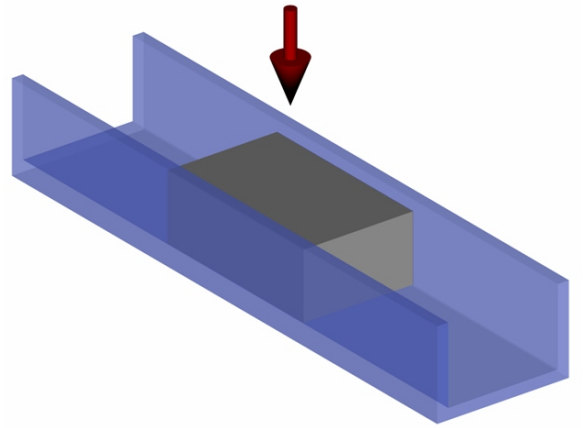

Figure 5.5. Schematic illustration of the channel die test.

It is commonly expected that the strain distribution field in the channel die tests reflects the metallurgical cross.

As was shown in Figure 5.1, the two CA spaces are attached to each FE gauss integration point in the present solution. During the first step, calculations are performed using the FE approach with the conventional flow stress model. In Figure 5.6 a comparison is made with the results obtained from the CAFE model.

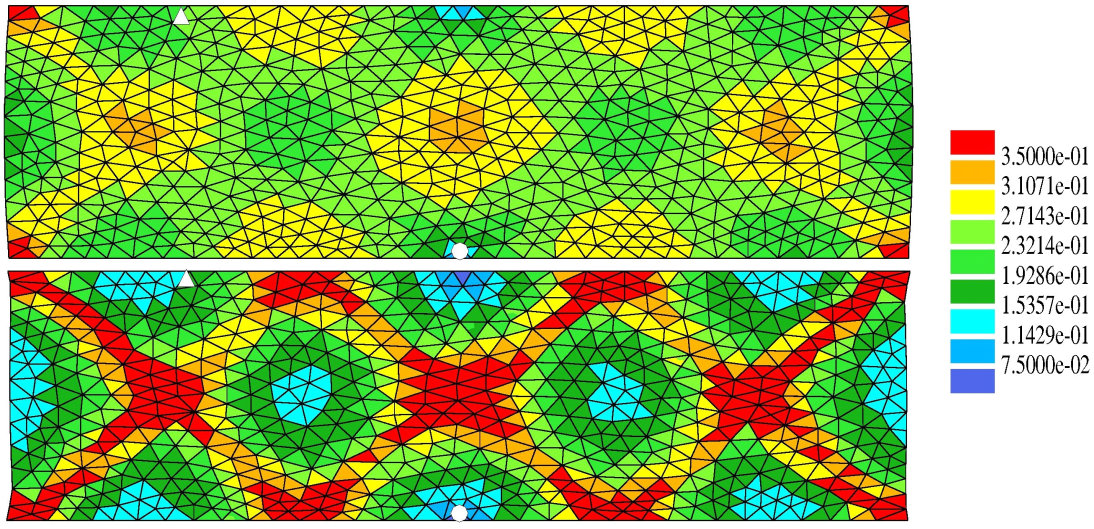

Figure 5.6. Strain distribution during the channel die tests calculated by the conventional FE model (top) and the CAFE model (bottom).

Analysis of the plots shows clearly that strain localization in the bands appears when the CAFE approach is applied. This is due to the development of micro shear and shear bands at the micro- and mezoscales, respectively, during the deformation process. These initial results show that the first goal of this work has been obtained. A proper tool capable of simulating strain localization phenomena has been developed based on the multi scale CAFE approach.

However, one of the major goals related to model flexibility is still not solved. During simulation, remeshing in the FE mesh is applied, and it is observed that the CAFE model gives inaccurate results. The problem concerning remeshing in the multi scale CAFE approach is the subject of the following part of this Chapter.

5.3. Remeshing Problem in the Multi Scale Approach

As previously described, the change between states using the predefined transition rules is due to the states of the neighbors of a selected cell and the cell itself in the previous time step. According to this essential definition of the CA method, the number of CA spaces in the CAFE approach has to remain constant during the calculations. This leads to problems whenever a complicated scheme of deformation or sample shapes are introduced and remeshing is necessary. As a consequence, the number of mesh nodes and gauss points may change, and a problem with attaching the CA spaces to the FE nodes appears (Figure 5.7). This leads to a lack of information from the microscale in some regions of the FE mesh, which eventually leads to inaccurate results.

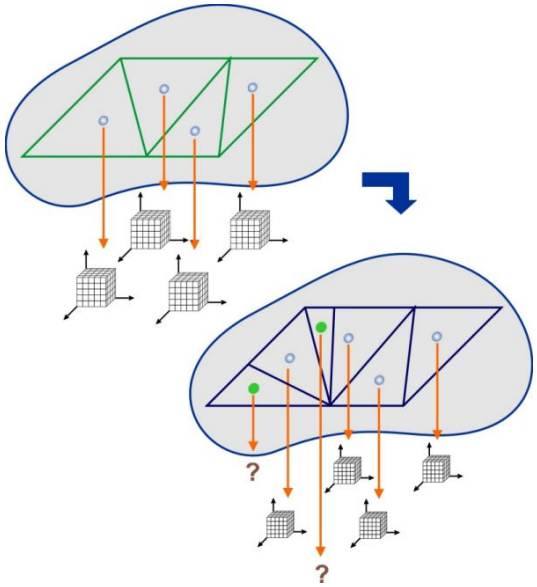

Figure 5.7. Remeshing problem – after the remeshing operation, there is a lack of information from several points in the material without underlying CA spaces.

To solve the problem with the remeshing operation, an alternative set of points is introduced in the domain. The idea of this solution is presented in [Mad05c], and a more detailed description is given below. In the proposed solution the number of so-called CA points remains constant during the deformation process, and a number of underlying CA spaces attached to each CA point also remains constant. This approach enables the remeshing process and a change in the number of nodes in the initial mesh. In each time step, an

exchange of information between the FE and CA points is performed using the interpolation technique based on the Smoothed Particle Hydrodynamics (SPH) method [Liu03].

The simplest approach would be to use a traditional interpolation procedure. However, when a large deformation occurs in the material, more accurate results are obtained using the SPH method, as this method is less sensitive to large displacements of FE nodes. The essential basis of the SPH method is described briefly below.

5.3.1. Smoothed Particle Hydrodynamics (SPH)

The Smoothed Particle Hydrodynamics method was developed by [Gin77, Luc77] to simulate astrophysical processes and was later improved upon by [Mon83, Mon05]. A breakthrough was made by the author of [Lib90] when this method was extended and gained the capability of working with the stress tensor. This allowed application of the SPH method to metallurgical problems. In this sense, SPH is a meshless Lagrangian method that uses a pseudo particle approach to calculate the field variables. The concept of an integral representation of a function $f(x)$ at location x in the SPH method is given by an integral of multiplication of the product of the function and an appropriate kernel function W_{ij}:

$$f(x) \cong \int f(x_j) W_{ij}(x - x_j, h_{sm}) dx \tag{5.9}$$

If we assume that a value of the $f(x)$ function is known only in a finite set of discrete points, equation (5.9) can be written by a summation:

$$\langle f(x) \rangle \cong \sum_{j=1}^{N} f(x_j) W_{ij}(x - x_j, h_{sm}) V_j \tag{5.10}$$

where: the $\langle\ \rangle$ – kernel approximation, W_{ij} – kernel function, h_{sm} – smoothing length of the support domain, V_j – volume associated with the j^{th} particle.

Equation (5.10) is a basic equation used in the SPH method. The value of the function at a point x is calculated by a summation of the contribution from a set of the neighboring particles (j subscript) from the support domain of the x particle (Figure 5.8). The Kernel function plays an important role, and due to that this function should meet several consistency conditions to be applicable in the SPH method [Liu03,Vig04]. The most important one is the *unity condition* expressed as follows:

$$\int W(x - x', h_{sm}) dx' = 1 \tag{5.11}$$

where: x – particle position, x' – particle neighbor position.

The second condition corresponds to the situation when the smoothing length h_{sm} approaches zero. The *delta function property* is then described by:

$$\lim_{h \to 0} W(x - x', h_{sm}) = \delta(x - x') \tag{5.12}$$

The third condition is related to the support domain of the smoothing function. Based on the idea of the *compact condition*, integration is localized only at the area of the support domain:

$$W\left(x-x^{'},h_{sm}\right)=0 \Leftrightarrow \left|x-x^{'}\right|>\kappa h_{sm} \tag{5.13}$$

where: κ – constant defining the support domain for the smoothing function.

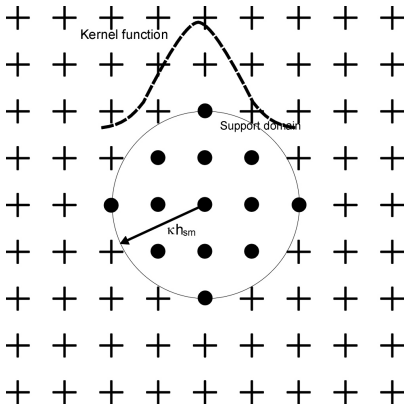

Figure 5.8. Support domain of the i^{th} particle.

Several Kernel functions, which meet these requirements, can be defined. The most commonly used examples of Kernel functions are:

- B – spline [Mon05]:

$$W\left(R,h_{sm}\right)=\alpha_d\begin{cases}\frac{2}{3}-R^2+\frac{1}{2}R^3 & 0\le R<1\\ \frac{1}{6}\left(2-R\right)^3 & 1\le R<2\\ 0 & R\ge 2\end{cases} \tag{5.14}$$

For one two and three dimensional space, $\alpha_d = 1/h_{sm}$, $15/7\pi\ h_{sm}{}^2$, $3/2\pi\ h_{sm}{}^3$, d – dimension.

- The quintic spline [Liu03]:

$$W\left(R,h_{sm}\right)=\alpha_d\begin{cases}\left(3-R\right)^5-6\left(2-R\right)^5+15\left(1-R\right)^5 & 0\le R<1\\ \left(3-R\right)^5-6\left(2-R\right)^5 & 1\le R<2\\ \left(3-R\right)^5 & 2\le R<3\\ 0 & R>3\end{cases} \tag{5.15}$$

For one, two and three dimensional space, $\alpha_d = 120/\ h_{sm}$, $7/478\pi\ h_{sm}{}^2$, $3/359\pi\ h_{sm}{}^3$

- Gaussian kernel:

$$W\left(R,h_{sm}\right)=\frac{1}{h_{sm}\sqrt{\pi}}e^{-R^2} \tag{5.16}$$

where: $R = \frac{\left| x - x_j \right|}{h_{sm}}$.

A detailed explanation of this method, including a description of essential boundary conditions, integration or parallelization and related problems can be found in the works [Fri04, Li00, Mon05]. In the work [Bon00], the author describes an approach leading to a modification of the SPH method to achieve more accurate numerical results. An additional factor in the Kernel function [Bon00] is introduced to achieve better consistency:

$$\hat{W}_{ij}(x) = W_{ij}(x)\alpha(x)\left[1 + \boldsymbol{\beta}(x)\left(x - x_j\right)\right] \tag{5.17}$$

where: $\hat{W}$ - corrected Kernel function.

Parameters $\alpha(x)$ and $\boldsymbol{\beta}(x)$ have to be evaluated by enforcing the consistency conditions described previously. Based on this they are written in the following form:

$$\beta(x) = \left[\sum_{j=1}^{N} V_j\left(x - x_j\right) \times \left(x - x_j\right) W_{ij}(x)\right]^{-1} \sum_{j=1}^{N} V_j\left(x_j - x\right) W_{ij}(x) \tag{5.18}$$

$$\alpha(x) = \left[\sum_{j=1}^{N} V_j W_{ij}(x)\left[1 + \boldsymbol{\beta}(x)\left(x - x_j\right)\right]\right]^{-1} \tag{5.19}$$

Such a method including equation (5.17) is called a Corrected Smoothed Particle Hydrodynamic (CSPH). Instead of using the described linear correction, a constant correction of the Kernel function is introduced in the form:

$$\hat{W}_{ij}(x) = \frac{W_{ij}(x)}{\sum_{j=1}^{N} V_j W_{ij}(x)} \tag{5.20}$$

Based on this approach more accurate results can be achieved, which is important when applied to the metal forming process. The work [Bon00] provides a detailed description of the defined energy function and boundary conditions applied during analysis. Several examples of applications of the CSPH method to forming processes are presented in that work.

To solve the problem with remeshing in the CAFE approach, the Author decided to use the interpolation procedure from the described CSPH method to exchange information between integration (FE points) and CA points. A proper code based on the theoretical background presented in this Chapter was implemented and attached to the previously created CA code. For the purpose of detailed analysis of the SPH method accuracy, equations (5.14) to (5.16) were included in the developed code with the correction coefficient described by equation (5.20). Preliminary analysis revealed that the most accurate interpolation results are obtained for the function (5.15). This Kernel function is later used in all the performed CAFE simulations.

At the beginning of simulation, an alternative set of CA points is created in the sample area. A proper algorithm was implemented by the Author, capable of point generation in various sample shapes (Figure 5.9).

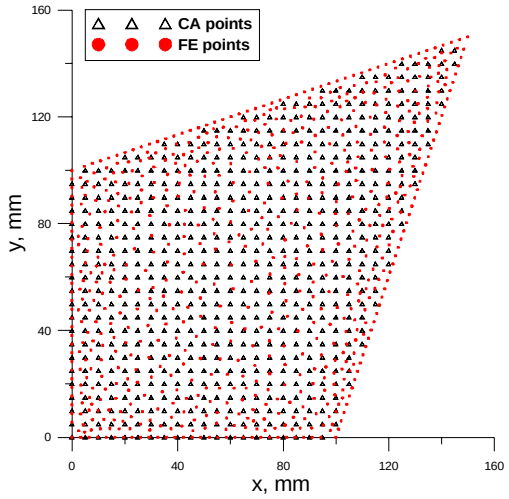

Figure 5.9. Illustration of CA points distribution among FE points in the sample.

The SPH interpolation in the CAFE approach is a two-step procedure in each time increment. In the first step, interpolation of the displacement field between the FE and CA points is performed to achieve a proper distribution of the CA points in the sample space (Figure 5.10), which is crucial to obtain accurate results. When the position of the CA points is updated, an approximation of the stress field from the FE points is performed. Information about stress values from the CA points is later sent to the underlying CA spaces, and calculation of the initiation and development of micro shear and shear bands is performed according to the CAFE approach described previously. To finalize the CAFE calculation, information about the modified stress values is sent from the CA points to the FE points using the same SPH interpolation procedure.

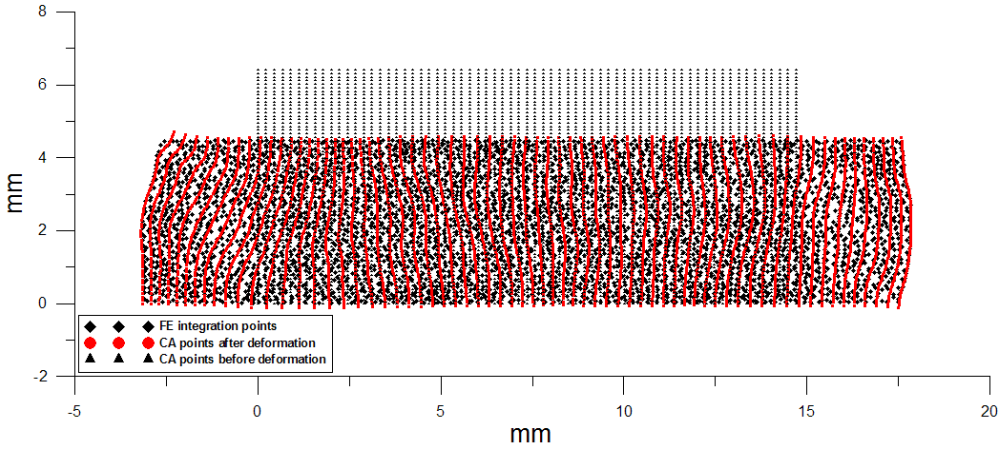

Figure 5.10. Position of the FE and CA points during the channel die tests, calculated by the developed CAFE model with the SPH interpolation procedure.

A schematic illustration of the extended CAFE procedure with the SPH interpolation part, called sphCAFE, is presented in Figure 5.11.

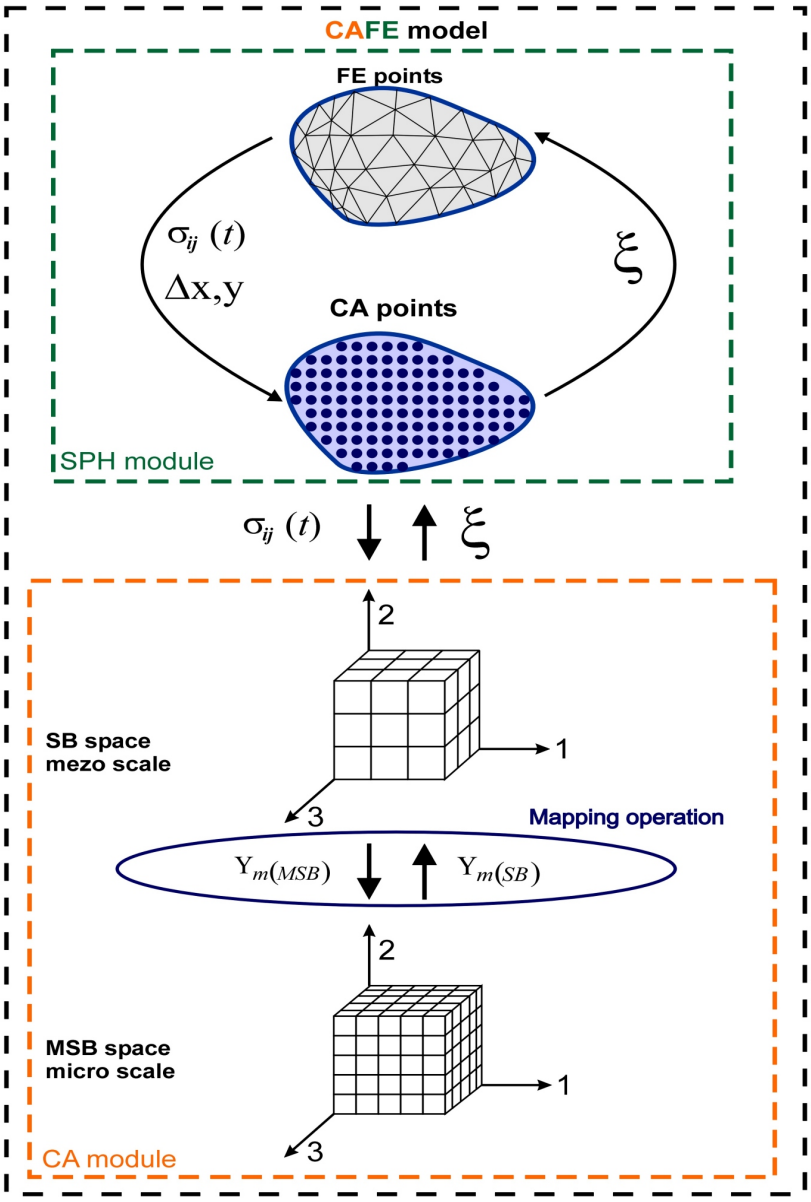

Figure 5.11. Schematic of the information flow between macro-, mezo-, and microscales of the extended CAFE model with the SPH part., where: σ_{ij} –stress tensor, ξ – correction coefficient, Y_m – the state of a selected *m* cell.

5.4. Channel Die Test Simulation with the Extended sphCAFE Model

Further simulation of the channel die compression were performed to test the developed CAFE model combined with the interpolation method. Results obtained for the channel die test are presented in Figure 5.12.

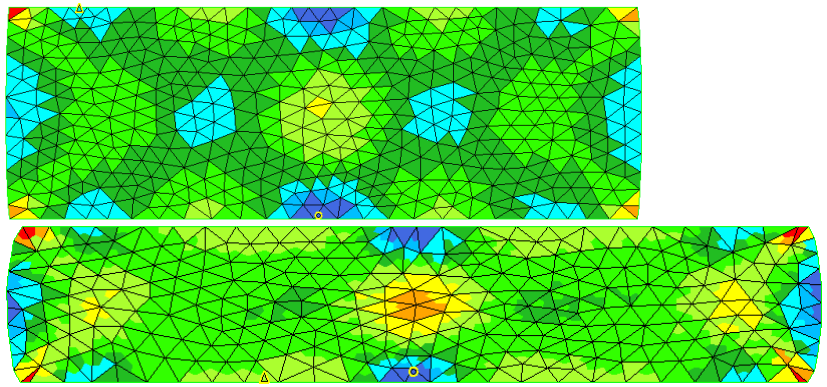

a)

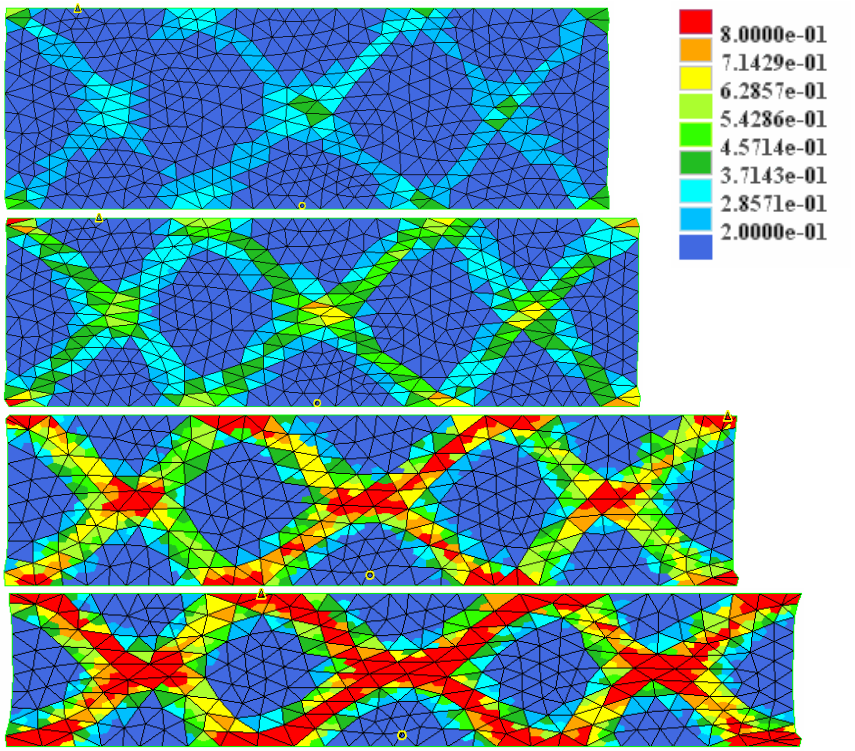

b)

Figure 5.12. Strain distribution during the channel die tests calculated by a) the conventional FE model and b) the CAFE model with friction coefficient 0.12. Results from (a) are directly comparable with the first and last figures from (b).

The distribution of the ξ parameter and distribution of the strain field were analyzed to evaluate how accurately the remeshing problem was solved. The obtained distributions before and after remeshing are shown in Figure 5.13. It is seen that after remeshing, the FE mesh has been rebuilt, and the distributions remain unchanged in the sample.

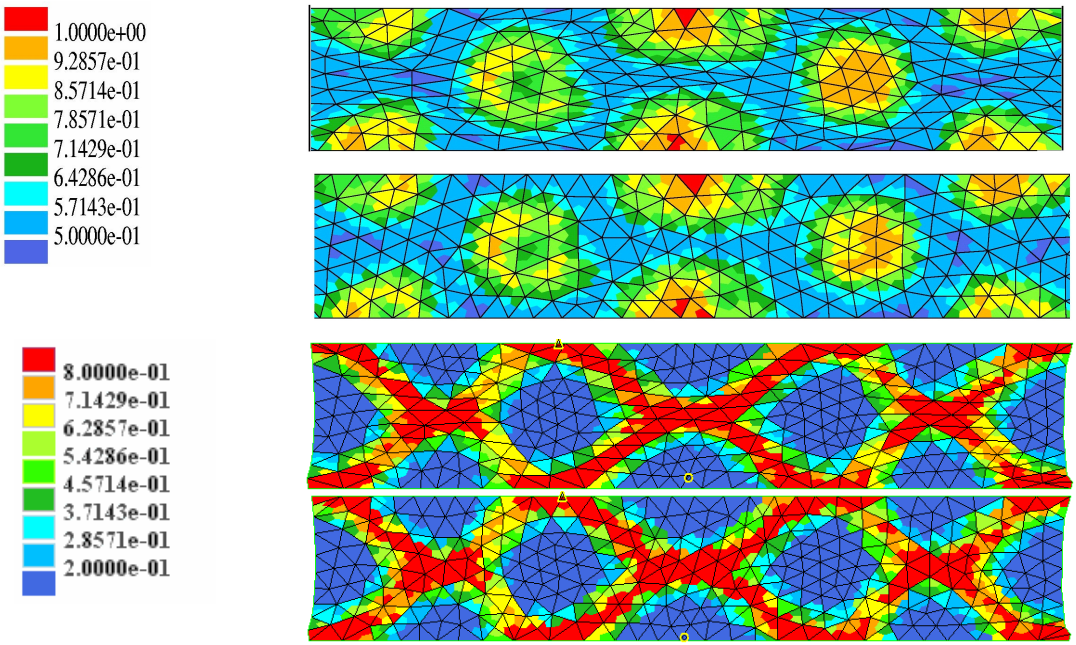

Figure 5.13. a) Correction coefficient ξ distribution and b) strain field distribution during the channel die tests calculated before remeshing (top) and after remeshing (bottom).

It is seen in Figure 5.12 that a strain localization phenomenon in the band of a width of more or less one finite element appears when the CAFE approach is applied. This is due to simultaneous development of the micro shear and shear bands at the micro- and mezoscale during the deformation process. A similar shape of the strain localization is observed in experimental work [Nou86] presented in Figure 2.5. It can be concluded that the developed CAFE model predicts real material behavior more accurately than the conventional FE model.

After solving the problems with remeshing, the developed CAFE model became capable of predicting material behavior not only during simple plastometric tests, but also in conditions of real industrial processes. This improves the predictive capabilities of the method and creates opportunities for proper validation of the results by comparison with experimental observations and leads to further development of this multi scale approach. This flexibility in application to various processes is one of the advantages of the proposed multi scale approach and was one of the goals of this work. Further examples of applications, as well as experimental validation, are presented in the following Chapters.

6. Applications of the CAFE Model

6.1. Extrusion

A series of simulations of extrusion processes (Figure 6.1) was performed using the developed CAFE model. Extrusion involves strong strain localization while the deformation process proceeds. Selection of this process was motivated by experimental observations showing a highly localized shear band zone with flow discontinuity that occurs in the deformation area [Lib92]. The shear zone influences the final product's microstructure and may lead to a coarse grain layer close to the surface. Results obtained from the conventional FE model are compared with the CAFE results in Figure 6.2. Several steps of deformation before the deformation reaches its steady state are presented to show evolution of the strain localization zone in the sample. The steel billet dimensions used in the simulation were: height 90 mm, diameter 60 mm, extrudate diameter 20 mm.

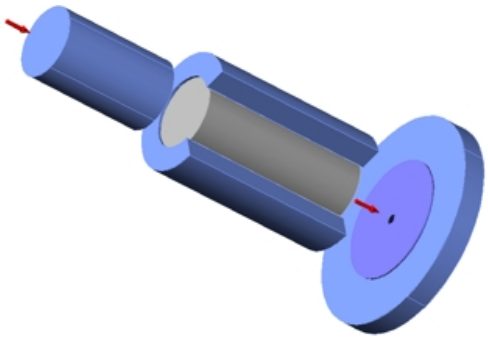

Figure 6.1. Illustration of the extrusion process.

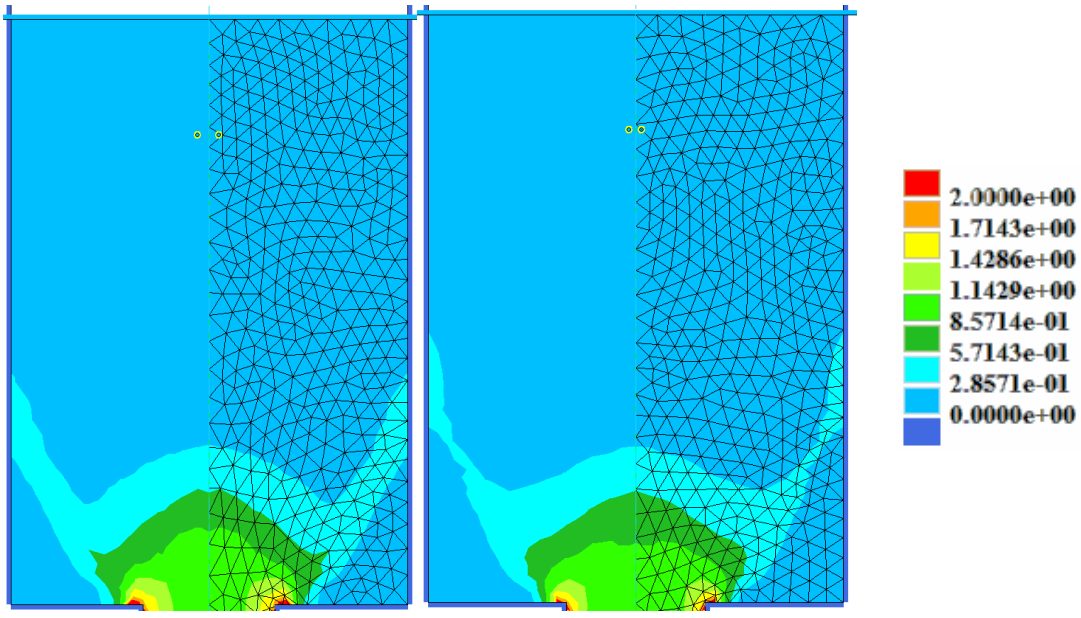

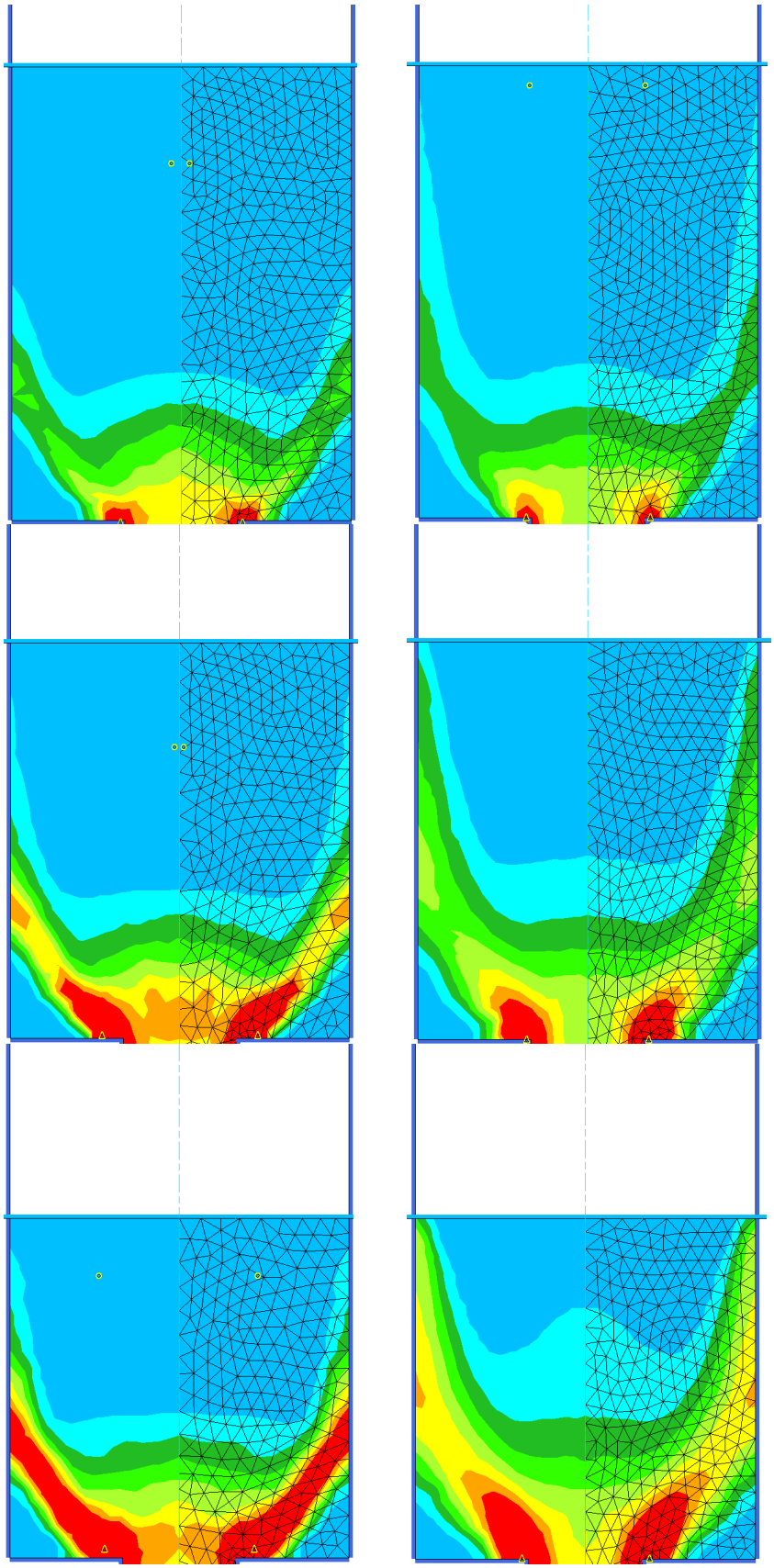

Figure 6.2. Development of strain localization in material obtained from the CAFE (left) and FE (right) models.

It is clearly seen that in the CAFE approach, the deformation zone is narrower, and the strain localization in this area is much higher than in the FE approach for the same deformation conditions. All these above mentioned differences are also clearly observed in the 3D graphs showing strain distribution (Figure 6.3).

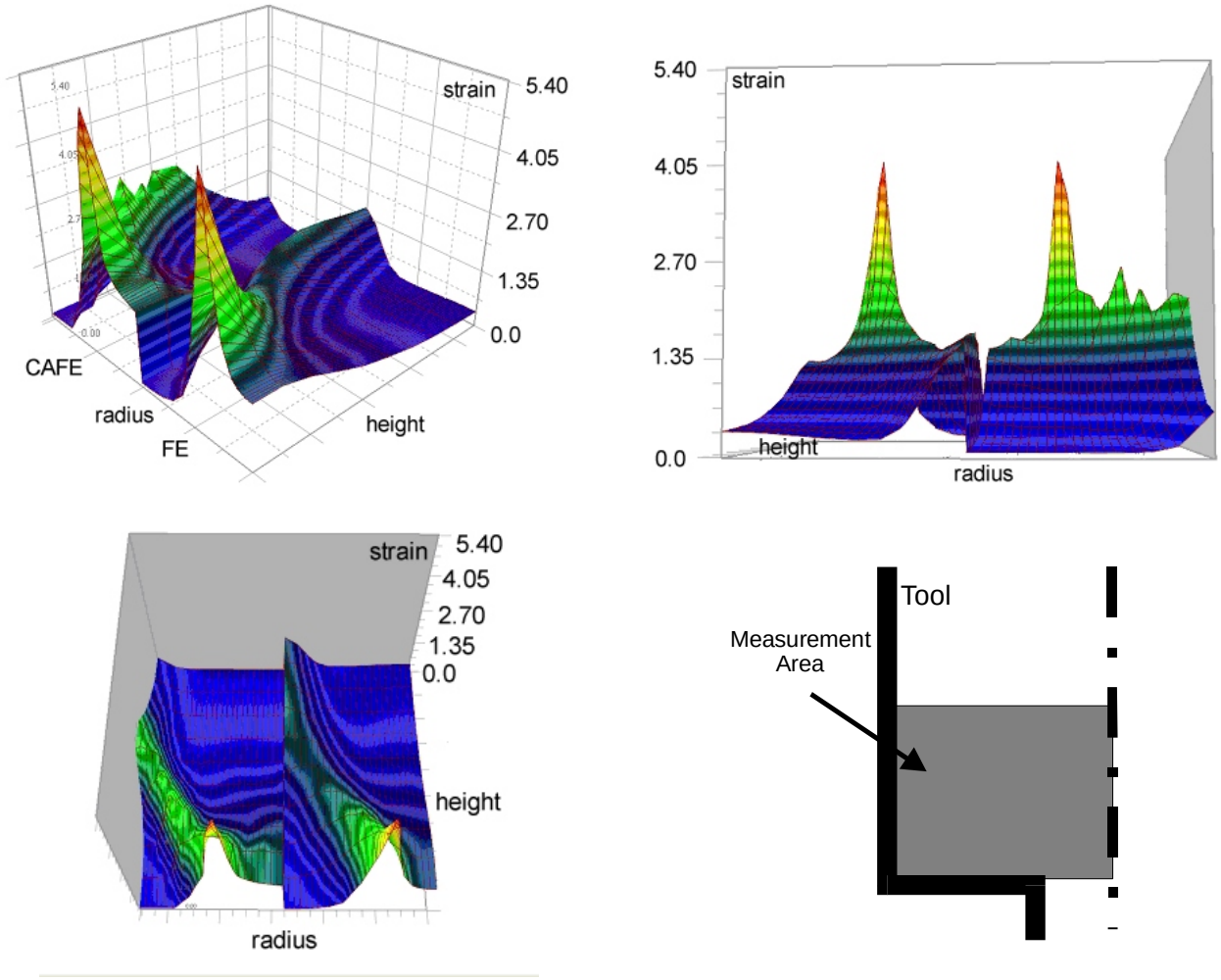

Figure 6.3. Strain field obtained from the CAFE and FE models during the extrusion process.

It is seen in this figure that the CAFE model predicts larger maximum values of strains and narrower strain localization zones, which are closer to experimental observations. In the conventional FE approach, larger values of strain near the tool surface are due to friction conditions, which is less visible in the CAFE results. Strain localization in the CAFE approach is an outcome from the development of micro shear and shear bands. It is clearly seen that strain is localized in the band, and that strain values outside the shear zone are lower in the CAFE approach than in the FE approach. The continuous FE approach gives more uniform strain distribution, smaller values in the shear zone and larger values in the remaining part of the sample. In addition, the transition between the lower and higher strain values in the FE approach is not so steep, which leads to the conclusion that strain is not localized in the shear zone. Contrary to the FE results, the developed CAFE model clearly shows strain

localization in the narrow band with a sharp transition between the shear zone and the remaining part of the material. Such behavior also provides the possibility for more detailed investigation of the dead zone. The values of strain in the shear zone seem to be a little scattered, which may be a result of the data acquisition frequency. The dead zone with strain values equal to zero in the CAFE approach is clearly distinguishable from the shear zone.

A comparison of the strain values predicted by both models was performed during analysis. The distribution of strain is presented along the dashed line shown in Figure 6.4.

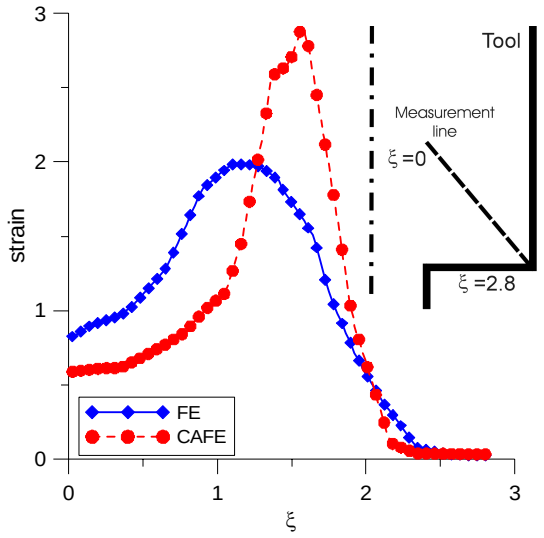

Figure 6.4. Comparison of the strain values calculated by the FE and CAFE approaches at the stage, in which steady state is obtained.

Analysis of results in Figure 6.4 shows that the CAFE model predicts higher strain localization in the shear band area than the conventional FE model. This agrees qualitatively with experimental observation as shown in Figure 6.5 [Lib92]. Such behavior is an outcome from the simultaneous development of micro shear and shear bands in the material.

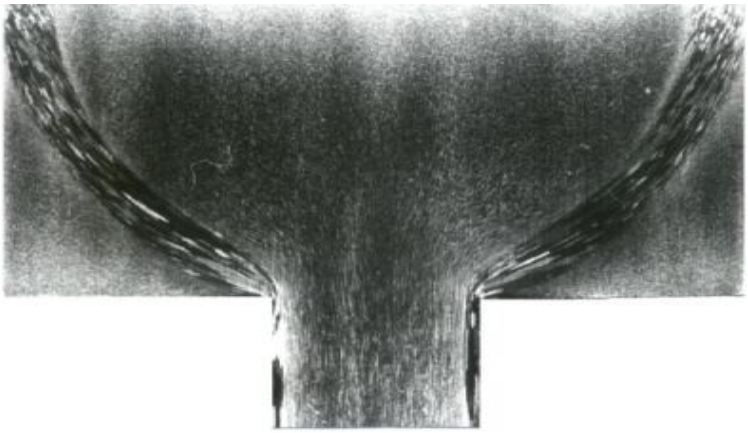

Figure 6.5. Photograph of shear zones in extruded aluminum [Lib92].

Modeling of the strain localization zone creates the possibility of computer aided design of the extrusion process and optimization of technological parameters with respect to the microstructure and properties of products. The presented results show immense capabilities of the developed CAFE model to predict micro shear and shear bands initiation and development, which finally leads to strain localization in the sample area during extrusion. The obtained results compared to the conventional FE simulation again show better qualitative agreement with the experimental observations published in literature.

6.2. Rolling

Similar analysis was performed for the flat rolling process (Figure 6.6). A comparison of the strain fields predicted by the FE and CAFE models is presented in Figure 6.7 and 6.8.

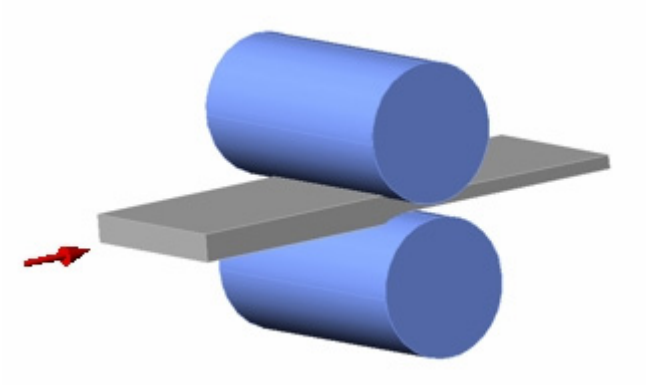

Figure 6.6. Schematic illustration of the flat rolling process.

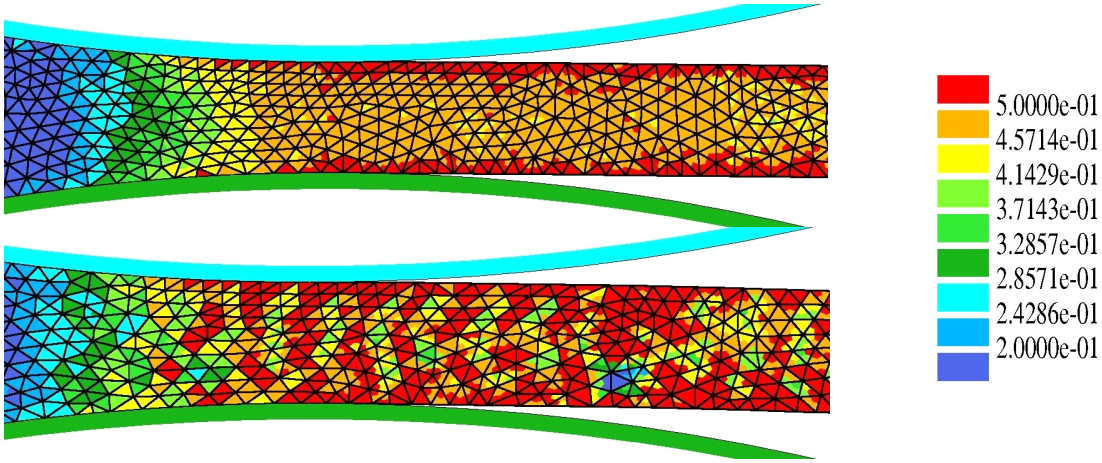

Figure 6.7. Comparison of the strain field distribution in 2D obtained from the FE (top) and CAFE (bottom) approaches for the flat rolling process.

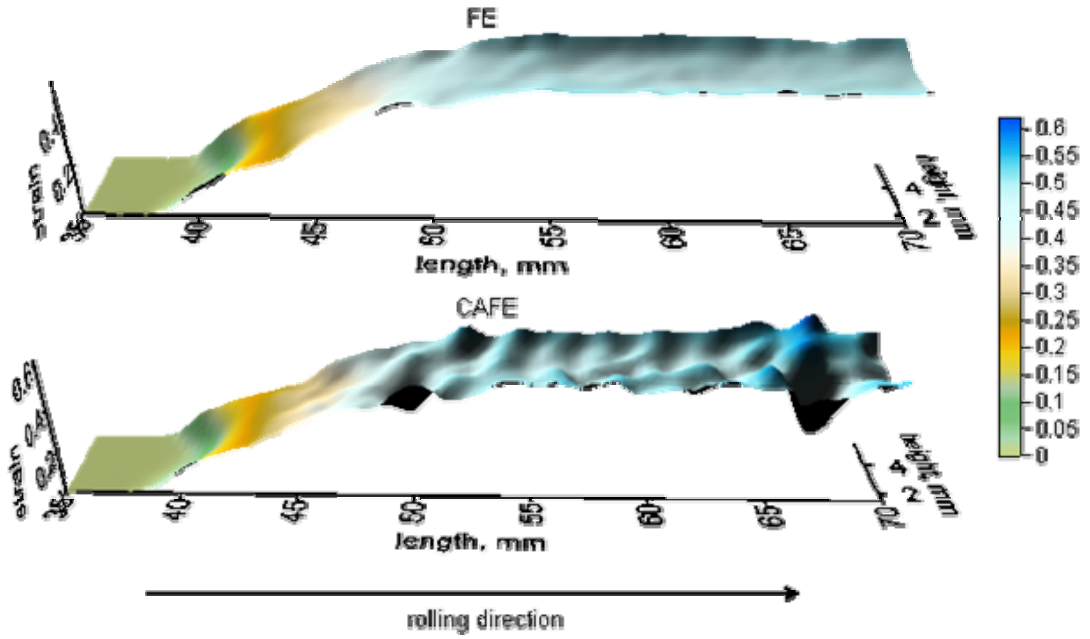

Figure 6.8. Strain field distribution visualized in 3D using the conventional FE (top) and developed CAFE (bottom) approaches.

The strain field obtained from the FE approach is uniform in the center and is characterized by higher values near the surface, which is a result of the influence of friction. For the same process parameters, results obtained from the CAFE model vary significantly from the FE results. In the case of CAFE simulation, the strain field is not uniform in the area of the sample. Strain localization in the bands aligned around 35-45^{o} with respect to the rolling direction appear as a result of the development of micro and macro shear bands in the MSB and SB cellular automata spaces, respectively.

However, it seems from literature knowledge that micro shear and shear bands develop in a more significant manner when the plane strain conditions appear in the sample during deformation. This is the first reason why rolling was selected as the process for experimental validation of the obtained results. Rolling is also a widely used industrial process, which was the second reason why it was selected for following experiments.

7. Experiments

To investigate the capabilities of the developed CAFE model in the description of real material behavior during deformation, a series of experiments was performed for three different materials. All the experiments were composed of material preparation, rolling trials as well as metallographic analysis, and were performed by the Author during his visit to the Center of Material and Fiber Innovation at Deakin University in Australia.

7.1. Materials

Materials such as Aluminum-6%Cu, OFHC Copper (Oxygen Free High Conductivity), and Brass 70-30 (CuZn30) were used to reveal strain localization development during cold rolling operations. All the selected materials are characterize by large differences in stacking fault energy (SFE). In aluminum, copper and CuZn30 the SFE is equal to ~200mJ/m^2, ~70mJ/m^2 and ~20mJ/m^2, respectively. Strong differences in the SFE are responsible for different abilities of selected material to undergo strain localization. The Author investigated experimentally the influence of the applied strain on formation of micro shear and shear bands. The experiments were based on optical microscopy observations. The chemical compositions of the materials used during the experiments are shown in Table 7.1:

Table 7.1 Chemical composition of materials used during experiments.

Al-6%Cu	**Al, %**	**Cu, %**	**Si, %**	**Fe, %**	**Zn, %**	**Others**
	92.45	6	0.4	0.7	0.3	0.15

OFHC Copper	**Cu, %**	**O,%**	**Others**
	99.95	0.02	0.03

Brass 70-30	**Cu, %**	**Zn,%**	**Others**
	70	30	-

7.2. Experiment Methodology

Materials as received have been cut to specific dimensions and subjected to a series of thermomechanical operations to obtain microstructures with a relatively uniform distribution of large grains. An exception was made for Aluminum-6%Cu, which was subjected to rolling operations as received. The applied experimental procedure is presented in Figure 7.1.

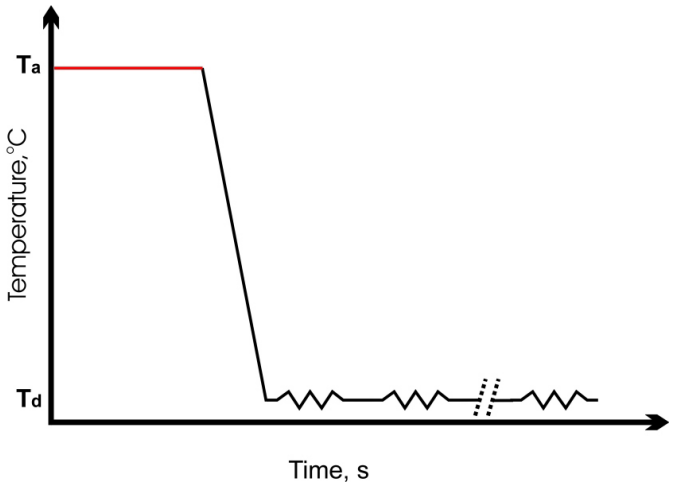

Figure 7.1. Experimental procedure: annealing and subsequent rolling trials.

For CuZn30 the annealing temperature T_a was selected as 600ºC for three hours, and for copper T_a was 800ºC for one hour. After preheating and air cooling, the prepared materials were subjected to several rolling operations in the two-high rolling mill (Figure 7.2) at $T_d = \pm 20$ºC.

Figure 7.2. Two-high rolling mill used in the experiments.

Rolling parameters and initial sample dimensions are given in Table 7.2.

Table 7.2 Rolling parameters and initial sample dimensions.

Sample length, mm	100
Sample width, mm	50
Sample height, mm	10
Roll diameter, mm	175
Rolling velocity, rmp	30
Lubricant	Mineral oil

After each pass in the rolling mill, part of the sample was cut off for further metallographic analysis. Such analysis involves grinding, polishing, etching and optical microscopic observations. When grinding was involved, three different grinding pads were used for all the materials: P240, P600 and P1200. However, for polishing operations (manual or automatic, Figure 7.3) different pads for different materials were used, usually starting with 15- or 9-micron pads finishing with a 1-micron pad (or instead using the colloidal silica suspension polishing - OPS). Polishing times for different materials also varied and were selected in order to obtain surfaces free of scratches, which were ready for etching and microscopic analysis.

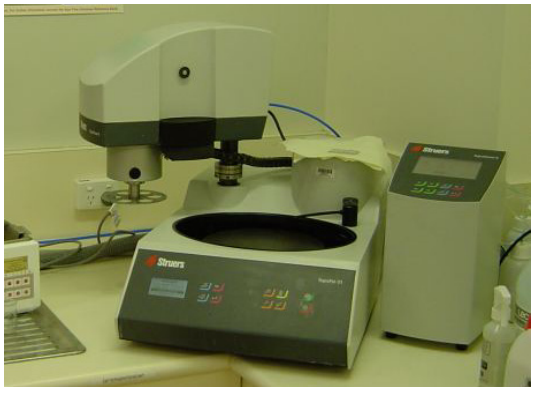

Figure 7.3. Manual and automatic polishing equipment available at the Center of Material and Fiber Innovation at Deakin University.

The etching procedure was also adjusted to each particular material to obtain a clear picture of the surface structure. All the details are shown in Table 7.3. The etching procedure was not applied to the aluminum alloy.

Table 7.3. Etchants used during material preparation.

Material	Etchant
Brass 70-30	20 ml distilled water 10 ml NH_4OH
OFHC Copper	25 ml distilled water 25 ml NH_4OH 10 ml H_2O_2

After preliminary observations, to obtain the most interesting results the Author decided to investigate the development of micro shear and shear bands on the samples' vertical cross sections parallel to the rolling direction (Figure 7.4).

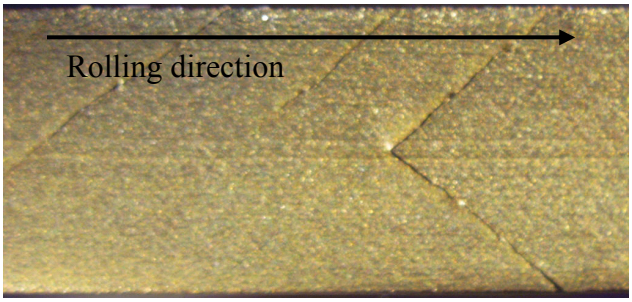

Figure 7.4 Vertical cross section of the rolled sample.

All the samples were rolled in a series of trials to obtain specific deformations accumulated in the material. After that the cross sections of the rolled samples were prepared by grinding and polishing to obtain a surface free of any scratches. To reveal micro shear bands and shear bands, the previously prepared samples were rolled with additional small rolling reduction (2-10%). Selected examples of the obtained results are presented in the following sections.

7.3. Results

7.3.1. Aluminum-6%Cu

According to the expectations due to large values of SFE, polycrystalline aluminum shows a weak tendency toward strain localization. Similar microstructures were observed after 65% rolling reduction obtained in two or several passes with additional 5% and 10% rolling reductions, which are shown in Figure 7.5.

a) b)

Figure 7.5. Results obtained after 65% reduction with a) 5% additional reduction and b) 10% additional reduction.

Figure 7.5 reveals microstructures composed of elongated grains in the rolling direction with the grain size equal to ~50μm. In such microstructures, two symmetrical families of highly visible micro shear bands aligned ±40° to the rolling direction are observed. It might be stated that they are active in parallel layers but aligned in an opposite manner (Figure 7.6).

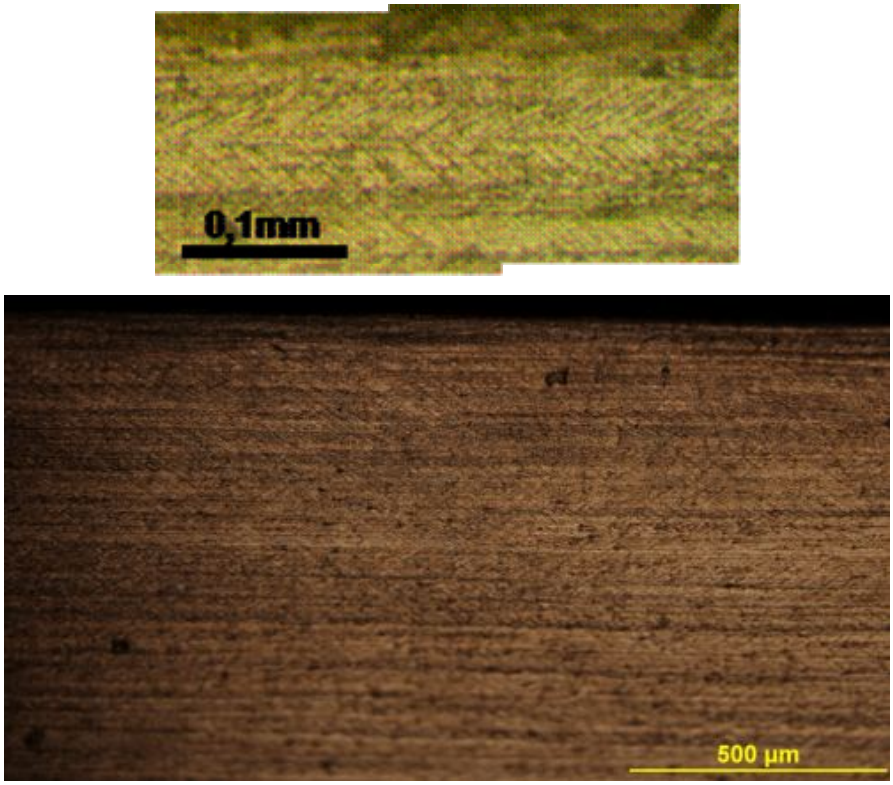

Figure 7.6. It is difficult micro shear bands aligned ±40° to the rolling direction observed in parallel layers but aligned in an opposite manner.

It is hard to observe a macroscopically aligned shear bands, which cross several grains and propagate throughout the entire sample. However, it may be observed that some micro shear bands cross between adjacent grains (Figure 7.7).

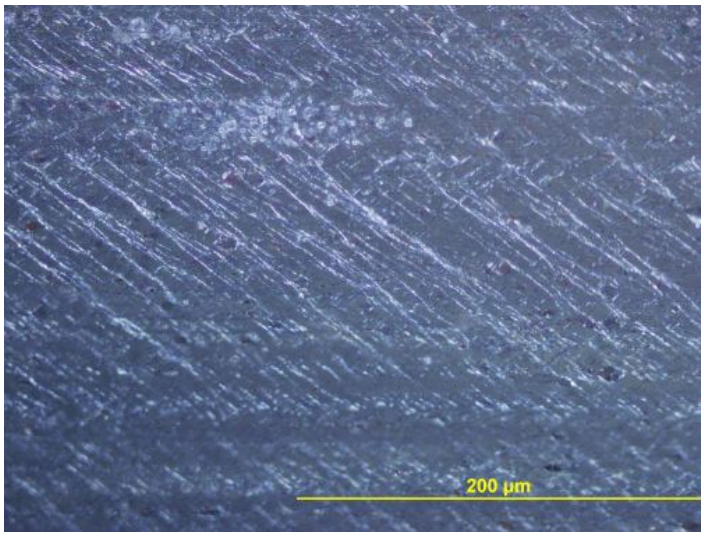

Figure 7.7. Initial stages of shear band development in aluminum.

7.3.2. OFHC Copper

Polycrystalline copper reveals a high tendency toward strain localization through the formation of micro shear and shear bands due to its much lower SFE values than in aluminum. The author observed development of layered structures composed of elongated grains when rolling reduction is 70% (obtained in two or seven passes), with an additional 5% or 10% reduction applied to reveal these microstructure features. Optical microscopy shows the formation of compact symmetrical families of micro shear bands aligned 35° to the rolling direction (Figure 7.8).

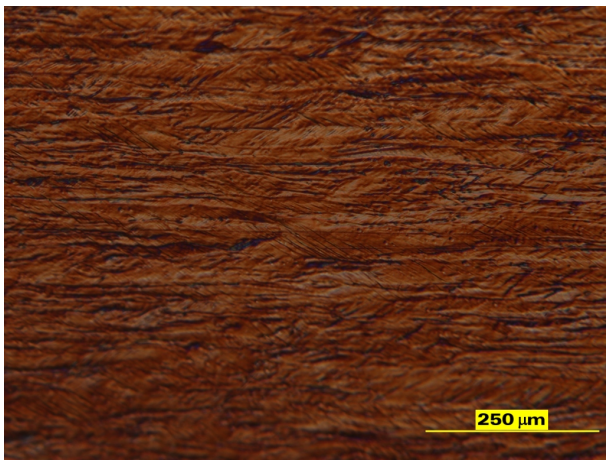

Figure 7.8. Symmetrical families of micro shear bands.

When additional rolling reduction is applied, development of crossing families of micro shear bands, which are also a precursor of shear band development at the macroscale, is observed on the samples' cross section (Figure 7.9).

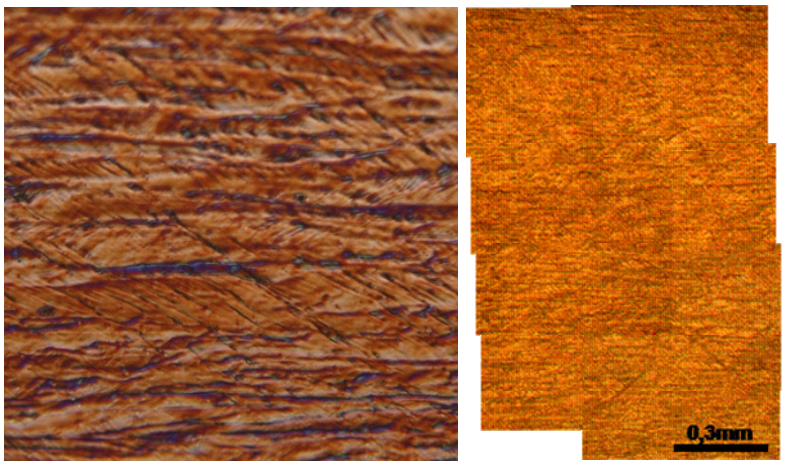

Figure 7.9. Initial stages of development of shear bands based from shear bands.

In the case of copper, crossing families of shear bands are highly visible throughout the entire sample, which leads to strain localization observed at the macroscale. This behavior is presented in Figure 7.10.

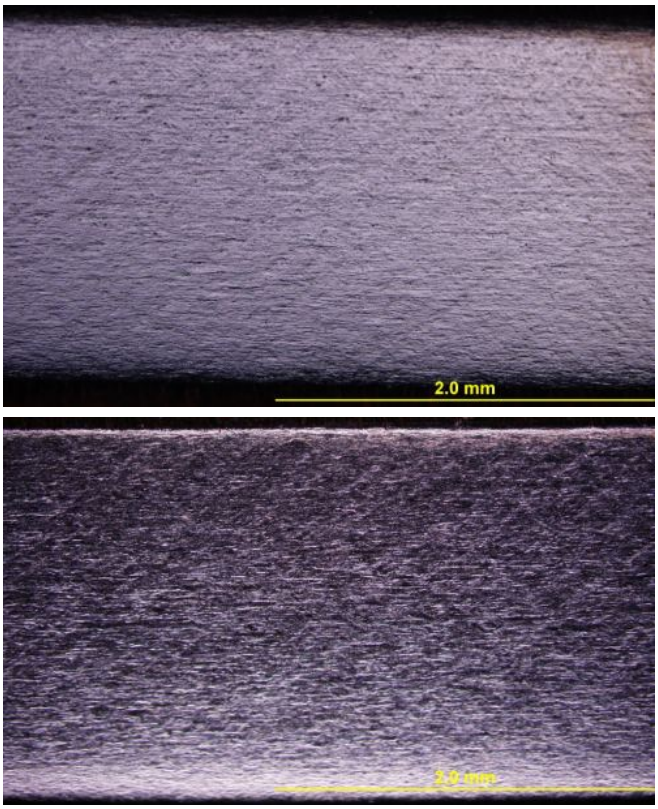

Figure 7.10. Shear bands observed in the entire sample under optical microscopy.

7.3.3. Brass 70-30

One phase brass CuZn30 has the highest value of SFE, which results in highly visible tendency toward strain localization. The author observed net shaped structures of shear band families crossing each other and aligned 35-40° to the rolling direction for medium rolling reductions (i.e. 50% and 5% of additional rolling reduction), which is shown in Figure 7.11.

Figure 7.11. Highly visible crossing families of shear bands obtained for relatively low rolling reductions 50% + 5% additional rolling reduction.

Micro shear bands develop on the background of elongated grains, in which a layered structure of twins and the surrounding matrix (T-M) may appear. Twins are important for metals with medium and high SFE values, in which for low rolling reductions (after 20%) an anisotropic structure composed of layered T-M features is responsible for slip restrictions in preferable slip systems. This results in the fast development of the micro shear and shear band deformation mode. After 55% reduction not only micro shear bands but also shear bands are observed in the whole range of the rolled sample, which is seen in Figure 7.12.

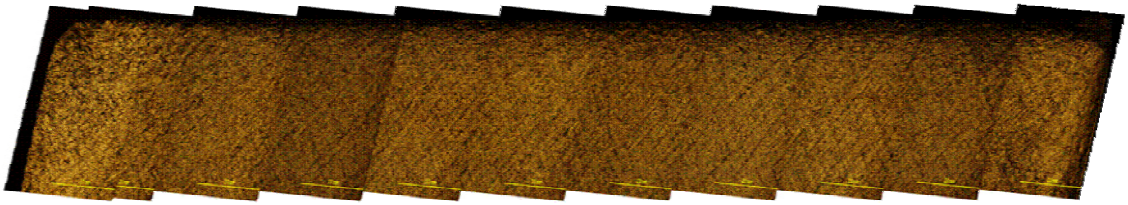

Figure 7.12. Crossing families of shear bands visible after 55% reduction in CuZn30.

After 80% reduction and 5% additional rolling, a very dense net of crossing families of shear bands is observed in the entire cross section of the sample (Figure 7.13).

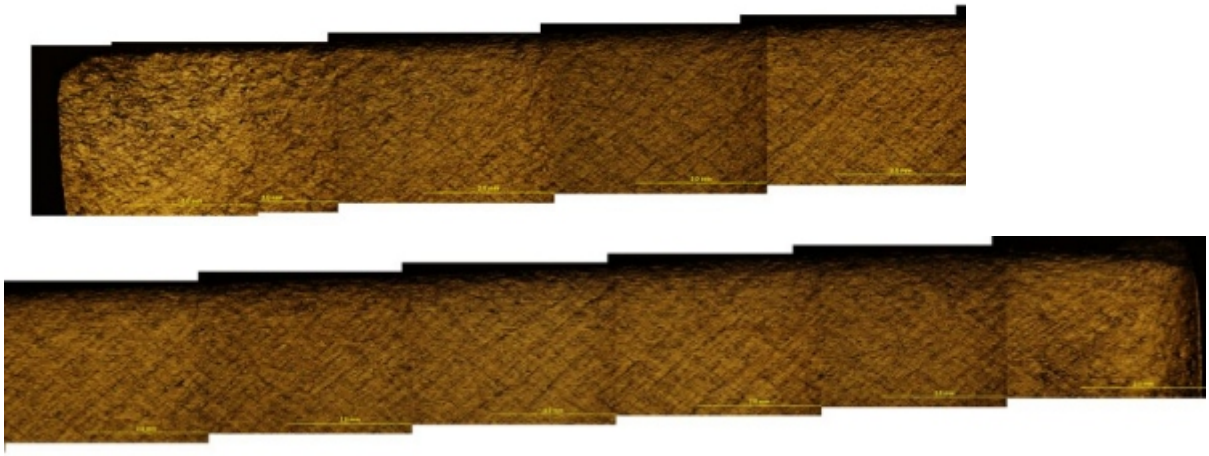

b)

Figure 7.13. Dense net of shear band families visible after 85% reduction in the entire cross section.

It is observed in Figure 7.14 that crossing families of shear bands run in the entire sample cross section starting at the top surface and finishing at the bottom. They are directly responsible for strain localization phenomenon.

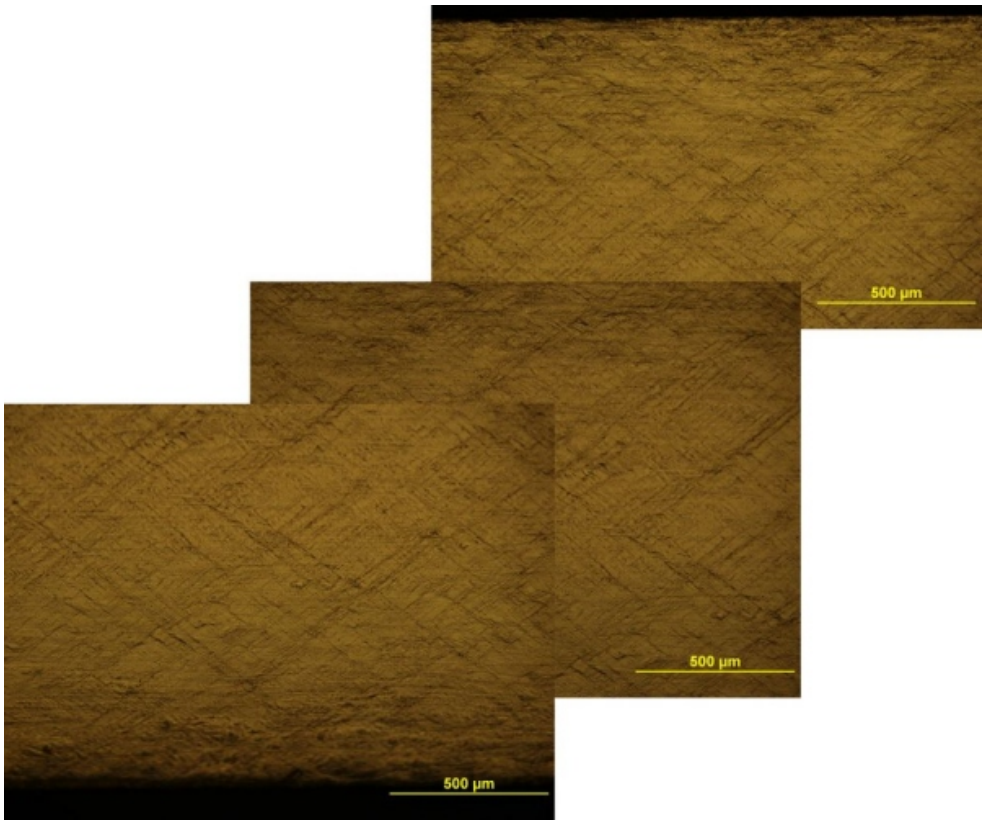

Figure 7.14. Magnification across sample height after 85% reduction.

Based on the collected and presented experimental results, a proper validation of the developed multi scale CAFE model for strain localization was performed by the Author. This comparison between experiment and simulation showed capabilities of the developed CAFE model and restrictions of the conventional FE approach in strain localization description. Numerical simulation results are presented in the next section.

7.4. Comparison Between CAFE and Experimental Results Obtained from Rolling

During the numerical simulation, OFHC Copper was selected as the material used for the presentation of results of model validation in rolling because of its medium value of SFE, which is between the SFE of aluminum and brass. Numerical simulations were designed to replicate experimental parameters and the dimensions of rolling operations performed on the two-high rolling mill. During the experiment copper samples were deformed up to 70-75% in either two or seven rolling passes. For comparison of the numerical simulation results with the experimental observations, the rolling process involving 70% reduction in 2 rolling passes was selected. Results obtained by the developed CAFE approach were compared with the conventional FE results to highlight different capabilities of these techniques. Figure 7.15 illustrates differences in strain distribution obtained after the first rolling pass.

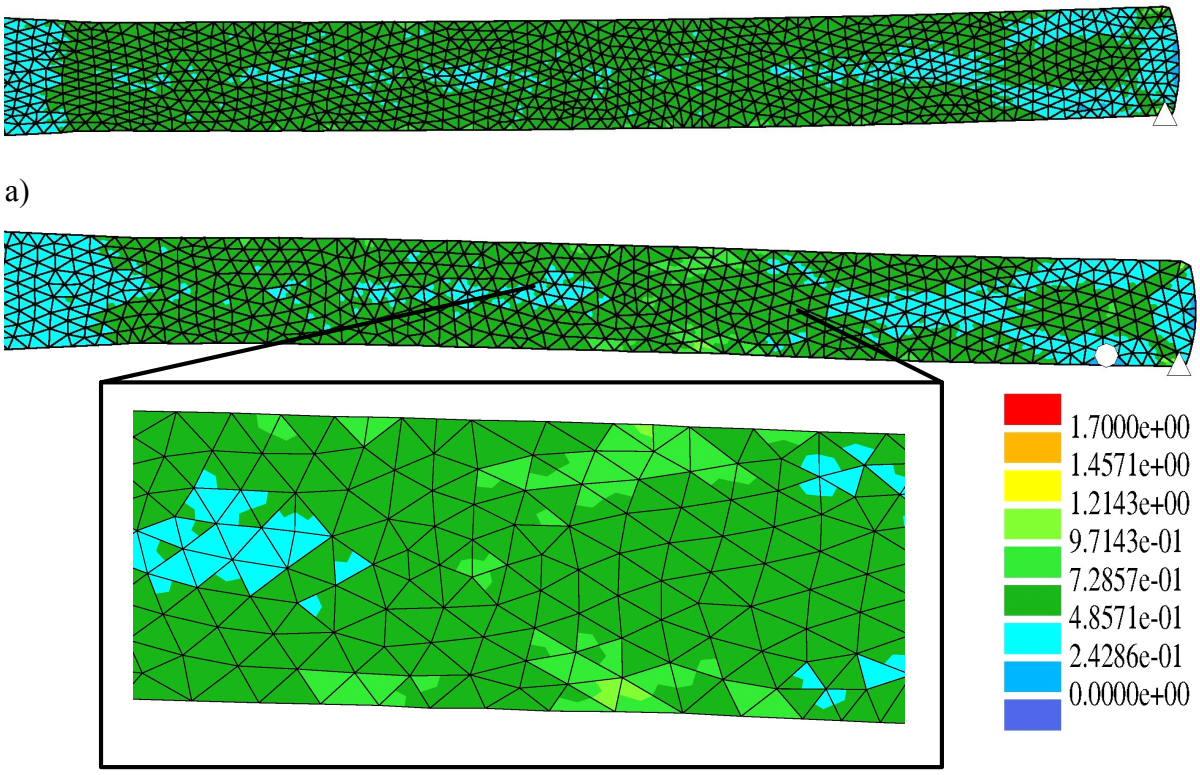

Figure 7.15. Strain distribution obtained from the a) conventional and b) CAFE simulation after the first rolling pass.

Strain distribution obtained from the conventional FE and CAFE simulations are very similar and uniform in the sample area. This is because the development of micro shear and shear bands in the CAFE model is slow for the applied rolling reduction. This is in agreement with experimental observations, in which for small rolling reductions strain localization in the sample is weak. However, in some regions a form of narrow bands with higher strain values than in the surrounding material is observed when the CAFE model is applied. High strain values are visible as two bands aligned in an opposite manner ±40-45º to the rolling direction, which is observed in the magnification in Figure 7.15b. These bands represent the initial stages of the strain localization process, which is (after another rolling trial) highly visible in the sample (Figure 7.9).

The predeformed sample was then subjected to the second rolling operation to obtain 70% reduction of the initial height. This is the same procedure applied during some experimental trials involving two rolling passes. Results of the simulation obtained after the second pass are presented in Figure 7.16.

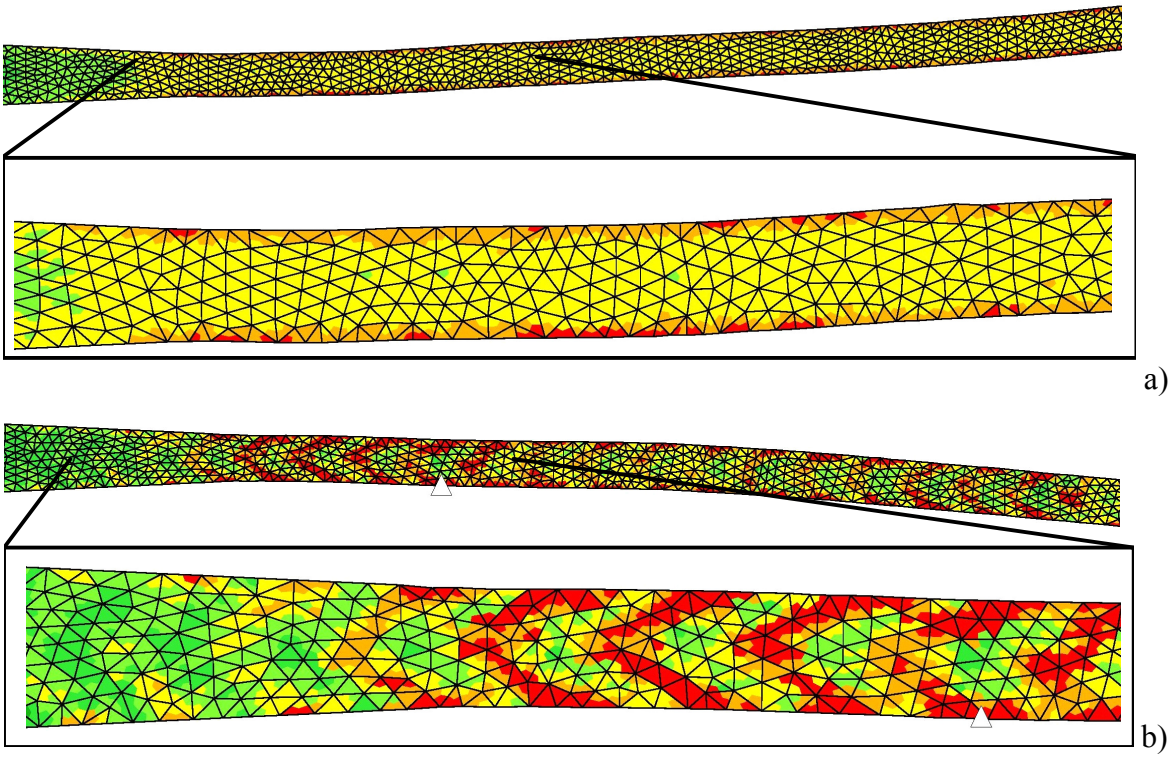

Figure 7.16. Strain distribution obtained after the second rolling pass from the a) conventional and b) CAFE simulation.

A highly localized deformation in the form of narrow bands aligned ±40-45º to the rolling direction is observed in Figure 7.16b, when the CAFE model is used for numerical modeling. Strain values visible as the bands, which are observed between highly localized regions in Figure 7.16b, carry medium strain values, when compared with the one observed in Figure 7.16a. Between the bands in Figure 16b, regions with low strain value are observed, which are not visible in the FE approach. In Figure 16a, strain distribution is relatively uniform except for the surface region, which is characterized by higher strains. Such behavior is well known and is due to friction between the rolls and the sample. It is not related to the micro shear or shear band phenomena. On the contrary, strain localization observed in Figure 7.16b is an outcome of the microstructural response to macroscopic loading conditions. Simultaneous development of micro shear and shear bands in the MSB and SB spaces, respectively, results in the macroscale in the form of strain localization observed in Figure 7.16b.

Results obtained from the developed CAFE model presented in Figures 7.15b and 7.16b are well comparable in a qualitative manner with real material behavior presented in Figures 7.9 and 7.10. At the same time, the conventional FE approach fails to describe these phenomena, which is seen in Figures 7.15a and 7.16a.

For further validation of the CAFE model, the Author decided to perform additional experiments involving channel die tests for OFHC Copper.

7.5. Experimental Validation for the Channel Die Test

OFHC Copper samples with specific dimensions: width = 10mm, height = 10mm, length = 8mm, were used during channel tests performed due to courtesy of Professor H. Paul from the Polish Academy of Science (PAN), Krakow, Poland. A comparison between the FE and CAFE results for the channel tests is presented in Figure 7.17.

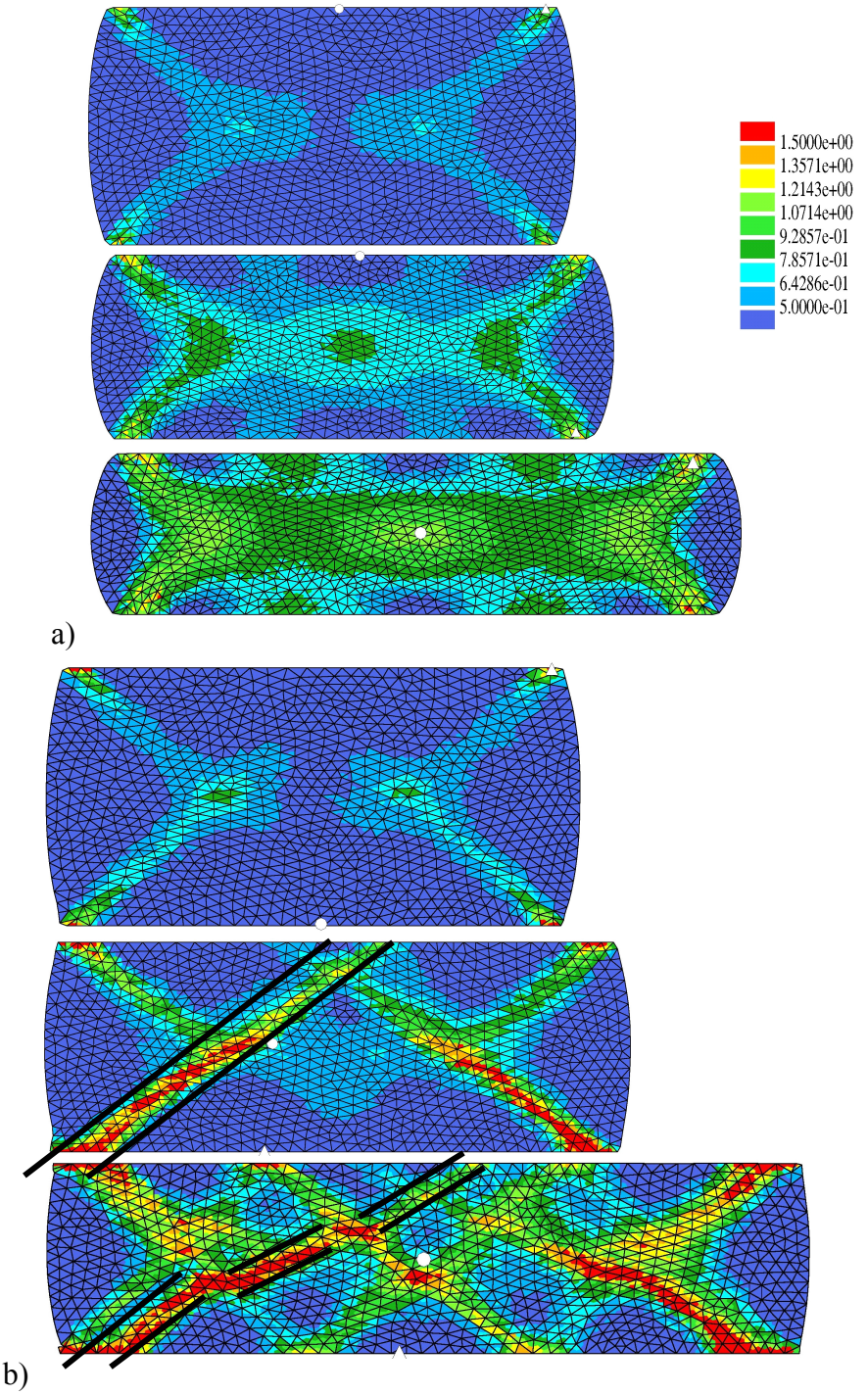

Figure 7.17. a) FE results for 30%, 40% and 50% reductions, b) CAFE results for 30%, 40% and 50% reductions.

The experimental result obtained after 40% reduction is shown in Figure 7.18.

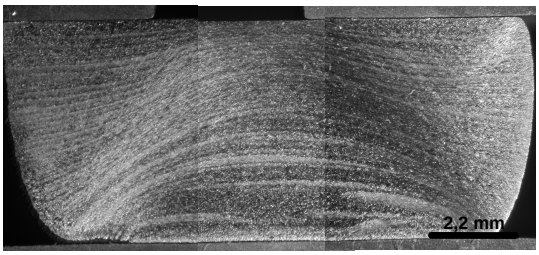

Figure 7.18. Experimental result after 40% reduction.

Similar to the results presented in Figure 7.15, the strain fields obtained for small deformations from the FE and CAFE approaches are comparable because micro shear bands and shear bands play negligible roles in material deformation. At 40% reduction, highly visible strain localization is observed as a result of shear band development in the entire sample. At the same time, it is observed that a second family of shear bands is developing. This second family of shear bands plays an important role during further deformation (50% reduction), when they are responsible for the movement (offset) of the primary shear band families. This process is illustrated in Figure 7.17b by two parallel solid lines. The result in Figure 7.17b obtained after 40% reduction is in very close agreement with the experimental result presented in Figure 7.18.

All the presented numerical results from the developed CAFE model describe real material behavior much better than the conventional FE approach used in this work. That is why after successful validation of the numerical results with experimental rolling and the channel test procedure, the CAFE model can be used to analyze and to solve problems that occur during industrial manufacturing operations. Selected examples of the CAFE model application are shortly described in the following section.

7.6. Selected Examples of Simulation of Other Forming Processes

The developed CAFE model is flexible and can be applied to simulation of any metal forming process, in which problems of the influence of micro shear and shear bands on crack resistance, final structure and properties of products is important. Three examples of applications of the CAFE model to simulate industrial forming processes were selected:

- bolts and connecting parts forging,
- extrusion with convex dies,
- equal channel angular pressing.

Results of simulation showing the capability of the CAFE model to predict strain localization are presented below.

7.6.1. Industrial Forging Operation

Materials used to manufacture these products (e.g., bainitic steels) are characterized from one side by elevated mechanical properties and fatigue resistance. From the other side they show a tendency toward micro crack initiation during forming. The latter phenomenon is caused mainly by micro shear and shear bands. Elimination of the micro cracks is important from the point of view of exploitation of final products, their durability and fatigue resistance. Thus, decreasing this effect is essential during the design of technology for future manufacturing processes.

The bolt forging operation shown in Figure 7.19 was selected for the FE and CAFE simulations.

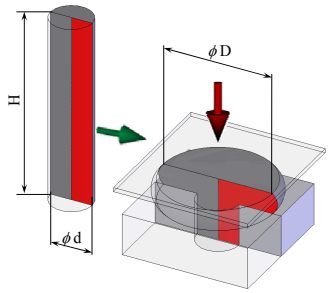

Figure 7.19. Bolt forging operation.

The CAFE simulation of bolt forging revealed strain localization development during deformation, which is shown in Figure 7.20b. This behavior is not properly predicted by FE analysis (Figure 7.20a).

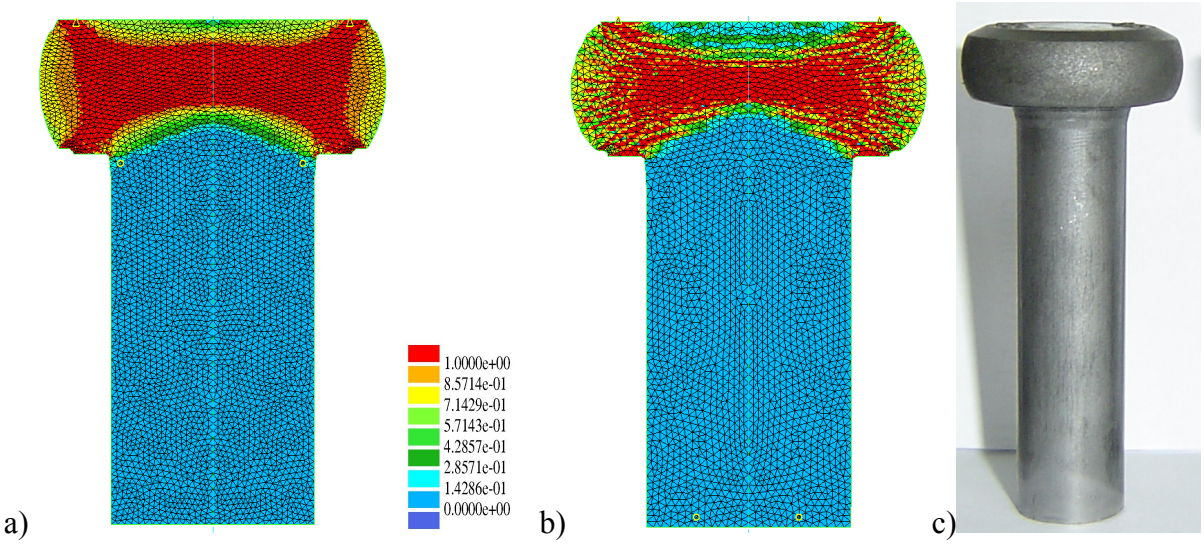

a) b) c)

Figure 7.20. Strain distribution obtained from the a) FE and b) CAFE method after the forging operation, c) shape after the real forging operation.

It is seen in Figure 7.20 that strain localization during the process is more accurately predicted by the CAFE model. Analysis of such results may lead to reducing of the probabilty of material failure during the manufacturing process or further exploitation conditions. It can also be the basis for investigating the influence of micro shear and shear bands on other microstructural processes (e.g., dynamic recrystalization [Hum04, Pau02]).

7.6.2. Extrusion with Various Die Shapes

Extrusion is one of the most important technologies used in the plastic working of metals and alloys. The ability to obtain the final shape of products in a single operation is the main advantage of this process. On the other hand, extrusion leads to nonhomogeneous structures and mechanical properties of final products. A coarse grain layer occurs close to the surface and leads to deterioration of product exploitation properties [Lib92, Kaz05]. This is mainly due to the existence of a dead zone and strain localization in the deformation area. Eliminating, or at least decreasing the effect of, this zone should lead to higher quality extrudates and to more efficient applications of extrusion. Proper design of extrusion dies may lead to a reduction of such a dead zone.

The CAFE calculations are performed for two different die shapes: convex dies with 100^o and 110^o angles. The main aim is to investigate the influence of the die shape on strain localization in material and dead zone development. Typical example of the experimental results is presented in Figure 7.21.

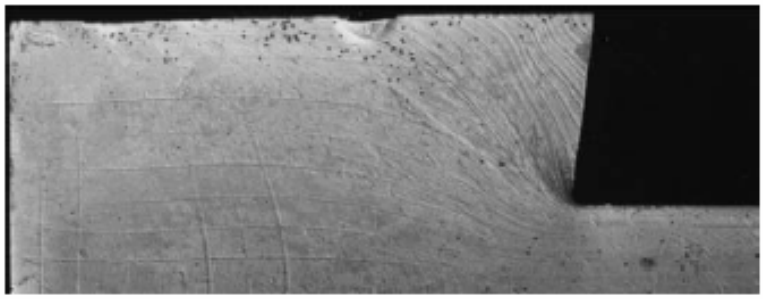

Figure 7.21. Example of experimental results obtained in [Kaz05] for the die angle 98^o.

Comparison of the results of the FE and CAFE simulations of the extrusion process with different die shapes is presented in Figure 7.22.

It is clearly seen that in the CAFE approach the deformation zone is narrower, and the strain localization in this area is much higher than in the FE approach for the same deformation conditions. Analysis of the results in Figure 7.22 shows that the CAFE model predicts higher strain localization in the shear band area than the conventional FE model. It agrees qualitatively with experimental observation, see for example [Lib92, Kaz05].

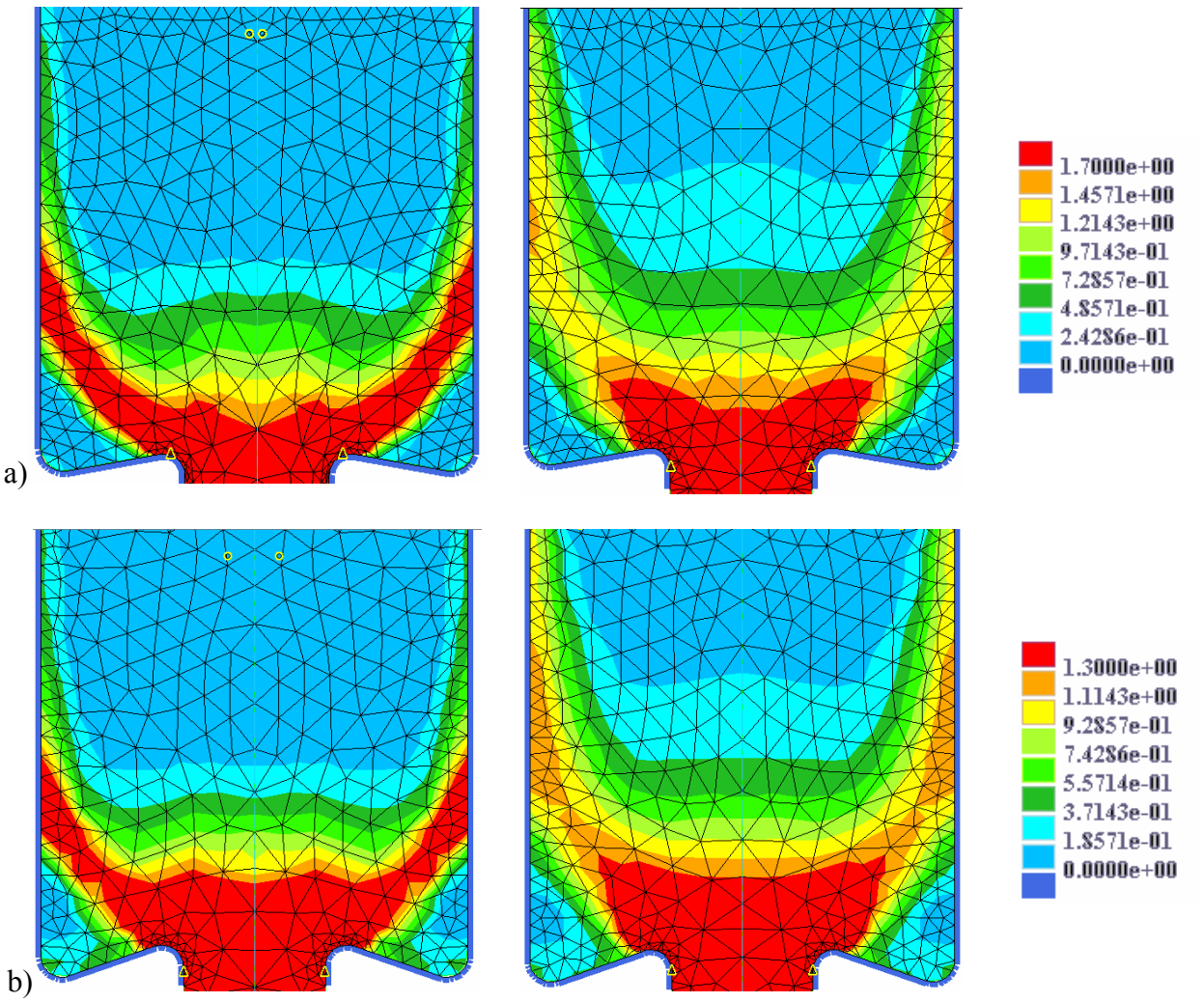

Figure 7.22. Comparison of the strain field distribution obtained from the CAFE (left) and FE (right) approaches in the extrusion process for various die angles a)100^{o}, b)110^{o},

7.6.3. Equal Channel Angular Pressing (ECAP)

Equal Channel Angular Pressing (ECAP) is one of the examples of discontinuous processes of Severe Plastic Deformation (SPD) [Ros04], in which strain localization plays an important role. SPD methods have enormous effects on the final microstructure and properties of metallic materials, which is the reason why a detailed understanding of these processes plays an important role in recent scientific research. The developed CAFE approach can be applied to simulate complicated deformation processes such as the ECAP process, which is shown in Figure 7.23.

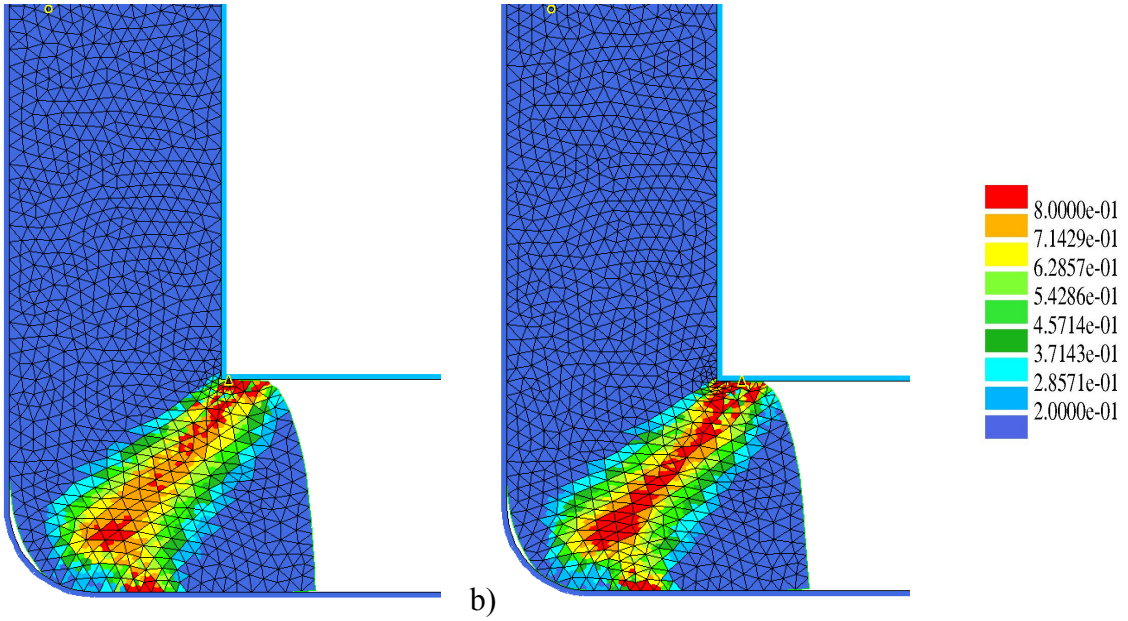

a) b)

Figure 7.23. Strain distribution obtained from the a) FE and b) CAFE simulation of the ECAP process.

Again strain localization appearing in the material due to the development of micro shear and shear bands is predicted by the CAFE approach for the ECAP process much better than by the FE approach.

The presented examples obtained from the CAFE model reveal the flexibility and wide range of possible applications to solve crucial problems during material manufacturing stages and further exploitation.

8. Conclusions

8.1. General Conclusions

The developed CAFE approach is an example of the new generation of knowledge based modeling methods. The idea of the CAFE model is based on the proper definition of transition rules, which control changes in cell states and replicate real material behavior. In the developed CAFE model the transition rules for micro shear and shear band development are created in an intelligent way based on knowledge gathered during the literature review, experimental observations and most importantly upon discussions between experienced researchers. This process is schematically presented in Figure 8.1.

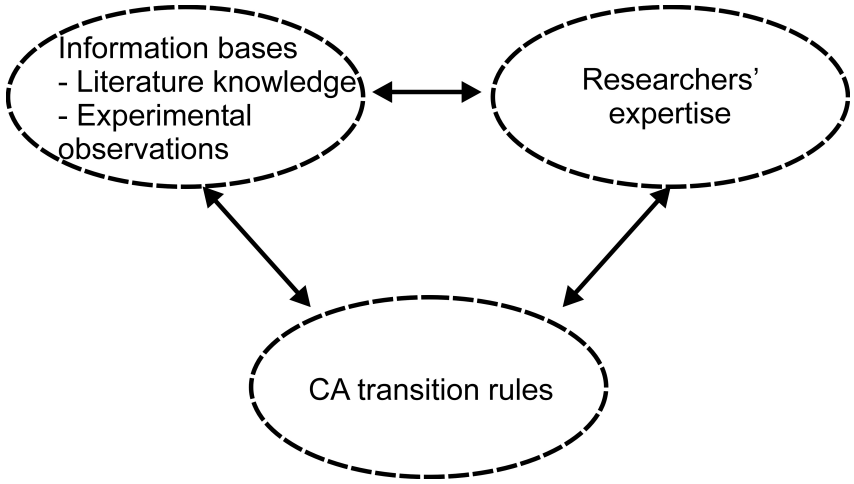

Figure 8.1. Information flow during the development of the knowledge based data base dedicated to the creation of the transition rules.

The CAFE approach developed by the Author and presented in detail in this work gives the possibility to create a model based on real physical aspects, and not only on arbitrarily selected parameters. This close relationship to the physics of phenomena of particular interest is the main advantage of the proposed approach. Another advantage is connected to the possibility of taking into account the multi scale nature of the modeled phenomena. The CAFE model for strain localization simulations represents a truly multi scale approach. The model is able to perform calculations at different scales in material from the micro- to macroscale. Furthermore, it gives possibilities of modeling interactions between phenomena at different scales. Because of this, it was possible to include the hierarchical character of strain localization in the CAFE model. Taking into account the complex relationship between micro shear bands and shear bands at the micro- and mezoscale,

respectively, is the main problem observed in conventional approaches described in Chapter 2.

Finally, the possibility to include in the solution stochastic and discontinuous phenomena taking place during deformation makes the developed CAFE model a very powerful investigative tool in comparison to the conventional approaches.

In the presented work, the Author described a complete cycle of development of the CAFE model. Initial work related to the literature review and experimental analysis described in Chapters 2 and 3 shows the idea how, based on available knowledge of specific phenomena, an alternative approach such as the CAFE model can be designed. Following that, a detailed discussion about crucial parameters (i.e., internal variables and transition rules) is described in Chapter 5. To support the statement that the CAFE method represents an artificial intelligence idea, the Author clearly showed how each part of the created CAFE model is related to physical observations. Furthermore, numerical results obtained from the strain localization CAFE model are presented in Chapter 6. They show that realistic material behavior, including stochastic phenomena taking place during deformation at two different scales, is properly replicated. Limitations of conventional methods in describing strain localization in different metal forming operations are compared with the CAFE results in Chapter 6. This comparison revealed the immense capabilities of the developed model in the simulation of real deformation processes. However, to obtain such a general form of the developed model, which does not constrain application to particular tests or particular processes but allows simulations of any metal forming process, the Author decided to solve a problem with remeshing. As an outcome, the model gained flexibility, which is one of the advantages of this approach. Finally, a series of experiments involving various metallic materials was performed for the purpose of validation and is described in Chapter 7. During analysis the model was applied to simple deformation processes, such as the channel die test and to real industrial processes (i.e., cold rolling). Comparison of the results obtained from the CAFE model with experimental results shows good qualitative agreement.

All the work performed by the Author and described in this PhD thesis confirms that the multi scale CAFE method is an efficient method for modeling strain localization development in material subjected to plastic deformation in real industrial processes. All the objectives formulated in the work and described in detailed in Chapter 4 have been successfully realized.

The main outcome from this work is the CAFE model for strain localization, which can be easily applied to various deformation processes, and which is a multi scale platform for further improvement (e.g., development of strain localization during processes with changes in the deformation path). The proposed multi scale approach fulfills industrial demand to create a computer aided design of processes involving strain localization.

8.2. Specific Conclusions

- Development of a working CAFE model dedicated to simulate a specific phenomenon or a group of interacting phenomena has to be preceded by a detailed literature review, experimental analysis and experts knowledge about the investigated problem. Gathering the knowledge is essential to identify transition rules in an intelligent manner.
- Proper definition of transition rules is a key step in the creation of the CAFE model. Transition rules replicate physical processes occurring in the deformed material. Determination of transition rules that do not properly reflect physical phenomena in the process will cause inaccurate results.
- Designing of the internal variables should also be performed on the basis of the gathered knowledge. The combination of the internal variables with the transition rules results in creation of the CAFE method.
- Detailed analysis of the sensitivity of the obtained results is of high importance because some of the defined transition rules can have negligible influence on the final results and unnecessarily extend computational cost. Selection of the defined transition rules is another important step during model development.
- The strain localization phenomenon is not restricted to any particular part of the sample and can appear anywhere in the area of the sample during the deformation process. Due to this, the CA spaces have to be applied in the entire area of the sample, which influences the computational cost. Parallelization of the developed code is a proper solution to this kind of problem.
- Application of the interpolation technique based on the SPH method is a good solution to overcome the problem with remeshing. It also provides the possibility to create a multi scale model for strain localization based on the combination of CA and meshless methods.
- Selection of the smoothing length parameter in the SPH method, which is responsible for the choice of support domain (neighboring points), is an important step. Defining the proper size of the support domain may lead to a reduction in calculation cost.
- There is a possibility to change the smoothing functions in the model. They should be selected based on the assessment of accuracy after some initial simulations.

8.3. Plans for Further Work

Based on experience gathered during the research described in this thesis, several directions of further development and improvement of the model can be established. First, transition rules developed in the current model can be modified to include processes leading to the propagation of micro shear and shear bands due to the change of the deformation path. It is well known from literature [Kor92] that micro shear bands and shear bands in such

processes become a major mechanism of deformation, which is a reason why further work in this area is needed.

Second, creation of a CA model, which includes microstructural features (e.g., grain orientation) in the explicit manner rather than implicit, should be performed. Taking into account the crystallographic aspects of deformation will result in further development of the model. The existing model can be modified, and a third CA space describing phenomena occurring in microstructures can be introduced. However, based on the existing transition rules and knowledge gathered during this work, a new 2D model for strain localization can also be established.

An algorithm for connecting the CAFE approach with *hp* adaptation methods will be developed, leading to even more accurate results in a specific part of the samples. That will create interesting possibilities of model application and reduction in computational cost.

Finally, at the end of the work dedicated to creation of the strain localization model, a complex multi scale model describing interactions between various phenomena occurring in the deformed material (i.e., dynamic recrystalization or phase transformation with micro shear and shear bands [Hum04, Pau02]) will be created. Such a complex model, which take into account interactions between these various phenomena, will create a powerful computational platform for detailed investigation of material behavior under thermomechanical processing and will help to solve several industrial problems.

9. Literature

[All06] Allix O., Multiscale strategy for solving industrial problems, Comp. Meth. Appl. Sci., 6, 2006, 107-126.

[Ana80] Anand L., Spitzig A., Initiation of localized shear bands in plane strain, J. Mech. Phys. Solids, 28, 1980, 113-128.

[Ana94] Anand L., Kalidindi S.R., The process of shear band formation in plane strain compression of fcc metals: effect of crystallographic texture, Mech. of Mat., 17, 1994, 223-243.

[Arm95] Armero F., Garikipati K., Recent advances in the analysis and numerical simulation of strain localization in inelastic solids, Proc. Conf. COMPLAS95, eds, Owen D.R.J., Onate E., Barcelona, 1995, 547-561.

[Bal03] Balokhonov R.R., Romanova V.A., Schmauder S., Makarov P.V., Simulation of meso–macro dynamic behavior using steel as an example, Comp. Mat. Sci., 28, 2003, 505-511.

[Bau96] Baudin T., Penelle R., Liu Y., Simulation of normal grain growth by cellular automata. Scr. Mat, 34, 1996, 1679–1683.

[Ber03] Berveiller M., Naddari A., Fakri N., Korbel A., The role of shear bands in the evolution of copper texture, Int. J. Plast., 8, 1992, 857-865.

[Bey00] Beynon J.H., Das S., Howard I.C., Palmier E.J., Shterenlikht A., The combination of cellular automata and finite elements for the study of fracture; the CAFE model of fracture., Proc. Conf., ECF14, eds, Neimitz A., Rokach I.V., Kocańda D., Gołoś K., Kraków, 2000, 241-248.

[Bey02] Beynon J.H., Das S., Howard I.C., Shterenlikht A., Extending the local approach to fracture; methods for direct incorporation of microstructural effects into finite element model of fracture, Proc. Conf. ASME2002, ed., Brust F.W., Vancouver, 2002, 229-237.

[Bli02] Blicharski M., Odkształcanie i pękanie, Uczelniane Wydawnictwa Naukowo-Dydaktyczne, Kraków, 2002, (in Polish).

[Boc03] Bochniak W., Korbel A., KOBO type forming forging of metals under complex conditions of the process, J. Mat. Proc. Techn., 134, 2003, 120-134.

[Bon00] Bonet J., Kulasegaram S., Correction and stabilization of smooth particle hydrodynamics method with applications in metal forming simulation, Int. J Numer. Meth. Engng., 47, 2000, 1189-1214.

[Bur04] Burbelko A., Mezomodelowanie krystalizacji metodą automatu komórkowego, Uczelniane Wydawnictwa Naukowo-Dydaktyczne, Kraków, 2004 (in Polish).

[Cha06] Chantrenne P., Atomic scale simulation: use of molecular dynamics, Mat. Konf. ESAFORM 2006, eds., Juster N., Rosochowski A., Glasgow, 123-127.

[Ciz02a] Cizek P., Characteristics of shear bands in an austenitic stainless steel during hot deformation, Mat. Sci. Eng. A324, 2002, 214-218.

[Ciz02b] Cizek P., Formation of shear bands during hot torsion of an austenitic stainless steel, Proc. Conf., Thermomech. Processing: Mechanics, Microstructure & Control, ed., Palmiere E.J., Mahfouf M., Pinna C., Sheffield, 2002, 289-295.

[Ciz04] Cizek P., Bai F., Rainforth M., Baynon J., Fine structure of shear bands formed during hot deformation of two austenitic steels, Mat. Trans., 45, 2004, 2157-2164.

[Che98] Chenot J.L., Bay F., An overview of numerical modeling techniques, J. Mat. Proc. Tech., 80-81, 1998, 8-15.

[Col93] Colas R., Grinberg A., Plastic instability in a heat-treatable aluminum alloy, Mat. Sci. Eng., A161, 1993, 201-208.

[Con76] Conway J.H., On numbers and games, Academic Press, New York, 1976.

[Cru04] Crumbach M., Goerdeler M., Gottstein G., Neumann L., Aretz H., Kopp R., Through-process texture modelling of aluminum alloys, Mod. Sim. Mater. Sci. Eng., 12, 2004, 1-18.

[Das02a] Das S., Palmiere E.J., Howard I.C., CAFE: a tool for modeling thermomechanical processes, Proc. Conf., Thermomech. Processing: Mechanics, Microstructure & Control, eds, Palmiere E.J., Mahfouf M., Pinna C., Sheffield, 2002, 296-301.

[Das02b] Das S., The effect of boundary conditions and material data representation on the simulation of deformation during hot rolling, PhD Thesis, University of Sheffield, Sheffield, 2002.

[Dau00] Daux C., Moes N., Dolbow N., Sukumar J., Belytschko T., Arbitrary branched and intersecting cracks with the extended finite element method, Int. J. Num. Met. Eng., 48, 2000, 1741-1760.

[Dav95] Davies C.H.J., The effect of neighborhoods on the kinetics of a cellular automaton recrystallization model, Scr. Metall. Mater., 33, 1995, 1139–1143.

[Dev89] Deve H.E., Asaro R.J., The development of plastic failure modes in crystalline materials: shear bands in FCC polycrystals, Metall. Trans. A, 20A, 1989, 579-593.

[Dav97] Davies C.H.J., Growth of nuclei in a cellular automaton simulation of recrystalization, Scr. Mater., 36, 1997, 35-40.

[Dav99] Davies C.H.J., Hong L., The cellular automaton simulation of static recrystallization in cold-rolled AA1050, Scr. Mater., 40, 1999, 1145–1150.

[Dil79] Dillamore I.L., Roberts J.G., Bush A.C., Occurrence of shear bands in heavily rolled cubic metals, Metal Sci. 13, 1979, 73-77.

[Din01] Ding R., Guo Z., Coupled quantitative simulation of microstructural evolution and plastic flow during dynamic recrystallization, Acta Mater., 49, 2001, 3163–3175.

[Din02] Ding R., Guo Z., Microstructural modelling of dynamic recrystallisation using an extended cellular automaton approach, Comp. Mat. Sci., 23, 2002, 209–218.

[Din04] Ding R., Guo Z., Microstructural evolution of a Ti–6Al–4V alloy during □-phase processing, experimental and simulative investigations, Mater. Sci. Eng., A 365, 2004, 172–179.

[Dug78] Duggan B.J., Hatherly M., Hutchinson W.B., Wakefield P.T., Deformation structures and textures in cold-rolled 70:30 brass, Metal Sci., 1978, 343-351.

[Emb84] Embury J.D., Korbel A., Raghunathan V.S., Rys J., Shear band formation in cold rolled Cu-6% Al single crystals, Acta Metall., 32, 1984, 1883-1894.

[Fen99] Feng H., Bassim M.N., Finite element modelling of the formation of adiabatic shear bands in AISI 4340 steel, Mat. Sci. Eng., A266, 1999, 255-260.

[Fri04] Fries T.P., Matthies H.G., Classification and overview of meshfree methods, Scientific Computing, Informatikbericht, 2003-3, Brunswick, 2004.

[Gan94] Gandin C. A., Rappaz M., A coupled finite element - cellular automaton model for the prediction of dendritic grain structures in solidification processes, Acta Metall., 42, 1994, 2233–2246.

[Gan99] Gandin C., Desbiolles J., Rappaz M., Thevoz P., A three-dimensional cellular automaton–finite element model for the prediction of solidification grain structures, Metall. Mater. Trans. A, 30A, 1999, 3153–3165.

[Gaw04] Gawąd J., Madej Ł., Szeliga D., Pietrzyk, M., Microstructure evolution modeling based on the rheological parameters using the cellular automaton technique, Proc. Conf. Forming 2004, Strebske Pleso, 2004, 67–70.

[Gaw05a] Gawąd J., Maciol P., Pietrzyk M., Multiscale modeling of microstructure and macroscopic properties in thixoforming process using cellular automaton technique, Arch. Metall. Mater., 50, 2005, 549-561.

[Gaw05b] Gawąd J., Madej Ł., Szeliga D., Pietrzyk M., Cellular automaton technique as a tool for a complex analysis of the microstructure evolution and rheological behaviour, Act. Met. Slov., 11, 2005, 45–53.

[Gaw05c] Gawad J., Madej Ł., Zastosowanie automatów komórkowych do wieloskalowej analizy zjawisk w inżynierii metali, Informatyka w Technologii Materiałów, 5, 2005, 142-162.

[Gin77] Gingold R.A., Monaghan J.J., Smoothed particle hydrodynamics: theory and application to non-spherical stars, Monthly Notices Royal Astronomical Society, 181, 1977, 375-389.

[Goe05] Goetz R., Particle stimulated nucleation during dynamic recrystallization using a cellular automata model, Scr. Mater., 52, 2005, 851–856.

[Goe98a] Goetz R., Seetharaman V., Modeling dynamic recrystallization using cellular automata, Scr. Mater., 38, 1998, 405–413.

[Goe98b] Goetz R., Seetharaman V., Static recrystallization kinetics with homogeneous and heterogeneous nucleation using a cellular automata model, Metal. Mater. Trans. A., 29, 1998, 2307–2321.

[Gui04] Guillemot G., Gandin C. A., Combeau, H., Heringer, R., A new cellular automaton - finite element coupling scheme for alloy solidification, Mod. Sim. Mater. Sci. Eng., 12, 2004, 545–556.

[Har88] Harren S.V., Deve H.E., Asaro R.J., Shear band formation in plane strain compression, Acta Metall., 36, 1988, 2435-2480.

[Hes91] Hesselbarth H., Göbel I., Simulation of recrystallization by cellular automata, Acta Metall., 39, 1991, 2135–2143.

[Hou78] Van Houtte P., Seviliano J.G., Aernoudt E., Models for shear band formation in rolling extrusion, Mettalkde, 1978, 426-432.

[How00] Howard I.C., Li Z.H., Sheikh M.A., Modeling the ductile to cleavage transition in steels and structures, ASTM STP 1360, eds, Paris P.C., Jerina K.L., Philadelphia, 2000, 152-168.

[Hum95] Humphreys F.J., Hatherly M., Recrystalization and related annealing phenomena, Pergamon, Elsevier Science Ltd., 1995.

[Hum04] Humphreys F.J., Nucleation in recrystallization, Mat. Sci. Forum, 467-470, 2004, 107-116.

[Jan04] Janssens K.G.F., Holm E.A., Foiles S.M., Introducing solute drag in irregular cellular automata modelling of grain growth, Mat. Sci. Forum, 467/470, 2004, 1045-1050.

[Kaz05] Kazanowski P., Browne H.M., Libura W., Misiolek W.Z., Mechanical and microstructural performance of convex dies in axisymetric extrusion – theory and experimental verification, Met. Sci. Eng., A404, 2005, 235-243.

[Kor83] Korbel A., Dobrzanski F., Richert M., Strain hardening of aluminium at high strains, Acta Metall., 31, 1983, 293-298.

[Kor85] Korbel A., Richter M., Formation of shear bands during cyclic deformation of aluminum, Acta Metall., 33, 1985, 1971-1978.

[Kor86a] Korbel A., Martin P., Microscopic versus macroscopic aspects of shear bands deformation, Acta Metall., 34, 1986, 1905-1909.

[Kor86b] Korbel A., Embury J.D., Hatherly M., Martin P.L., Erbsloh H.W., Microstructural aspects of strain localization in Al-Mg alloys, Acta Metall., 34, 1986, 1999-2009.

[Kor88] Korbel A., Martinh P., Microstructural events of macroscopic strain localization in prestrained tensile specimens, Acta Metall., 36, 1988, 2575-2586.

[Kor90] Korbel A., The model of microshear banding in metals, Scr. Mat. Mater., 24, 1990, 1229 – 1231.

[Kor92] Korbel A., Perspectives of the control of mechanical performance of metals during forming operations, J. Mater. Proc. Techn, 34, 1992, 41-50.

[Kor95] Korbel A., Bochniak W., The structure based design of metal forming operations, J. Mat. Proc. Tech., 53, 1995, 229-237.

[Kor97] Korbel A., Ciura F., The mechanical instability of the metal substructure and formation of pseudo periodic substructure in thermodynamically stable and unstable phases, J. Mat. Proc. Tech., 64, 1997, 231-238.

[Kor98] Korbel A., Structural and mechanical aspects of homogeneous and non-homogeneous deformation in solids, Courses and Lectures – No. 386, Springer, 1998, 21-98.

[Kor04] Korbel A., Bochniak W., Refinement and control of the metal structure elements by plastic deformation, Scr. Mater., 51, 2004, 755–759.

[Kro01a] Kroc J., Paidar V., Modelling of the effect of triple junctions on grain boundary migration by a cellular automaton, J. Phy., 11, 2001, 85–92.

[Kro01b] Kroc J., Simulation of dynamic recrystallization by cellular automata, PhD Thesis, Charles University, Prague, 2001.

[Kro02] Kroc J., Application of cellular automata simulations to modelling of dynamic recrystallization, Lecture Notes in Computer Science, 2329, 2002, 773–782.

[Kro03] Kroc J., Paidar V., Modelling of recrystallization and grain boundary migration by cellular automata, Mat. Sci. Forum, 426/432, 2003, 3873–3878.

[Kro05] Kroc J., Influence of lattice anisotropy on models formulated by cellular automata in presence of grain boundary movement, a case study, Mater. Sci. Forum, 482, 2005, 195–198.

[Kul00] Kułakowski K., Automaty Komórkowe, Ośrodek Edukacji Niestacjonarnej, Kraków, 2000 (in Polish).

[Lan05] Lan Y.J., Xiao N.M., Li D.Z., Li Y.Y., Mesoscale simulation of deformed austenit decomposition into ferrite by coupling a cellular automaton method with a crystal plasticity finite element model, Acta Mater., 53, 2005, 991-1003.

[Lee91] Lee W.B., Chan K.C., A criterion for the prediction of shear band angles in F.C.C. metals, Acta Metall. Mater., 39, 1991, 411-417.

[Li00] Li S., Liu W.K., Numerical simulation of strain localization in inelastic solids using mesh-free methods, Int. J. Num. Met. Eng., 48, 2000, 1285-1309.

[Lib90] Libersky L.D., Petschek A.G., Smooth particle hydrodynamics with strength of materials. Advances in the free lagrange method, Lecture Notes in Physics, 395, 1990, 248-257.

[Lib92] Libura W., Zasadzinski J., The influence of strain gradient on material structure during extrusion of the AlCu4Mg alloy, J. Mat. Proc. Tech., 34, 1992, 517-524.

[Liu87] Liu Yi-Lin L., Delaey E., Aernoudt E., Arkens O., Substructure development and mechanical properties in cold-rolled aluminium alloy 3004, Mat. Sci. Eng., 96, 1987, 125-137.

[Liu03] Liu G.R., Liu M.B., Smoothed particle hydrodynamic: a meshfree particle method, World Scientific Publishing, 2003.

[Luc77] Lucy L.B., A numerical approach to the testing of fusion process, Astronomical Journal, 88, 1977, 1013-1024.

[Mad04] Madej Ł., Hodgson P., Gawad J., Pietrzyk M., Modeling of rheological behavior and microstructure evolution using cellular automaton technique, Proc. Conf. ESAFORM 2004, ed., Støren, S., Trondheim, 2004, 143–146.

[Mad05a] Madej Ł., Żmudzki A., Pietrzyk M., Możliwości uwzględnienia wpływu wymuszonej zmiany drogi odkształcenia na naprężenie uplastyczniające w procesach plastycznej przeróbki metali, Proc. Conf. KomPlasTech 2005, eds, Piela A., Lisok J., Grosman F., Ustroń, 2005, 207-214 (in Polish).

[Mad05b] Madej Ł., Pietrzyk M., Pidvysotskyy V., Kuziak R., Analiza wrażliwości naprężenia uplastyczniającego, wyznaczonego z próby ściskania pierścieni, na współczynnik tarcia i wymiary próbki, Informatyka w Technologii Materiałów, 5, 2005, 83-94 (in Polish).

[Mad05c] Madej Ł., Hodgson P.D., Pietrzyk M., The remeshing problem in the multi scale strain localization CAFE approach, Lecture Series on Computer and Computational Sciences, 4, 2005, 365-368.

[Mad05d] Madej Ł, Talamantes-Silva J., Howard I.C., Pietrzyk M., Modeling of the initiation and propagation of the shear band using the coupled CAFE model, Arch. Metall. Mater., 50, 2005, 563-573.

[Mad06a] Madej Ł., Hodgson P.D., Pietrzyk M., Multi scale analysis of material behavior during deformation processes, in: Foundation of Materials Design, eds, Krzysztof J. Kurzydlowski, Boguslaw Major and Pawel Zieba, Research Signpost, Kerala, 2006, 17-47.

[Mad06b] Madej Ł., Hodgson P.D., Pietrzyk M., Multi scale rheological model for discontinuous phenomena in materials under deformation conditions, Comp. Mat. Sci., 35, 2006, (in press).

[Mak00a] Makarov P.V., Romanova V.A., Mesoscale plastic flow generation and development for polycrystals, Theor. Appl. Fract. Mech., 33, 2000, 1-7.

[Mak00b] Makarov P.V., Localized deformation and fracture of polycrystals at mesolevel, Theor. Appl. Fract. Mech., 33, 2000, 23-30.

[Mak01] Makarov P.V., Schmuader S., Cherepanov O.I., Smolin I.Yu., Romanova V.A., Balokhonov R.R., Saraev D.Yu., Soppa E., Kizler P., Fisher G., Hu S., Ludwig M., Simulation of elastic-plastic deformation and fracture of materials at micro-, meso- and macrolevels, Theor. Appl. Fract. Mech., 37, 2001, 183-244.

[Mal03] Malarz K., Automaty komórkowe, Wydział Fizyki i Techniki Jądrowej AGH, Kraków, 2003 (in Polish).

[Mar99] Marx V., Reher F. R., Gottstein G., Simulation of primary recrystallization using a modified three-dimensional cellular automaton, Acta Mater., 47, 1999, 1219–1230.

[Mon83] Monaghan J. J., Gingold R. A., Shock simulation by the particle method SPH, J. Comp. Phys., 52, 1983, 374-389.

[Mon05] Monaghan J. J., Smoothed particle hydrodynamic, IPAM, Notes, 2005.

[Mor85] Morii K., Mecking H., Nakayama Y., Development of shear band in F.C.C single crystals, Acta Metall., 33, 1985, 379-386.

[Mro06] Mrozek A., Burczyński T., Analysis of the material behaviour at the nanoscale, Proc. Conf. 35th Solid Mechanics, Kraków, 2006, 283-284.

[Mro07] Mrozek A., Kuś W., Burczyński T., Application of the coupled boundary element method with atomic model in the static analysis, Computer Methods in Materials Science, 7, 2007, 284-288.

[Muk04] Mukhopadhyay P., Loeck M., Gottstein, G., Simulation of microstructure evolution during recrystallization using a high-resolution three-dimensional cellular automaton, J. Phy., 120, 2004, 225–230.

[Nak87] Nakayama Y., Morii K., Microstructure and shear band formation in rolled single crystals of Al.-Mg alloy, Acta Metall. 35, 1987, 1747-1755.

[Nav04] Nave M., Barnett, M., Microstructures and textures of pure magnesium deformed in plane-strain compression, Scr. Mater., 51, 2004, 881-885.

[Neu66] Von Neumann J., Theory of self reproducing automata, ed., Bamk A.W., University of Illinois, Urbana, 1966.

[Nou80] Nourbakhsh S., Nutting J., The high strain deformation of an aluminum-4% copper alloy in the supersaturated and aged conditions, Acta Metall., 28, 1980, 357-365.

[Nou86] Nourbakhsh S., Vujic D., High strain plane strain deformation of 70-30 brass in a channel die, Acta Metall., 34, 1986, 1083-1090.

[Oli01] Oliferuk W., Korbel A., Bochniak W., Energy balance and macroscopic strain localization during plastic deformation of polycrystalline metals, Mat. Sci. Eng., A319-321, 2001, 250-153.

[Oli95] Olivier J., Continuum modelling of strong discontinuities in solid mechanics, Proc. Conf. COMPLAS'95, eds, Owen D.R.J., Onate E., Barcelona, 1995, 455-479.

[Pas06] Paszyński M., Kopernik M., Madej Ł., Pietrzyk M., Automatic hp adaptivity to improve accuracy of heat transfer model and linear elasticity problems in engineering solving, J. Machine Eng., 16, 2006, 73-82.

[Pau02] Paul H., Driver J.H., Jasienski Z., Shear banding and recrystallization nucleation in a Cu-2%Al alloy single crystal, Acta Mater., 50, 2002, 815-830.

[Pec92] Pecherski R. B., Modelling of large plastic deformations based on the mechanism of micro-shear banding. Physical foundation and theoretical description in plane strain, Arch. Mech., 44, 1992, 563-584.

[Pec98a] Pecherski R.B., Continuum mechanics description of plastic flow produced by micro-shear bands, Technische Machanik, 18, 1998, 107-115.

[Pec98b] Pecherski R. B., Macroscopic effect of micro-shear banding in plasticity of metals, Acta. Mech., 131, 1998, 203-224.

[Qia04] Qian M., Guo Z., Cellular automata simulation of microstructural evolution during dynamic recrystallization of an HY-100 steel, Mater. Sci. Eng., A, 365, 2004, 180-185.

[Raa98] Raabe D., Computational material science: the simulation of materials microstructures and properties, Weinheim, New York, 1998.

[Raa02] Raabe D., Cellular automata in materials science with particular reference to recrystallization simulation, Ann. Rev. Mater. Res., 32, 2002, 53–76.

[Raa04] Raabe D., Mesoscale simulation of spherulite growth during polymer crystallization by use of a cellular automaton, Acta Mater., 52, 2004, 2653–2664.

[Raa05] Raabe D., Hantcherli L., 2D cellular automaton simulation of the recrystallization texture of an IF sheet steel under consideration of Zener pinning, Comp. Mater. Sci., 34, 2005, 299–313.

[Ric95] Richert M., Korbel A., The effect of strain localization on mechanical properties of Al99,992 in the range of large deformations, J. Mat. Proc. Tech., 53, 1995, 331-340.

[Rol01] Rollett A., Raabe D., A hybrid model for mesoscopic simulation of recrystallization, Comp. Mater. Sci., 21, 2001, 69–78.

[Ron06] Rondanini M., Barbato A., Cavalloti C., A multi scale model of the Si CVD process, Proc. Conf., MMM 2006, 98-101.

[Ros04] Rosochowski A., Olejnik L., Richert M., Metal forming technology for production bulk nanostructured materials, Steel-Grips, 3, 2004, 35-44.

[Rou89] Rousselier G., Devaux J.C., Mottel G., Devesa G., A methodology of ductile fracture analysis based on damage mechanics: an illustration of a local

approach of fracture, in Non linear fracture mechanics: Volume II, eds, Landers J.D., Saxena A., Merkle J.G., ASTM STP 995, Philadelphia, 1989, 332-354.

[Sea05] Searles T., Tiley J., Tanner A., Williams R., Rollins B., Lee E., Kar S., Banerjee R., Fraser H.L., Rapid characterization of titanium microstructural features for specific modelling of mechanical properties, Meas. Sci. Technol., 16, 2005, 60-69.

[Sem82] Sematin S.L., Laohoti G.D., The occurrence of shear bands in the isothermal hot forging, Metal. Trans. A, 13A, 1982, 275-287.

[She98] Sherry A.H., Beardsmore D.W., Lidbury D.P.G, Sheikh M.A., Howard I.C., Remanent life assessment using the local approach - a prediction of the outcome of the NESC experiment, Mech. Eng. Pub., S539/006, 1998, 87-103.

[Shi05] Shiari B., Miller R.E., Curtin W.A., Coupled atomistic/discrete dislocation simulations of nanoindentation at finite temperature, J. Engng Mater. Technol, 127, 2005 358-367.

[Sht03] Shterenlikht A., 3D CAFE Modeling of transitional ductile – brittle fracture in steels, PhD Thesis, University of Sheffield, Sheffield, 2003.

[Str01] Strouboulis T., Copps K., Babuska I., The generalized finite element method, Comp. Met. App. Mech. Eng., 190, 2001, 4081-4193.

[Svy05] Svyetlichnyy D., Milenin A., Modelowanie procesów rekrystalizacji za pomocą automatów komórkowych, Proc. Conf. KomPlasTech05, eds, Piela, A., Lisok, J., Grosman, F., Ustroń, 2005, 115-122 (in Polish).

[Sze02] Szeliga D., Pietrzyk M., Identification of rheological and tribological parameters, Metal forming science and practice, A State-of-the-art Volume in Honour of Professor J.A. Schey's 80th Birthday, ed., Lenard J.G., Elsevier, Amsterdam, 2002, 227-258.

[Sze06] Szeliga D., Gawad J., Pietrzyk M., Inverse analysis for identification of rheological and friction models in metal forming, Comp., Meth., App., Mech. Eng., 195, 2006, 6778-6798.

[Ter03] Terrier V., Two-dimensional cellular automata and their neighborhoods, Theor. Comp. Sci., 312, 2004, 203-222.

[Vig04] Vignjevic R., Review of development of the smooth particle hydrodynamics (SPH) method, Proc. Conf. DCSSS, Cranfield, 2004.

[Waj04] Wajda W., Modelowanie procesów przeróbki plastycznej z uwzględnieniem efektów mikorpasm ścinania, PhD thesis, AGH, Kraków, 2004 (in Polish).

[Wol94] Wolfram S., Universality and complexity in cellular automata, Physica, D 10, 1994.

[Yu05] Yu Q., Esche S. K., A multi-scale approach for microstructure prediction in thermo-mechanical processing of metals, J. Mater. Proc. Tech., 169, 2005, 493–502.

[Zhu03] Zhu Q., Abbod M.F., Talamantes-Silva J., Sellars C.M., Linkers D.A., Beynon J.H., Hybrid modeling of aluminum-magnesium alloys during thermomechanical processing in terms of physically based, neuro-fuzzy and finite element models, Acta Mater., 51, 2003, 5051-5062.

[Zie06] Zienkiewicz O.C., Morgan K., Finite elements and approximation, Dover Publications, UK.